National Library of Canada
Bibliothèque nationale du Canada

Canadian Theses Service
Services des thèses canadiennes

Ottawa, Canada
K1A 0N4

CANADIAN THESES

THÈSES CANADIENNES

NOTICE

The quality of this microfiche is heavily dependent upon the quality of the original thesis submitted for microfilming. Every effort has been made to ensure the highest quality of reproduction possible.

If pages are missing, contact the university which granted the degree.

Some pages may have indistinct print especially if the original pages were typed with a poor typewriter ribbon or if the university sent us an inferior photocopy.

Previously copyrighted materials (journal articles, published tests, etc.) are not filmed.

Reproduction in full or in part of this film is governed by the Canadian Copyright Act, R.S.C. 1970, c. C-30. Please read the authorization forms which accompany this thesis.

AVIS

La qualité de cette microfiche dépend grandement de la qualité de la thèse soumise au microfilmage. Nous avons tout fait pour assurer une qualité supérieure de reproduction.

S'il manque des pages, veuillez communiquer avec l'université qui a conféré le grade.

La qualité d'impression de certaines pages peut laisser à désirer, surtout si les pages originales ont été dactylographiées à l'aide d'un ruban usé ou si l'université nous a fait parvenir une photocopie de qualité inférieure.

Les documents qui font déjà l'objet d'un droit d'auteur (articles de revue, examens publiés, etc.) ne sont pas microfilmés.

La reproduction, même partielle, de ce microfilm est soumise à la Loi canadienne sur le droit d'auteur, SRC 1970, c. C-30. Veuillez prendre connaissance des formules d'autorisation qui accompagnent cette thèse.

THIS DISSERTATION
HAS BEEN MICROFILMED
EXACTLY AS RECEIVED

LA THÈSE A ÉTÉ
MICROFILMÉE TELLE QUE
NOUS L'AVONS REÇUE

NL 339 (r. 86/01)

Canada

National Library of Canada
Bibliothèque nationale du Canada

Ottawa, Canada
K1A 0N4

98

TC –

0-315-23295-1

CANADIAN THESES ON MICROFICHE SERVICE – SERVICE DES THÈSES CANADIENNES SUR MICROFICHE

PERMISION TO MICROFILM – AUTORISATION DE MICROFILMER

• Please print or type – Écrire en lettres moulées ou dactylographier

AUTHOR – AUTEUR

Full Name of Author – Nom complet de l'auteur

Kathryn Isabella Story

Date of Birth – Date de naissance	Canadian Citizen – Citoyen canadien
May 31, 1959	☒ Yes / Oui ☐ No / Non
Country of Birth – Lieu de naissance	**Permanent Address – Résidence fixe**
Canada	10528 - 76 St Edmonton, Alberta T6A 3B3

THESIS – THÈSE

Title of Thesis – Titre de la thèse

Synthesis and Kinetic Studies of Model Compounds for the Acylation Step in Cysteine Protease Mediated Hydrolysis.

Degree for which thesis was presented Grade pour lequel cette thèse fut présentée	Year this degree conferred Année d'obtention de ce grade
M.Sc.	1985
University – Université	**Name of Supervisor – Nom du directeur de thèse**
Alberta	Robert S. Brown

AUTHORIZATION – AUTORISATION

Permission is hereby granted to the NATIONAL LIBRARY OF CANADA to **microfilm** this thesis and to **lend** or **sell copies of the film.**

The author reserves other publication rights, and neither the thesis nor extensive extracts from it may be printed or otherwise reproduced without the author's written permission.

L'autorisation est, par la présente, accordée à la BIBLIOTHÈQUE NATIONALE DU CANADA de **microfilmer** cette thèse et de **prêter** ou de **vendre des exemplaires du film.**

L'auteur se réserve les autres droits de publication; ni la thèse ni de longs extraits de celle-ci ne doivent être imprimés ou autrement reproduits sans l'autorisation écrite de l'auteur.

ATTACH FORM TO THESIS – VEUILLEZ JOINDRE CE FORMULAIRE À LA THÈSE

Signature	Date
Kathryn I. Story	July 31, 1985

NL-91 (r. 84/03)

Canada

THE UNIVERSITY OF ALBERTA

SYNTHESIS AND KINETIC STUDIES OF CHEMICAL MODELS FOR THE ACYLATION STEP IN CYSTEINE PROTEASE MEDIATED HYDROLYSIS

by

(C) KATHRYN ISABELLA SKOREY

A THESIS

SUBMITTED TO THE FACULTY OF GRADUATE STUDIES AND RESEARCH

IN PARTIAL FULFILMENT OF THE REQUIREMENTS FOR THE DEGREE

OF MASTER OF SCIENCE

DEPARTMENT OF CHEMISTRY

EDMONTON, ALBERTA

FALL, 1985

THE UNIVERSITY OF ALBERTA

RELEASE FORM

NAME OF AUTHOR Kathryn Isabella Skorey

TITLE OF THESIS Synthesis and Kinetic Studies of Model Compounds for the Acylation Step in Cysteine Protease Mediated Hydrolysis

DEGREE FOR WHICH THESIS WAS PRESENTED M.Sc.

YEAR THIS DEGREE GRANTED 1985

Permission is hereby granted to THE UNIVERSITY OF ALBERTA LIBRARY to reproduce single copies of this thesis and to lend or sell such copies for private, scholarly or scientific research purposes only.

The author reserves other publication rights, and neither the thesis nor extensive extracts from it may be printed or otherwise reproduced without the author's written permission.

Kathryn I. Skorey

PERMANENT ADDRESS

.....

.....

DATED July 31 1985

THE UNIVERSITY OF ALBERTA

FACULTY OF GRADUATE STUDIES AND RESEARCH

The undersigned certify that they have read, and recommended to the Faculty of Graduate Studies and Research for acceptance, a thesis entitled SYNTHESIS AND KINETIC STUDIES OF CHEMICAL MODELS FOR THE ACYLATION STEP IN CYSTEINE PROTEASE MEDIATED HYDROLYSIS submitted by KATHRYN ISABELLA SKOREY in partial fulfilment of the requirements for the degree of Master of Science.

.....
Supervisor

.....

.....

.....

Date..June 20...1985.....

DEDICATION

To my husband, Michael

For his steadfast support and love

ABSTRACT

Papain is one of the sulfhydryl-containing proteolytic enzymes found in nature. The active site of the enzyme consists of 40 amino acids including a cysteine, histidine and aspartic acid residue. Currently, it is believed that the thiol group of cysteine 25 and the imidazole group of histidine 159 exist as a thiolate-imidazolium ion pair at physiological pH. The sulphur of the ion-pair is believed to be nucleophilically active in attacking the carbonyl of an ester or amide to form a tetrahedral intermediate which subsequently collapses to the S-acyl enzyme intermediate. Hydrolysis of the S-acyl intermediate regenerates the original enzyme and a carboxylic acid.

In this work, three imidazole-thiol model compounds, 4(5)-mercaptomethylimidazole (**15a**), N-methyl-2-mercaptomethylimidazole (**16a**), and 2-mercaptomethylimidazole (**17a**) were synthesized. Studies were then performed to determine if a thiolate-imidazolium species can form at physiological pH and if such a zwitterionic species is nucleophilically active in attacking p-nitrophenylacetate (PNPA).

The aforementioned compounds were prepared from their hydroxymethylimidazoles by treatment with thionyl chloride to give the chloromethylimidazoles which were subsequently treated with benzyl mercaptan to give the

S-benzyl compounds. Reduction of the S-benzyl compounds with sodium in liquid ammonia yielded the final mercaptan products. These products (**15a-17a**) were isolated and purified as their HCl salts.

The acylation of the mercaptomethylimidazoles (**15a-17a**) by p-nitrophenylacetate as a function of pH was studied and compared with the similar data for the respective imidazoles 4(5)-methylimidazole (**15b**), 1,2-dimethylimidazole (**16b**) and 2-methylimidazole (**17b**).

Analysis of the pH versus log k_{cat} plots (where k_{cat} is the second order rate constant for nucleophilic attack on PNPA) of **15a-17a** gave two pKa's representing the deprotonation of the imidazole and the thiol functional groups. The reactivity of **15a** around neutrality was the same as that of 4(5)-methylimidazole (**15b**) indicating little thiolate anion reactivity in this pH region. However, **16a** and **17a** both showed reactivity 10 to 15 fold greater than their corresponding imidazoles 1,2-dimethylimidazole (**16b**) and 2-metnylimidazole (**17b**) respectively.

Microscopic pKa determinations for the model compounds were attempted by two methods: one method using data from potentiometric titrations and another method using UV-visible spectra titration data. The microscopic pKa's from the two methods were compared and the accuracy of each method was discussed. The pKa's calculated from the UV-visible titration data were

believed to be less accurate than the pKa's calculated from the potentiometric titration data. The latter pKa's were then used to determine the concentration of all microscopic species at any pH.

Evidence is presented from analysis of the pKa's that **16a** and **17a** exist primarily as zwitterionic species around neutrality. It is in this zwitterionic form that the thiolate is active which in turn yields the observed rate enhancement around pH 6.5 to 8.0.

These models **16a** and **17a** are believed to be the first examples where cooperativity between intramolecular imidazole and thiol in a nucleophilic acylation process has been demonstrated.

ACKNOWLEDGEMENTS

I would like to thank Dr. R.S. Brown for his guidance and encouragement in this project. I would also like to thank J.P. Street for his helpful suggestions and discussions.

TABLE OF CONTENTS

CHAPTER		PAGE
I.	INTRODUCTION	1
	Background	1
	Acylation	2
	Deacylation	6
	Catalytic Site: Structure and Mechanism	7
	Model Studies	16
	Summary	21
II.	RESULTS AND DISCUSSION	23
	Introduction to Research	23
	Synthesis	26
	Catalytic Studies: Acylation Rates	31
	pKa Determinations	47
	(1) Potentiometric Titrations	47
	(2) UV-visible Spectra Titrations	49
	Concentration of Zwitterion	70
	Product Study	86
	Deacylation	93
III.	EXPERIMENTAL	95
BIBLIOGRAPHY		115
APPENDIX 1.	Non-Linear Least Squares Program	126
APPENDIX 2.	Derivation of Kinetic Expression for Figures 4 and 5	127
APPENDIX 3.	Simm's Method to Determine the pKa's by Potentiometric Titration	129

CHAPTER PAGE

APPENDIX 4. Determination of Microscopic Dissociation Constants using UV-Visible Spectrophotometric Titration Data..... 131

APPENDIX 5. Determination of the Concentration of each species I, II, III and IV..... 134

APPENDIX 6. Diagram of a Specially-Designed UV Cell for the UV-Visible Spectra Titrations..... 137

LIST OF TABLES

TABLE		PAGE
1	Second order rate constant data for the reaction of PNPA with 4(5)-mercaptomethylimidazole hydrochloride.	34
2	Second order rate constant data for tne reaction of PNPA with N-methyl-2-mercaptomethyl-imidazole hydrochloride.	36
3	Second order rate constant data for the reaction of PNPA with 2-mercaptomethylimidazole hydrochloride.	38
4	Second order rate constant data for the reaction of PNPA with 4(5)-methylimidazole.	40
5	Second order rate constant data for the reaction of PNPA with 1,2-dimethylimidazole.	41
6	Second order rate constant data for the reaction of PNPA with 2-methylimidazole.	42
7	Macroscopic pKa's determined by potentiometric titration.	48
8	Microscopic pKa's based on potentiometric titration.	50
9	Computed values for pM and α from UV-visible titration data of 4(5)-mercaptomethylimidazole hydrochloride.	63
10	Computed values for pM and α from UV-visible titration data of N-methyl-2-mercaptomethylimidazole hydrochloride.	64
11	Computed values for pM and α from UV-visible titration data of 2-mercaptomethylimidazole hydrochloride.	65
12	Microscopic pKa's based on UV-visible spectra titrations.	66
13	Concentration of the microscopic species as a function of pH for 4(5)-mercaptomethylimidazole hydrochloride.	71

TABLE		PAGE
14	Concentration of the microscopic species as a function of pH for N-methyl-2-mercaptomethylimidazole hydrochloride.	73
15	Concentration of the microscopic species as a function of pH for 2-mercapto-methylimidazole hydrochloride.	75
16	Total thiolate anion concentration as a function of pH.	77
17	Computed rate constants for the attack of the various ionic forms of (4)5-mercaptomethylimidazole, N-methyl-2-mercaptomethylimidazole and 2-mercapto-methylimidazole on PNPA.	82
18	Absorbance versus time data at λ = 402 nm for the reaction of equal-molar quantities of PNPA and 4(5)-mercapto-methylimidazole, N-methyl-2-mercapto-methylimidazole and 2-mercaptomethyl-imidazole at pH 7.8.	87

LIST OF FIGURES

FIGURE		PAGE
1	The active site region of papain reproduced from reference 1.	3
2	Depiction of the "UP and DOWN" mechanism of acylation for papain proposed by Angelides and Fink from reference 36.	14
3	Plot of the second order rate constant (k_{cat}) versus pH for 4(5)-mercaptomethylimidazole (**15a**), N-methyl-2-mercaptomethylimidazole (**16a**) and 2-mercaptomethylimidazole (**17a**).	43
4	Reaction scheme for the attack on PNPA by 4(5)-mercaptomethylimidazole, N-methyl-2-mercaptomethylimidazole and 2-mercaptomethylimidazole.	46
5	Reaction scheme for the attack on PNPA by the imidazole compounds, 4(5)-methylimidazole, 1,2-dimethylimidazole and 2-methylimidazole.	46
6a	UV-visible spectrum as a function of pH for 4(5)-mercaptomethylimidazole hydrochloride (1.33×10^{-4} M).	51
6b	Plot of absorbance versus pH at λ = 240 nm for 4(5)-mercaptomethylimidazole hydrochloride (1.33×10^{-4} M).	52
7a	UV-visible spectrum as a function of pH for N-methyl-2-mercaptomethylimidazole hydrochloride (1.09×10^{-4} M) from pH 3.1 to 6.3.	53
7b	UV-visible spectrum as a function of pH for N-methyl-2-mercaptomethylimidazole hydrochloride (1.09×10^{-4}) from pH 6.3 to 8.7.	54
7c	UV-visible spectrum as a function of pH for N-methyl-2-mercaptomethylimidazole hydrochloride (1.09×10^{-4}) from pH 8.7 to 11.5.	55

FIGURE		PAGE
7d	Plot of absorbance versus pH at λ = 262 nm for N-methyl-2-mercaptomethylimidazole hydrochloride (1.09×10^{-4} M).	56
8a	UV-visible spectrum as a function of pH for 2-mercaptomethylimidazole hydrochloride (1.37×10^{-4} M).	57
8b	Plot of absorbance versus pH at λ = 255 nm for 2-mercaptomethylimidazole hydrochloride (1.37×10^{-4} M).	58
9	Plot of pM versus α for 4(5)-mercaptomethylimidazole, N-methyl-2-mercaptomethylimidazole and 2-mercaptomethylimidazole.	60
10	UV spectra from 200 to 400 nm of the disulfide and mercaptan of N-methyl-2-mercaptomethylimidazole hydrochloride (2.92×10^{-5} M).	68
11	Plot of the concentration of the microscopic species versus pH for 4(5)-mercaptomethylimidazole hydrochloride.	72
12	Plot of the concentration of the microscopic species versus pH for N-methyl-2-mercaptomethylimidazole hydrochloride.	74
13	Plot of the concentration of the microscopic species versus pH for 2-mercaptomethylimidazole hydrochloride.	76
14	Plot of the total thiolate concentration versus pH for 4(5)-mercaptomethylimidazole, N-methyl-2-mercaptomethylimidazole and 2-mercaptomethylimidazole.	78
15	Plot of $1/Abs - 1/Abs_f$ versus time for the reaction of 4(5)-mercaptomethylimidazole, N-methyl-2-mercaptomethylimidazole and 2-mercaptomethylimidazole with PNPA at equal molar concentrations of 4×10^{-4} M.	89

I. INTRODUCTION

BACKGROUND

Papain is one of the sulfhydryl containing proteinases found in certain plant and some simple bacterial sources.[1] Other examples of the cysteine proteinases are ficin[2a] from the fig tree, chymopapain,[2b] which, like papain can be isolated from papaya latex, bromelain[2c] from pineapple, mexicain[2d] from the leaf or fruit of Pileus mexicanus, ascelpain[2e] from milkweed rot, euphorbain[2f] from the latex of Eurphorbia lathyrus, and actinidin[2g] from the fruit of the Chinese gooseberry or Kiwifruit. The enzymes from animal tissue, called cathepsins, belong to this group as well as clostridiopeptidase B[3a] and streptococcal proteinase[3b] from bacteria. The latter are probably used as exotoxins to break down the cellular proteins of the invaded host.[4]. Plant derived cysteine proteinases may be defence-related by protecting the plant from invasion by fungi and parasitic insects.[5]

Both papain and bromelain have enjoyed commercial application as meat tenderizing agents,[6a] in cosmetic preparations,[6b] clinically[6c] and in the food preparation industry.[6d]

Structurally and kinetically, more is known about papain because of its relative abundance and ease of isolation.[7] Drenth, et al., obtained a complete X-ray

crystal structure of the nonactivated disulfide derivative of papain at a resolution of 2.8 Å.[8] The active site region is reproduced in Figure 1.[8]

It is on the basis of these structures that much of the present mechanistic interpretation of the activity of cysteine containing proteases is based.[9] A brief review of papain with emphasis on mechanistic studies is presented.

ACYLATION

Papain is sufficiently robust to permit kinetic studies between pH 2.8 and 10.8.[10] Several studies[11,12] of the mechanism of peptide and ester hydrolysis catalyzed by papain have indicated that the hydrolysis is a two step process in which a bound substrate is converted into an intermediate thiolester (acylation) which is subsequently cleaved to regenerate the enzyme (deacylation) as in eqn. 1.

$$1.\quad \underset{G}{E\text{-}SH} + R\overset{O}{\overset{\|}{C}}X \underset{k_{-1}}{\overset{k_1}{\rightleftharpoons}} \underset{G}{ESH} : R\overset{O}{\overset{\|}{C}}X \xrightarrow[k_{-2}]{k_2} \underset{G}{ES\text{-}}\overset{O}{\overset{\|}{C}}R \xrightarrow[k_{-3}]{H_2O} \underset{G}{E\text{-}SH} + HO\overset{O}{\overset{\|}{C}}R$$

To ellucidate the mechanism and groups important for catalysis, Smith and Parker studied the pH-rate profile for α-N-benzoyl-L-arginine ethyl ester (BAEE).[13] They observed a bell-shaped pH profile for the acylation step (k_2 in eqn. 1) implying the involvement of two groups having a pKa of 8.2 and 4.3.[13] They assigned

Figure 1: The Active Site Region of Papain
Reproduced from reference 1.

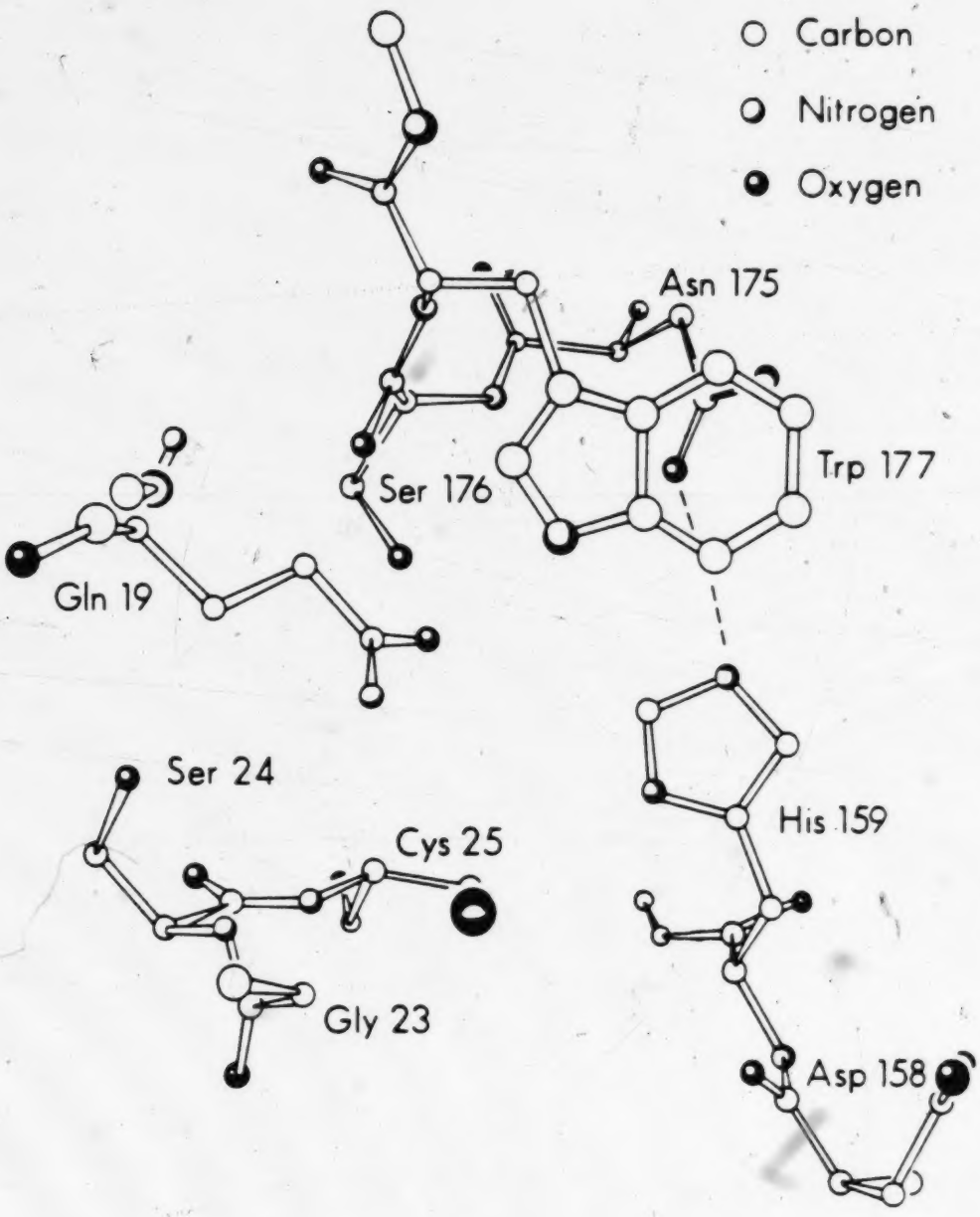

these pKa's to a cysteine SH and a carboxylate respectively.[13,14]

To study Smith and Parker's proposal, Bender used a simpler model system in which p-nitrophenylacetate (PNPA) was hydrolyzed by o-mercaptobenzoic acid (1) (eqn. 2).[15]

2. 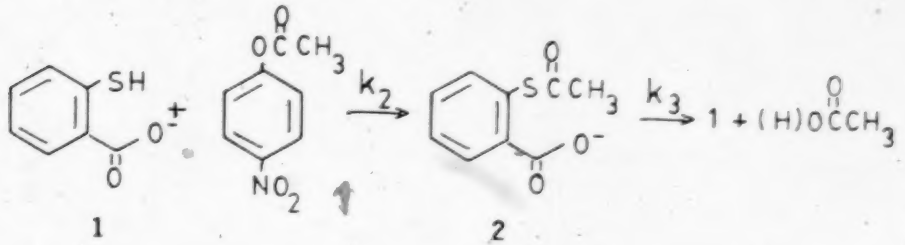

1 2

The thiolate anion of **1** was found to be an effective nucleophile toward PNPA (k_2 = 1 $M^{-1}sec^{-1}$ between pH 6-8) but the intermediate thioaspirin (**2**) hydrolyzed slowly (k_3 = (7 ± 3) x 10^{-6} sec^{-1}) suggesting that a carboxylate has weak catalytic power for thiol ester hydrolysis and will not account for the fast rate of acyl enzyme hydrolysis observed normally with papain (k_3 = 1-10 sec^{-1}). Furthermore, the X-ray structure[8] of papain shows that Asp 158 is 0.75 nm from the sulphur atom of Cys 25, whereas His 159 is only 0.34 nm from the sulphur atom suggesting that His 159 is more likely to be involved with Cys 25 than Asp 158.

That a thiolester acyl enzyme intermediate exists has been shown by spectrophotometric detection. Lowe and Williams[16] added papain to a solution of o-methylthiohippurate **3** and observed a strong absorption band at

313 nm indicating the presence of the dithioester **4**.

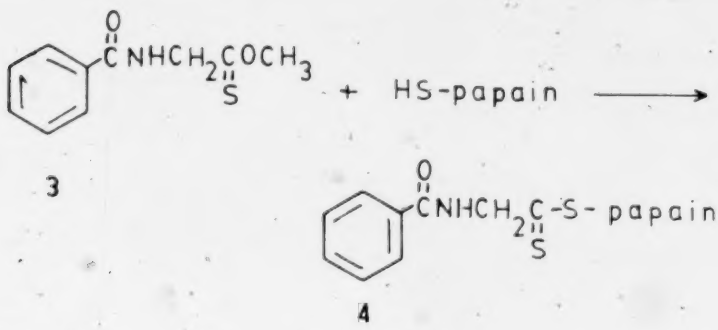

3.

3

4

A similar observation was made for bromelain indicating that it too ultilizes a cysteine SH as a nucleophile.[17] Storer, Murphey and Cary[16b] have verified the presence of the dithioester (**4**) from reaction 3 by Raman spectroscopy. Brubacker and Bender[18] also observed spectrophotometrically the acyl intermediate from trans-cinnamoylimidazole and papain.

Scott, et al.,[19] observed directly the production of a thioacyl intermediate prepared from papain and [^{13}C=O]-N-benzoylimidazole by adapting the techniques of cryoenzymology to a ^{13}C-NMR experiment. They observed the presence of ^{13}C=O at 196.0 ppm which slowly disappeared with $t_{1/2}$ > 30 minutes at -6 ^{o}C. More recently, Scott, et al.,[20] observed both diastereoisomers of the hemithioacetals formed by the complexation of papain and the inhibitory aldehyde N-acetylphenylalanylglycinal and differentiated between the isomers by NMR titration with 2,2'-dipyridyl disulfide at pH 7 and 4.

DEACYLATION

Deacylation of the thiol ester intermediate depends on a group with a pKa of 3.3 to 4.7 depending on the particular intermediate being studied.[18,21] A solvent kinetic isotope effect of 2.75 for α-N-benzyl-L-argininyl papain,[21a] 2.7 for benzoyl papain[21b] and 3.35 for trans-cinnamoyl papain[18a,b] has been observed for the deacylation step. This indicates that a general base mechanism may be occurring.

The rate constants for deacylation of substituted benzoyl papains show a ρ value of 2.74 ± 0.32 indicative of rate-limiting nucleophilic attack at the benzoyl carbon.[21b] Hubbard and Kirsch[22] have found that reactions of anionic nucleophiles with substituted benzoyl esters have ρ values > 2, while those for neutral nucleophiles have ρ values < 1.4. Kirsch believes that the large value for benzoyl papain suggests that the carboxylate anion of Asp 158 acts as a general base in controlling deacylation. However, Kirsch's conclusions may be incorrect as they are based on ρ values derived from O-esters, while it is known that a S-ester is formed in papain.

Other evidence[13,21a] has been given that a carboxylate (perhaps Asp 158) is associated with the deacylation stepbased on the low pKa of 4.5 and a negligible heat of ionization.[3] However, Lowe[23] found that the

apparent pKa for deacylation of cinnamoyl papain was reduced from 4.65 in water to 4.15 in 20% aqueous dioxane. This finding supports ionization leading from a charged to a neutral species ($H^+IM \rightarrow IM$) and argues against that from a neutral to a charged species ($COOH \rightarrow COO^-$). This solvent effect implies the involvement of an imidazole group (His 159) over that of a carboxylate group.

More recently, Lewis, et al.,[24a] have shown by ^1H-NMR titrations, potentiometric titrations and fluorescence studies that the pKa of His 159 is decreased from 8 to 4.3 when the thiol group is blocked in the form of papain-S-SCH_3. This suggests that His 159 is the group formally responsible for the low pKa of 4 in the deacylation step.

CATALYTIC SITE: STRUCTURE AND MECHANISM

A. Structure

Finkle and Smith[25] studied the reaction of papain with iodoacetamide as a means of labelling the reactive thiol. The enzyme was completely inhibited with the production of S-carbamoylmethylcysteine suggesting the importance of a thiol in the active site mechanism. The position of the active thiol was established by Light[9c] by converting papain to the mono-^{14}C-S-carboxymethyl derivative using ^{14}C-labelled iodoacetate. The radio-

active peptide was found to be in the sequence Gly-Ser-Cys-Trp identifying the reactive thiol group as cysteine 25.

Kinetic studies by Husain and Lowe[26] have suggested that histidine also plays an essential role in the active site. Husain and Lowe[26] alkylated both the Cys 25 and a second nucleophile in the active site with 1,3-dibromoacetone. Inhibition of the enzyme was observed. This reagent should be capable of alkylating a second nucleophile within a range of about 5 Å, coinciding with His 159 as shown in eqn. 4.

4.

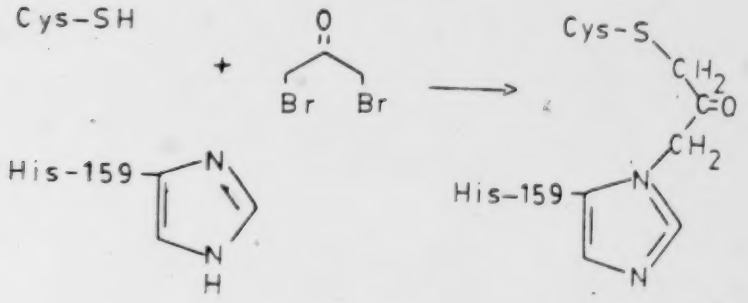

By alkylating with labelled 1,3-dibromo-(2-^{14}C)acetone, Husain and Lowe were able to confirm the site of alkylation as the N-1 of His 159.

It has been found that when Trp 177[27] or Asp 158[28] is blocked, papain loses its activity suggesting either that these groups are involved in catalysis or that such blockage alters the active site region.

The X-ray crystal structure by Drenth[8] confirmed these earlier findings substantiating that Cys 25, His

159 and Trp 177 do exist in the active site. However, it should be noted that because of the problem of air oxidation, papain has never been crystallized in its native form, but rather as an activatable or nonactivatable enzyme with the Cys 25 blocked as a disulfide (papain-S-SCH_3) or as a sulfinic acid respectively.[8d] In these forms, the enzyme has been found to be roughly ellipsoidal and can be divided into two parts each containing 100 residues. In the center of each half is a hydrophobic core.[24] The enzyme contains a large active site comprised of 40 residues. Both cysteine 25 and histidine 159 are found in the cleft. Glutamine 19 and tryptophan 177 are situated near cysteine 25, the latter residue forming the boundary of the cleft. Asparagine 175 is buried behind Trp 177 and forms a hydrogen bond with N-2 atom of His 159. At a distance of 7 A from the imidazole ring of His 159, aspartic acid 158 can be found.

B. Mechanisms

Common to all mechanistic theories is the presence of a thiolester intermediate and the involvement of Cys 25, His 159 and possibly Asp 158.

Reaction pathways such as that in eqn. 5 appear reasonable to describe the acylation of papain by a substrate, but the exact mechanism is still under contention.

5. 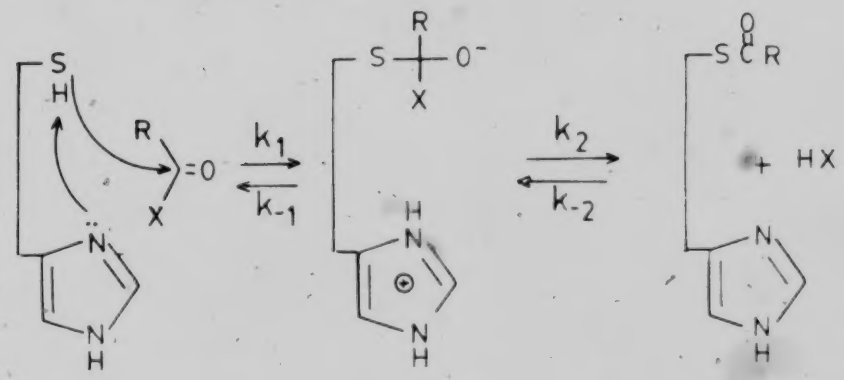

From the small solvent isotope effect observed for alkylation of papain at pH(pD) = 5.5, Polgar[29] concludes that no general base term is present for thiol alkylation. However, for acylation by amides or anilide substrates the situation is less clear. At neutrality, nucleophilic attack of the thiolate is not rate determining, but breakdown of the tetrahedral intermediate is ($k_1 > k_2$ in eqn. 5).[30] Nevertheless, thiols generally appear to react as their anions and require no general base assistance for acylation by esters.[31]

It was Polgar[32] who first suggested the possibility of the thiolate-imidazolium ion pair existing between the pH's of 4.2 and 8 with the thiolate acting as a powerful nucleophile towards a substrate. This was based on a UV absorption spectrum which he assigned to the thiolate anion at pH's less than 8. Although Polgar's interpretation of the UV spectrum has been ques-

tioned,[33] his hypothesis has been supported on the basis of other studies by Lewis, et al.[24a]

Lewis, et al.,[24a] studied the potentiometric titration difference between papain and papain-S-SCH_3 and contended that about 90% of the papain exists in its zwitterionic (thiolate-imidazolium) form between pH 4 and 8.

The existence of the thiolate-imidazolium ion pair as the attacking nucleophile is attractive as it does not require an unprecedented general base catalysis for thiol attack and also because it appears to provide a general acid for assisting the breakdown of the tetrahedral intermediate. It has been established by Jencks and Hupe[34] that the nucleophilic reactivity of thiolate anions towards esters will increase with the basicity of the anion and the efficiency of an acid catalyst will increase with its acidity. At neutral pH, a normal cysteine will predominately exist in the unreactive protonated form while an imidazole will exist in the less acidic protonated form. If the thiol and the imidazole can interact to form a thiolate-imidazolium ion pair, then the pKa of the thiol can decrease and the pKa of the imidazolium ion can increase. The basic thiolate anion can attack the carboxyl carbon atom of the substrate resulting in a decreased negative charge density on the thiolate. This decreased negative charge should cause a decrease in the pKa of the imidazolium cation of His 159 which in turn makes it a better

general acid to assist the leaving group departure from the tetrahedral intermediate if such is required. This would result in enhanced catalytic ability for the thiolate-imidazolium species over that which would be predicted on the basis of thiolate alone.[35]

Such a mechanism involving the thiolate-imidazolium ion pair as the active species at physiological pH for acylation of papain was also proposed by Angelides and Fink.[36]

They studied the reaction between papain and N-carbobenzoxy-L-lysine methyl ester at subzero temperatures in aqueous DMSO.[36a] Using the "cryoenzymology" approach they were able to slow the reaction for acylation and deacylation of papain with this ester and study the individual reaction steps.

Fink[36a] proposed the following reaction scheme (eqn. 6) to describe acylation and deacylation of an ester by papain.

$$6.\quad E + S \underset{k_{-1}}{\overset{k_1}{\rightleftharpoons}} ES_1 \underset{k_{-2}}{\overset{k_2}{\rightleftharpoons}} I_2 \underset{k_{-3}}{\overset{k_3}{\rightleftharpoons}} EA + P_1 \xrightarrow{k_4} E + P_2$$

The reaction occurs first with rapid substrate binding ($k_1 > 1$ sec^{-1} at -65 °C) to form an ES complex followed by a conformation change ($k_{obs} > 10^3$ sec^{-1} extrapolated to 25 °C) in which His 159 moves from H-bonding to the amide H of the side chain of Asn 175 to electrostatic interaction with Asp 158 (I_2). In this state (I_2), the

enzyme exists as a thiolate-imidazolium pair. Reaction 3 involves the formation of the acyl enzyme EA (k_3 = 10 sec^{-1} extrapolated to 25 ^{o}C). The final hydrolysis (reaction 4) of the acyl enzyme is the slowest, since the hydrolysis of acyl enzyme is the rate limiting step for this and other esters.[1]

Fink, et al.,[36b] also studied the acylation with an amide substrate, N-carboenzyoxy-L-lysine-p-nitroanilide. From their findings with this amide, they proposed a mechanism similar to the above with the amide substrate involving two forms of the unliganded active site called UP and DOWN. The schematic representation of this mechanism is given in Figure 2.

In this mechanism, papain exists in the UP conformation at pH values above 9 and below 4, corresponding to the crystallographically determined structure[8] in which the N-2 hydrogen of the imidazole of His 159 is H-bonded to the amide hydrogen of the side chain of Asn 175 (E in Figure 2). At pH values between 4 and 8, papain exists mainly as the DOWN conformer E' in which the imidazole is protonated and forms an ionic bond to the carboxylate side chain of Asp 158. Isomerization of E to E' is considered to involve rotation of the imidazole group of His 159 about its α-β axis by 79^{o} and about its β-γ plane by 35^{o} and repositioning of the carboxy side chain of Asp 158 by rotation of $C_{(\alpha)}$ - $C_{(\beta)}$ by 35^{o} and of $C_{(\beta)}$ - $C_{(\gamma)}$ by 68^{o}. (It is important

Figure 2: "Up and Down" Acylation Mechanism proposed by Angelides and Fink (ref. 36)

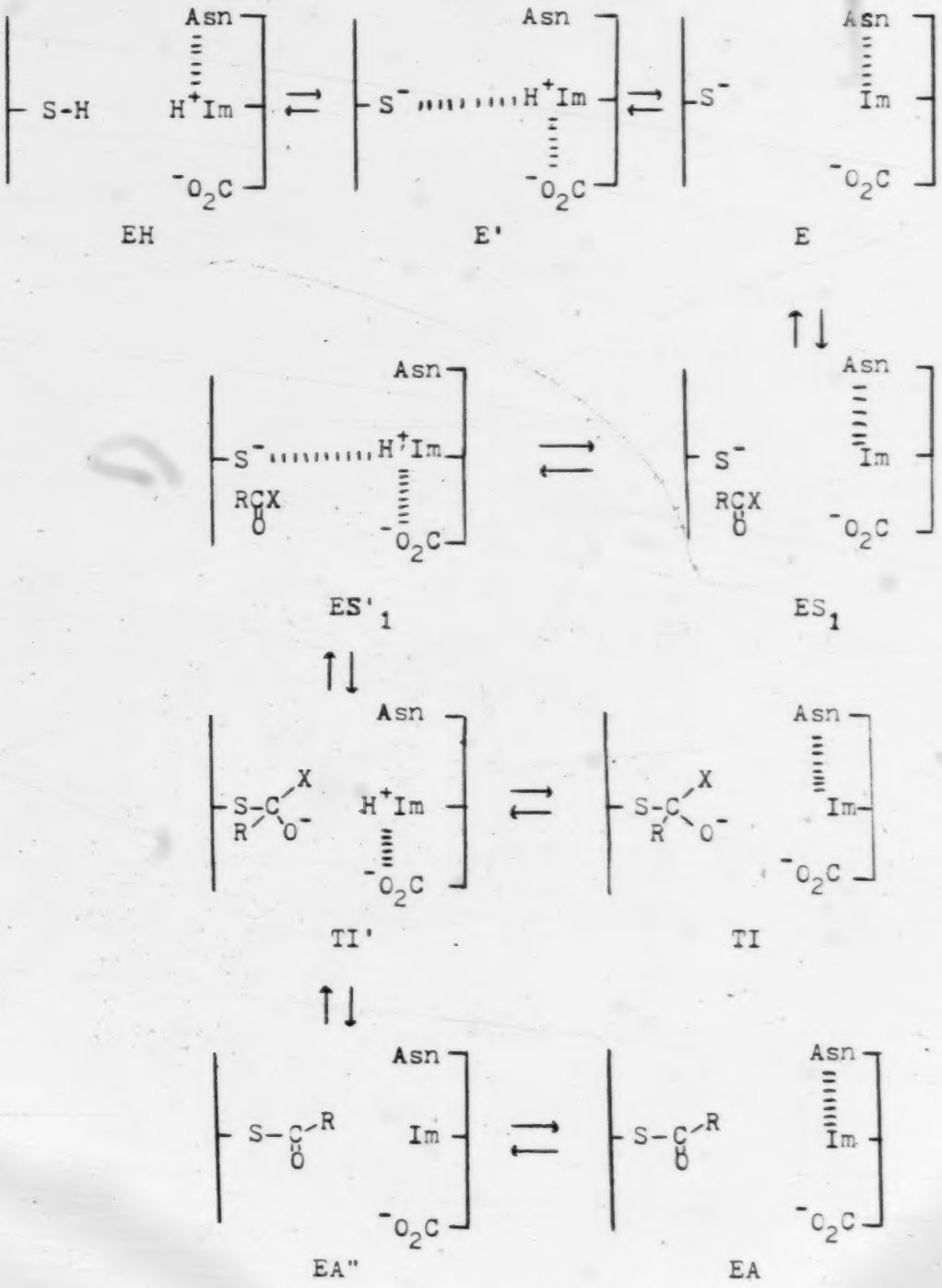

to note that the X-ray structure[8] was of the oxidized papain and was only resolved to 2.8 Å so that the degrees of rotation can only be considered as rough estimates at best.)

For the DOWN form the pKa of the thiol is 4 and the imidazole is 8; hence at neutral pH, the imidazolium-thiolate zwitterion can exist.

The catalytic reaction involves binding of the substrate to the UP conformation (E) to give the complex ES_1 followed by movement of His 159 to the DOWN position ES'. This quickly forms a tetrahedral intermediate by nucleophilic attack of the thiolate anion of Cys 25 on the peptide carbonyl carbon to give TI'. Collapse of the tetrahedral intermediate would give the acyl-enzyme, EA" which could isomerize rapidly to the UP form of the acyl-enzyme EA. In the DOWN position, the imidazolium ion is in an appropriate orientation to facilitate a proton transfer to the leaving group by the N-2 proton.

For deacylation, the first step would involve the imidazole in the EA (UP) form acting as a general base catalyst giving the tetrahedral intermediates TI and TI'. Collapse of the intermediate would involve the pathway given in eqn. 7.

7. $$TI \rightleftharpoons TI' \rightleftharpoons ES_1' \longrightarrow ES_1 \longrightarrow E \rightleftharpoons E'$$

The UP-DOWN transition mechanism of Fink's requires the presence of a carboxyl group in the active

site as well as the thiol and imidazole groups. Several studies by Brocklehurst, et al.,[37] have supported the possibility of a carboxyl group from Asp 158 participating in the mechanism for papain. In his study with certain reactivity probes in acidic media, he found that the reactivity of papain's thiol group was controlled by two groups each having pKa values approximately 4. One pKa of 4 was suggested to be associated with the ionization of the carboxyl group of aspartic acid 158 while the other pKa of 4 was due to the ionization of the imidazole group of His 159. It is worth noting that this additional pKa due to the carboxyl group has not been found in similar proteinases of ficin and actinidin.

Lewis, et al.,[24a,38] also found three ionizations with pKa's of 3.2, 3.9 and 8.4 at 25 ^{o}C for the pH-rate profile of papain-catalyzed hydrolysis of N-α-benzoyl-L-arginine p-nitroanilide. These were assigned to Cys 25 (pK = 3.2), Asp 158 (pK = 3.9) and His 159 (pK = 8.4).

MODEL STUDIES FOR ACYLATION

Model studies have been undertaken to try and mimic the proposed mechanism of papain with esters and amides.

Thiol Catalysis of Ester Hydrolysis

Only four groups have tried to provide some evidence for the cooperativity between thiol and imidazole in small molecules. Schneider[39] studied the hydrolysis

of p-nitrophenylacetate catalyzed by **5** n = 1,2, **6** and **7** by observing the appearance of p-nitrophenolate anion at 400 nm between pH 6.5 and 9.5.

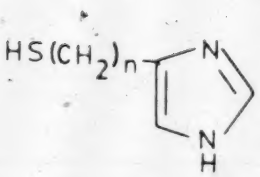

5 n=1,2

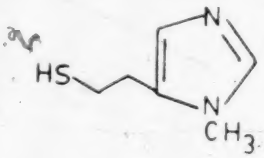

6

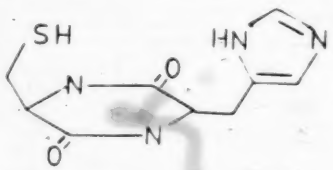

7

He observed rates at pH's below 7 that were faster than could be accounted for simply on the basis of thiolate attack alone.

Schneider interpreted these observations in terms of a mechanism whereby the imidazole either acts as a general base (eqn. 8) or as a pre-rate-determining H-abstractor to create a catalytically competent zwitterion (eqn. 9).

8.

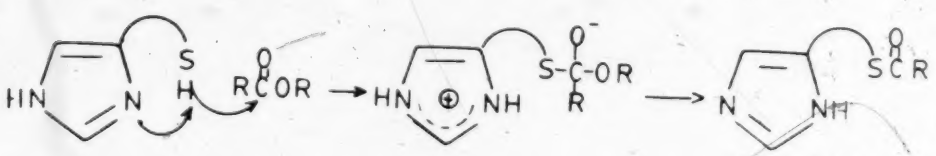

9. 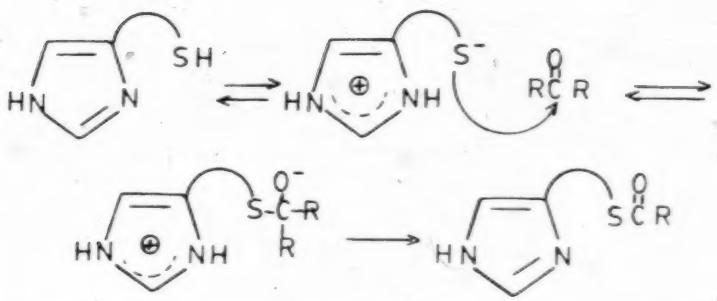

Schneider did not investigate isotope effects which in principle would have distinquished between 8 and 9 since 8 should show a primary kinetic isotope effect but not 9. (In practice, the solvent isotope effect would be more difficult to interpret since the equilibrium distribution of zwitterion form in 9 would be altered by the solvent change.[40])

Schneider also failed to compare his results with the catalysis afforded by imidazole alone toward the hydrolysis of PNPA and did not study the full pH range from 5 to 11 for acylation or deacylation of his compounds.

Lochon[41] investigated the reaction of 2-alkylthiolbenzimidazoles (**8**) with PNPA and found results similar to those reported by Schneider.

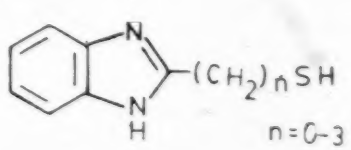

8

Lochon interpreted the excess catalytic activity over

that which can be accounted for on the basis of [RS^-] alone, to a general base mechanism akin to that given in eqn. 8. However, no solvent isotope effects were investigated, and the involvement of a zwitterion was given no consideration. Furthermore, Lochon did not report his experimental conditions or control experiments, which makes evaluation of the data very difficult. Also, he based his findings on only three pH experimental points and did not obtain the full pH rate profile which would have better substantiated his conclusions.

Overberger, et al.,[42] investigated the possible cooperativity between imidazole and thiol in copolymers of vinylimidazole and vinyl thiol. Catalytic rate constants observed were first order in copolymer and PNPA, but showed only additive rather than cooperative effects of the imidazole and thiol.

Klotz, et al.,[43] reacted a series of peptides having various arrangements of cysteine and histidine residues with substituted phenyl acetates. They observed no cooperative effect of a histidine group for the acylation of the cysteine residue.

It should be noted that all the above authors used the term "catalyst" incorrectly to described their model compounds. These compounds were not true catalysts as they did not "turn over" during the reaction with PNPA.

Thiol Catalysis of Amide Hydrolysis

Papain catalyzes the hydrolysis of both ester and amides (peptides) with roughly the same k_{cat} values.[1] However, for amide hydrolysis, formation of the acyl intermediate is rate limiting[1,29] while deacylation of the acyl intermediate is rate limiting for ester hydrolysis. On the basis of cryoenzymology data for the acylation of papain by an amide, Fink[36] has favored the imidazolium-thiolate anion as the active catalyst for amide hydrolysis.

A model study by Schneider and Wenck[39a] using the thiol imidazole (**9**) reacting with maleimide (**10**) to give the adduct (**11**), failed to show any cooperativity between the thiol and imidazole. (However, this model system does not pertain to hydrolysis of an amide.)

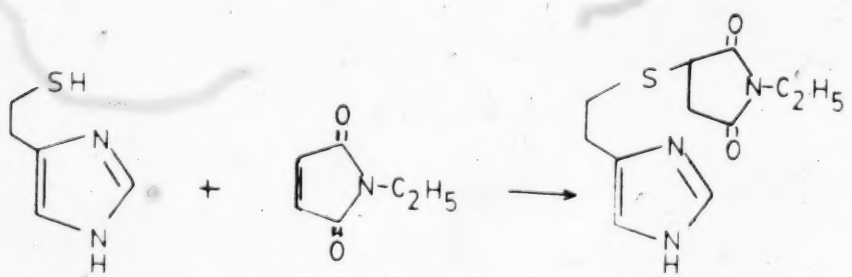

9 10 11

Fersht[31d] was able to show that a closely positioned thiolate imidazolium ion pair could catalyze the formation of a thiolester from an amide based on data for the attack of CF_3CH_2SH on a variety of amides.

McDonald, et al.,[44] have demonstrated the nucleo-

philic character of a thiol towards acylation by an amide using N-propyl-2-mercaptomethyl-benzamide (**12**). The hydrolysis of this thiol amide compound was found to proceed by rapid intramolecular nucleophilic attack by the thiol to displace propylamine and form a thiol-lactone as in eqn. 10. The hydrolysis of this thiol-lactone was very slow suggesting that a more reactive nucleophile than water was required.

10. 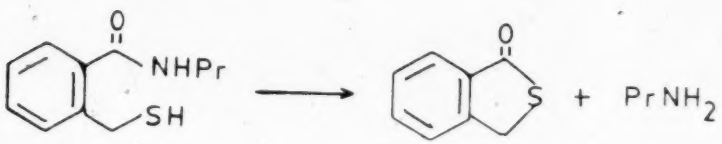

SUMMARY

The mechanism of acylation and deacylation of esters and amides (peptides) by papain has yet to be fully determined. The acylation step has been most extensively investigated and several theories have been proposed. Currently, the imidazolium-thiolate anion as the catalytically active species at physiological pH appears to be the most viable answer to the high reactivity of a thiol in papain towards substrates.[24] Co-operativity between His 159 and Cys 25 has been shown[24,37,38] with the possibility of cooperativity also existing between Asp 158 and His 159.[37]

All previous models incorporating both imidazole and thiol units studied as nucleophilic catalysts towards the hydrolysis of PNPA have failed to demonstrate any significant kinetic involvement of zwitterions. No previous models have shown a significant cooperative effect in the catalysis of hydrolytic processes at physiological pH as is thought to occur in cysteine proteinases.

The following report will describe the synthesis of three imidazole-thiol models **15a**, **16a** and **17a** as well as kinetic studies of their reactivity with p-nitrophenylacetate.

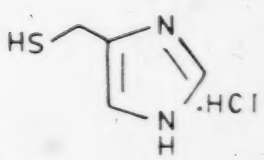

15a

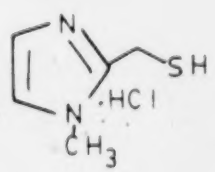

16a

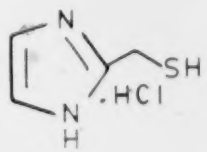

17a

These models along with a model recently synthesized by J.P. Street[45] are believed to be the first models that do show cooperativity between imidazole and thiol by existing primarily as zwitterions at physiological pH. Furthermore, these models show that the zwitterions are nucleophilic towards PNPA.

II. RESULTS AND DISCUSSION

INTRODUCTION TO RESEARCH

Several authors[24] have proposed that in the active site of papain, Cys 25 and His 159 exist as an imidazolium-thiolate anion pair at physiological pH and that it is in this form that papain is catalytically active. However, no model incorporating a thiol and imidazole unit has been able to show conclusively any cooperativity between these groups at neutral pH.

Therefore, it was necessary to show that an imidazole adjacent to a sulfhydryl group could be kinetically beneficial in promoting thiol attack on an ester (PNPA), and that by altering the ΔpKa between the imidazolium and sulfhydryl units, one could change the nucleophilic reactivity of the model. A summary of the approach is given below.

Compounds **15a**, **16a** and **17a** are believed to fit the above requirements for a model system. These compounds have an imidazole unit close to a thiol. The pKa of the imidazole can be altered by either methylating the N-1 nitrogen (the pKa increases by +0.34 units in methylating the N-1 nitrogen on imidazole)[46d] and/or changing the position of the methylthiol group on the imidazole ring. (Repositioning the methylthiol group from the 4(5) to 2-position is anticipated to inductively increase the imidazole's pKa.)[46d]

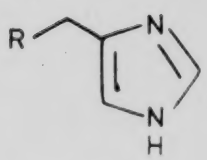

15a R = SH
15b R = H

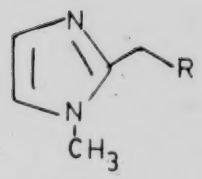

16a R = SH
16b R = H

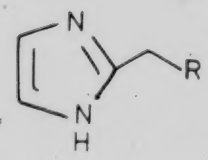

17a R = SH
17b R = H

For these model compounds, there are four species (controlled by four microscopic pKa values) that exist in solution as shown in eqn. 11.

11.

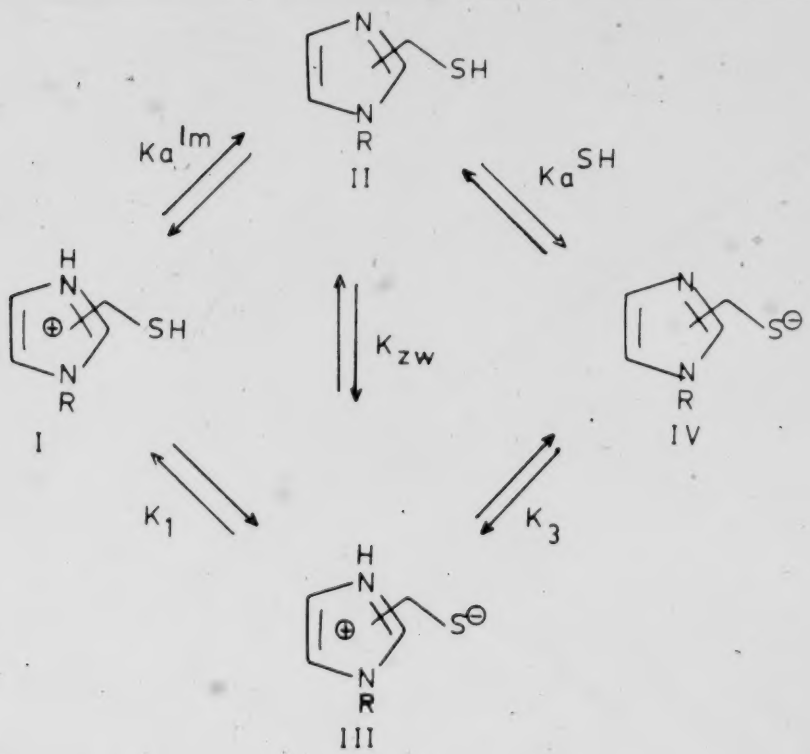

Since the nucleophilic activity of a thiol is pro-

portional to the thiolate anion concentration,[15,31,46a] then from eqn. 11, one can see that there are two possible thiolate anions, III and IV each undoubtedly capable of being an effective nucleophile toward PNPA.

By altering the pKa of the imidazole, the ΔpKa for ionization of the imidazole (pKa^{Im}) and the thiol (pKa^{SH}) from the neutral form (IMSH) (where $\Delta pKa = pKa^{SH} - pKa^{Im}$) can be reduced. Calculations (vide infra) suggest that if the $\Delta pKa < 2$ units, substantial amounts of zwitterionic material having a nucleophilic thiolate anion will be available at neutral pH.

Comparison of the pH versus rate profiles of the imidazole-thiol models **15a**, **16a** and **17a** with their respective methyl imidazole compounds **15b**, **16b** and **17b** would determine if any difference in rate of appearance of p-nitrophenoxide was due to the presence of the thiol group.

Potentiometric or UV-visible spectra titrations of the model compounds and their thiol protected compounds in principle allows the determination of the microscopic pKa's (as given in eqn. 11) for **15a**, **16a** and **17a**. From the microscopic pKa's, it is possible to determine the concentration of each species (I, II, III, and IV) over the pH range 3 to 11 and determine which of the species is responsible for any enhanced nucleophilic attack on PNPA at physiological pH.

SYNTHESIS

Compounds **15a-17a** were synthesized based on the procedure of F. Schneider.[39] Modifications in the workup procedures resulted in overall higher yields than were reported in the literature.[39] Once the hydroxymethylimidazoles were prepared, the synthetic scheme for the preparation of **15a**, **16a**, and **17a** was the same, as shown in Scheme 1.

The 4(5)-hydroxymethylimidazole compound (**21**), was prepared according to the procedure of Schunack.[47] Formamidine acetate (**18**) and 1,3-dihydroxyacetone were reacted with liquid ammonia at 50 °C. The resulting crude oil (**19**) was immediately converted to the picrate (**20**) giving an increased yield of 60% from the reported[47] 40%. The picrate salt was then converted to the hydrochloride salt (**21**) according to the procedure of Totter and Darby.[48] (eqn. 12).

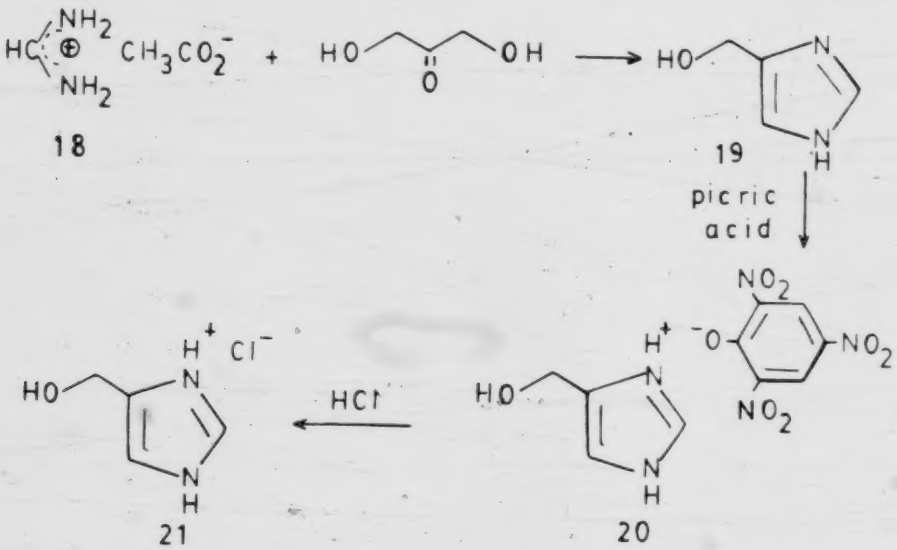

12.

Scheme 1: Synthetic scheme for the preparation of 15a, 16a and 17a.

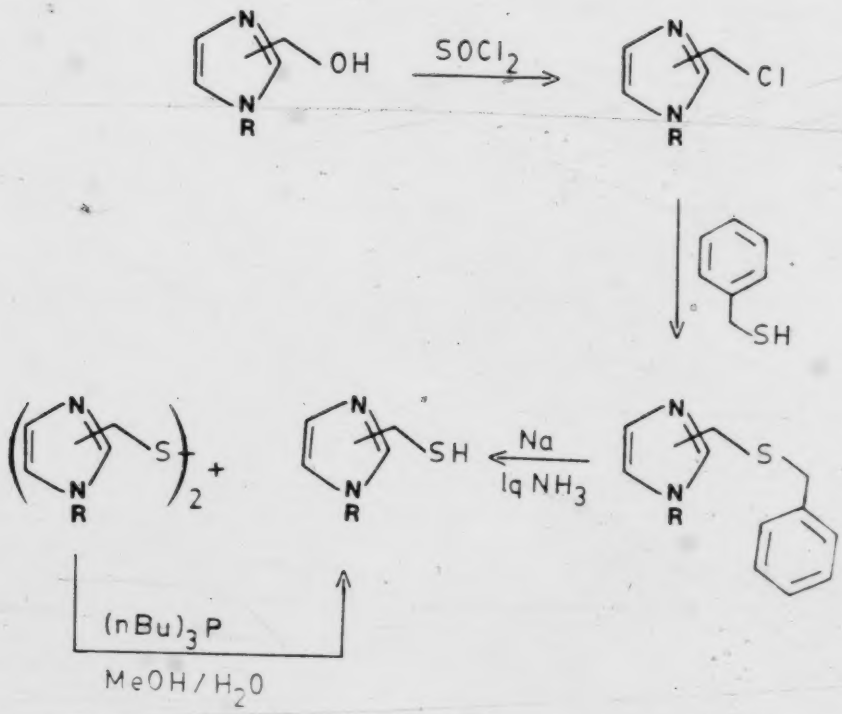

Formation of N-methyl-2-hydroxymethylimidazole, (**23**) was attempted by reacting the corresponding 2-lithioimidazole (**22**) with formaldehyde gas[49] as given in eqn. 13.

13.

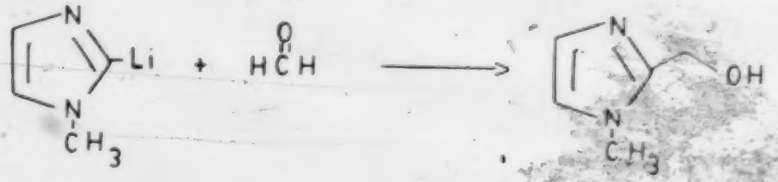

22 **23**

No reaction occurred due mainly to the difficulty of introducing the formaldehyde gas into the system by thermal decomposition of paraformaldehyde.

The method was repeated using dimethylformamide in replace of formaldehyde as in eqn. 14. This resulted in formation of the N-methyl-imidazole-2-carboxaldehyde (**24**) in 83% yield.

14.

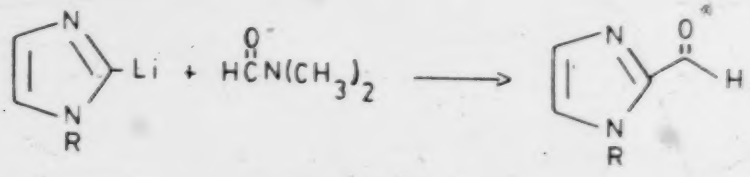

22 R = CH_3 **24** R = CH_3

25 R = $CH(OEt)_2$ **26** R = H

For the formation of the 1-H-imidazole-2-carboxaldehyde, the N-1 position was protected using a diethoxylmethyl function (R = $CH(OEt)_2$)[50a], (**25**) and the route given in eqn. 14 was followed. This protecting

group is readily hydrolyzed under neutral or mildly acidic conditions[50b] unlike other protecting groups which require strong acid conditions.[51] A yield of 76% was obtained for 1-H-imidazole-2-carboxaldehyde (**26**) using this protecting group.

Subsequent reduction of the carboxaldehydes (**24**) and (**26**) with $NaBH_4$ yielded the 2-hydroxymethylimidazoles (**27**) and (**28**,) respectively, as in eqn. 15.[52]

15.

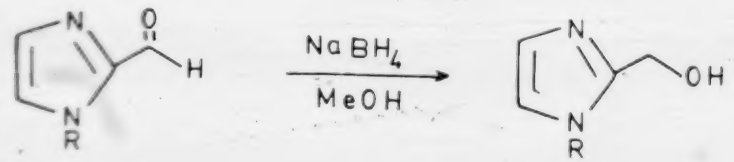

22 R = CH_3 **27** R = CH_3

26 R = H **28** R = H

The chloromethylimidazoles (**29-31**) were prepared in >90% yield from the alcohols using freshly distilled thionyl chloride (eqn. 16).[53]

16.

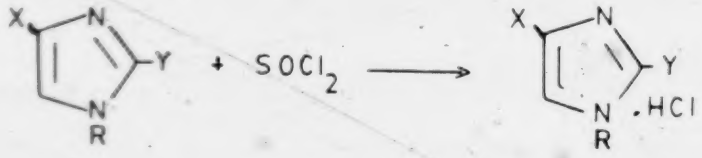

23 R=H; Y=H; X=CH_2OH **29** R=H; Y=H; X=CH_2Cl

27 R=CH_3; Y=CH_2OH; X=H **30** R=CH_3; Y=CH_2Cl; X=H

28 R=H; Y=CH_2OH; X=H **31** R=H; Y=CH_2Cl; X=H

Direct substitution of the chlorides by NaSH gave a low yield of <10% of the mercaptomethyl product, along

with 90% recovered starting material. The more nucleophilic benzyl mercaptan gave the S-benzylmercaptomethylimidazoles (**32-34**) in quantitative yields[53c] (eqn. 17).

17. 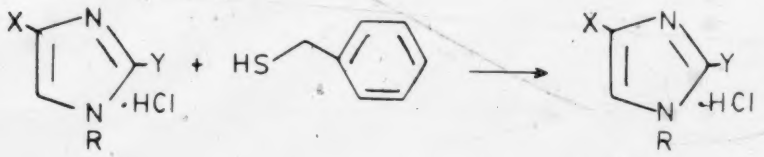

29 R=H; Y=H; X=CH_2Cl

30 R=CH_3; Y=CH_2Cl; X=H

31 R=H; Y=CH_2Cl; X=H

32 R=H; Y=H; X=$CH_2SCH_2C_6H_5$

33 R=CH_3; Y=$CH_2SCH_2C_6H_5$ X=H

34 R=H; Y=$CH_2SCH_2C_6H_5$ X=H

Reduction of the S-benzylmethylimidazoles with sodium metal in liquid ammonia gave the final mercaptan products (**15a, 16a, 17a**) in ~60% yield as shown in eqn. 18.[39d] To reduce the possibility of oxidation of the thiols to their respective disulfides, the reaction mixtures were acidified with 20% ethanolic HCl and not 10% aqueous HCl as given in the literature.[39d] This allowed a faster evaporation of the solvent and resulted in less disulfide formation. Any disulfide that was formed however, could be quickly reduced to the mercaptan using tributylphosphine as shown in eqn. 19.[54]

18. 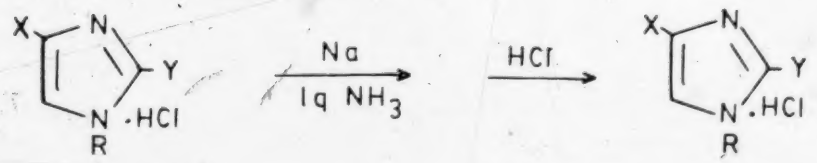

32 R=H; Y=H; X=$CH_2SCH_2C_6H_5$

33 R=CH_3; Y=$CH_2SCH_2C_6H_5$; X=H

34 R=H; Y=$CH_2SCH_2C_6H_5$; X=H

15a R=H; Y=H; X=CH_2SH

16a R=CH_3; X=H; Y=CH_2SH

17a R=H; X=H; Y=CH_2SH

19. 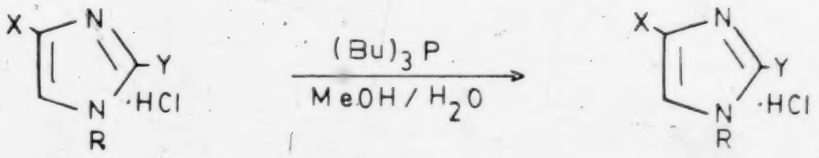

15c R=H; Y=H; X=$CH_2S_2C_4H_5N_2$

16c R=CH_3; Y=$CH_2S_2C_5H_8N_2$; X=H

17c R=H; Y=$CH_2S_2C_4H_5N_2$; X=H

15a R=H; Y=H; X=CH_2SH

16a R=CH_3; X=H; Y=CH_2SH

17a R=H; X=H; Y=CH_2SH

RESULTS

(A) Catalytic Studies

Acylation Rates of **15a-17a** by PNPA

The acylation rates were followed spectrophotometrically using a Cary 210 UV-VIS spectrophotometer interfaced to a computer for data collection. The rate of acylation of **15a,b**, **16a,b**, and **17a,b** by p-nitrophenylacetate was followed by observing the rate of appear-

ance of p-nitrophenoxide at 400 nm.

All buffers were oxygen-acid type and were prepared to 0.1 M, μ = 0.3 M (KCl) in triply distilled water.

Reactions were initiated by injecting 5 ul of a stock solution of 2.6×10^{-2} M p-nitrophenylacetate in ethanol into 3 ml of deoxygenated (argon) buffer in a 1-cm quartz cell thermostated at 37.5 ^{o}C followed by an injection of a 10 to 100 fold excess of the thiol (as its HCl salt) or the imidazole. All experiments were followed to completion and the observed pseudo-first-order rate constants were obtained by fitting the absorbance versus time data to a standard exponetial equation via a non-linear least squares program.[65] (See Appendix 1.)

The rate equation for the attack on p-nitrophenylacetate (PNPA) by a nucleophilic species is given in eqn. 20.

$$20.\quad \text{Rate} = \left(k_{H^+}[H^+] + k_{OH^-}[OH^-] + k_{H_2O}[H_2O] + k_{buff}[Buff] + k_{cat}[Cat]\right)[PNPA]$$

where [Buff] is the buffer concentration and [Cat] is the concentration of the compounds **15a,b-17a,b.**

The rate equation reduces to:

$$21.\quad \text{Rate} = \left(k' + k_{cat}[Cat]\right)[PNPA]$$

where $k' = k_{H^+}[H^+] + k_{OH^-}[OH^-] + k_{H_2O}[H_2O] + k_{buff}[Buff]$ and corresponds to the observed pseudo-first-order rate

constant at zero catalyst concentration.

The second order rate constant k_{cat} was obtained from the slope of the linear least squares treatment of the data for k_{obs} versus [added thiol] at each pH according to eqn. 22.

22. $k_{obs} = k' + k_{cat}[\text{added thiol}]$

The results from the reaction of PNPA with 4(5)-mercaptomethylimidazole (**15a**), N-methyl-2-mercaptomethylimidazole (**16a**), and 2-mercaptomethylimidazole (**17a**) as their HCl salts along with their respective imidazoles **15b**, **16b**, and **17b** are given in Tables 1, 2, 3, 4, 5 and 6, respectively. The second order rate constants (k_{cat}) versus pH profiles for the reaction of PNPA with these compounds are shown in Figure 3.

No buffer catalysis was observed for any of the compounds. D_2O solvent kinetic isotope effects were evaluated at pD = 10.0 in 0.1 M potassium carbonate D_2O. No significant deuterium isotope effect was observed.

The simplest reaction scheme involving zwitterions that can be postulated to explain the pH rate profiles for thiol-imidazole attack on PNPA is shown in Figure 4. Bender and Turnquist[55] have found that imidazole-catalyzed hydrolysis of PNPA is first order in imidazole and independent of imidazolium ion concentration. Thus the imidazolium ion does not appear to be catalytically active towards PNPA. For this reason, the imidazolium-

Table 1. Second Order Rate Data for the reaction of PNPA with 4-Methylmercaptoimidazole hydrochloride, **17a**.[a]

Buffer[b]	pH[c]	k_{cat}[d] ($M^{-1}min^{-1}$)	log k_{cat}
0.1 M Acetate	5.20	1.91	0.28
0.1 M Succinate	5.80	7.02	0.85
"	6.40	21.8	1.34
"	6.60	26.3	1.42
0.1 M Phosphate	6.80	35.4	1.54
"	7.14	51.7	1.71
"	7.40	63.6	1.80
"	7.60	73.8	1.87
"	7.80	94.8	1.98
0.1 M Borate	8.00	112	2.04
"	8.40	239	2.37
"	8.80	419	2.62
"	9.20	681	2.83
"	9.50	1163	3.06
"	9.80	1304	3.12
"	10.0	1820	3.26
"	10.2	1847	3.27
	10.4	1859	3.27
	10.6	2301	3.36
	11.0	2087	3.32
0.05 M Borate[e]	9.00	561	2.75
0.10 M Borate[e]	9.00	560	2.75
0.1 M Carbonate[f]	10.0	1500	3.18

a. Reaction conducted at 37±0.3 °C. $[PNPA]_0 = 4 \times 10^{-5}$ M.

b. Buffers were made in triply-distilled water to μ = 0.3 M and were degassed in argon prior to use.

c. pH was measured before and after reaction and did not deviate by more than 0.03 pH units.

d. Calculated by linear least squares treatment of the slope of the plots of k_{obs} versus [added thiol]. Std. deviation was < 1 % for computer fit of k_{cat}.

e. Test for Buffer catalysis. None was found.

f. Values obtained in D_2O Buffer at μ = 0.3 M.

pD = pH(meter reading) + 0.4 units.[45]

Table 2. Second Order Rate Data for the reaction of PNPA by N-Methyl-2-methylmercaptoimidazole hydrochloride, **16a**.[a]

Buffer[b]	pH[c]	k_{cat} ($M^{-1}min^{-1}$)	log k_{cat}
0.1 M Succinate	5.50	16.1	1.21
"	6.00	28.9	1.46
"	6.25	53.9	1.73
"	6.50	60.6	1.78
0.1 M Phosphate	6.68	80.4	1.90
"	6.82	111	2.04
"	7.12	121	2.09
"	7.40	121	2.08
"	7.70	167	2.22
0.1 M Borate	8.00	185	2.26
"	8.24	209	2.32
"	8.44	309	2.49
"	8.86	452	2.65
"	9.00	512	2.71
"	9.16	577	2.76
"	9.50	777	2.89
0.1 M Carbonate	9.86	791	2.90
"	10.27	918	2.96
"	10.37	847	2.93
0.05 M Borate[e]	7.80	146	2.16
0.30 M Borate[e]	7.80	146	2.16
0.1 M Carbonate[f]	10.10	794	2.90

a. Reaction conducted at 37±0.3 °C. $[PNPA]_o = 4 \times 10^{-5}$ M.

b. Buffers were made in triply-distilled water to μ = 0.3 M and were degassed under argon prior to use.

c. pH was measured before and after reaction and did not deviate by more than 0.03 pH units.

d. Calculated by linear least squares treatment of the slope of the plots of k_{obs} versus [added thiol]. Std. deviation was < 1% for computer fit of k_{cat}.

e. Test for buffer catalysis. None was found.

f. Values obtained in D_2O Buffer at $\mu = 0.3$ M.

pD = pH(meter reading) + 0.4 units[45]

Table 3. Second Order Rate Data for the reaction of PNPA by 2-Mercaptomethylimidazole hydrochloride, **17a**.[a]

Buffer[b]	pH[c]	k_{cat}[d] ($M^{-1}min^{-1}$)	log k_{cat}
0.1 M Acetate	5.30	12.5	1.10
0.1 M Succinate	5.60	15.4	1.19
"	6.00	30.5	1.48
"	6.25	37.5	1.57
0.1 M Phosphate	6.60	69.6	1.84
"	6.85	87.6	1.94
"	7.10	119	2.07
"	7.26	162	2.21
"	7.70	207	2.32
0.1 M Borate	8.20	277	2.44
"	8.40	406	2.61
"	8.86	605	2.78
"	9.20	733	2.87
"	9.55	911	2.96
"	9.75	1145	3.06
"	10.10	1106	3.04
"	10.36	1042	3.02
0.05 M Borate[e]	7.75	170	2.23
0.30 M Borate[e]	7.90	239	2.37
0.1 M Carbonate[f]	10.00	1059	3.02

a. Reaction conducted at 37±0.3 °C. $[PNPA]_0 = 4 \times 10^{-5}$ M

b. Buffers were made in triply-distilled water to μ = 0.3 M and were degassed under argon prior to use.

c. pH was measured before and after reaction and did not deviate by more than 0.03 pH units.

d. Calculated by linear least squares treatment of the slope of the plots of k_{obs} versus [added thiol]. Std. deviation was < 1 % for computer fit of k_{cat}.

e. After adjusting for pH differences and errors in k_{cat}, buffer catalysis was believed to be negligable.

f, Values obtained in D_2O Buffer at $\mu = 0.3$ M.

pD = pH(meter reading) + 0.4 units[45]

Table 4. Second Order Rate Data for the reaction of PNPA with 4(5)-Methylimidazole, **15b**[a]

Buffer[b]	pH[c]	k_{cat}[d] ($M^{-1}min^{-1}$)	log k_{cat}
0.1 M Succinate	5.20	0.81	-0.09
"	5.65	1.51	0.18
"	6.25	4.00	0.60
"	6.60	8.60	0.93
0.1 M Phosphate	6.95	14.0	1.15
"	7.20	27.1	1.43
"	7.52	43.0	1.63
"	7.65	49.0	1.69
"	7.80	61.5	1.79
0.1 M Borate	8.00	63.0	1.80
"	8.40	75.0	1.88
"	9.00	82.5	1.92
"	9.60	99.0	1.99
"	10.00	100	2.00
0.1 M Carbonate	10.60	105	2.02
"	11.00	102	2.01
0.1 M Carbonate[e]	10.0	79.4	1.90

a. Reaction conducted at 37±0.3 °C. $[PNPA]_0 = 4 \times 10^{-5}$M.

b. Buffers were made in triply-distilled water to μ = 0.3 M.

c. pH was measured before and after reaction and did not deviate by more than 0.03 pH units.

d. Calculated by linear least squares treatment of the slope of the plots of k_{obs} versus [added thiol]. Std. deviation was < 1 % for computer fit of k_{cat}.

e. Values were obtained in D_2O Buffer at μ = 0.3 M. pD = pH(meter reading) + 0.4[45]

Table 5. Second Order Rate Data for the reaction of PNPA by 1,2-Dimethylimidazole, **16b**[a]

Buffer[b]	pH[c]	k_{cat}[d] ($M^{-1}min^{-1}$)	log k_{cat}
0.1 M Phosphate	6.57	0.34	-0.47
"	7.47	2.10	0.32
"	7.77	3.30	0.52
0.1 M Borate	8.00	3.89	0.59
"	8.42	5.58	0.75
"	8.87	6.70	0.82
"	9.30	7.50	0.88
"	9.42	7.36	0.87
0.1 M Carbonate	10.00	7.80	0.89
0.1 M Carbonate[e]	10.10	7.08	0.85

a. Reactions were conducted at 37.5 ± 0.3 °C. $[PNPA]_0 = 4 \times 10^{-5}$ M.

b. Buffers were made in triply-distilled water to μ = 0.3 M.

c. pH was measured before and after reaction and did not deviate by more than 0.03 pH units.

d. Calculated by linear least squares treatment of the slope of the plots of the k_{obs} versus [added thiol]. Std. deviation was < 1 % for computer fit of k_{cat}.

e. Values were obtained in D_2O Buffer at μ = 0.3 M. pD = pH(meter reading) + 0.4 units[45].

Table 6. Second Order Rate Data for the reaction of PNPA by 2-Methylimidazole, **17b**.[a]

Buffer[b]	pH[c]	k_{cat}[c] ($M^{-1}min^{-1}$)	log k_{cat}
0.1 M Phosphate	6.75	1.26	0.10
"	7.07	2.61	0.42
"	7.37	4.41	0.62
"	7.70	6.54	0.82
0.1 M Borate	8.15	9.54	0.98
"	8.10	9.00	0.95
"	8.50	10.8	1.03
"	8.75	11.7	1.07
"	8.85	12.7	1.10
"	9.00	12.8	1.11
"	9.40	13.4	1.13
0.1 M Carbonate	10.10	15.6	1.19
0.1 M Carbonate[e]	10.00	12.6	1.10

a. Reactions were conducted at 37.5 ± 0.3 °C. $[PNPA]_0 = 4 \times 10^{-5}$ M.

b. Buffers were made with triply-distilled water to μ = 0.3 M.

c. pH was measured before and after reaction and did not deviate by more than 0.03 pH units.

d. Calculated by linear least squares treatment of the slope of the plots of k_{obs} versus [added thiol]. Std. deviation was < 1 % for computer fit of k_{cat}.

e. Values obtained in D_2O Buffer at μ = 0.3 M. pD = pH(meter reading) + 0.4 units[45].

Figure 3: Plot of the second order rate constant (k_{cat}) versus pH for nucleophilic attack by 15a-17a on p-nitrophenylacetate at 37 °C in aqueous buffer solutions. 4(5)-mercaptomethylimidazole hydrochloride (15a) △ ; N-methyl-2-mercapto-methylimidazole hydrochloride (16a) ▽ ; 2-mercaptomethylimidazole hydrochloride (17a) ○ ; 4(5)-methylimidazole (15b) ● ; 1,2-dimethyl-imidazole (16b) ◇ ; 2-methylimidazole (17b) X ; Symbols in squares at pD (pH) = 10 and 10.1 are the values obtained in D_2O potassium cartonate buffer.

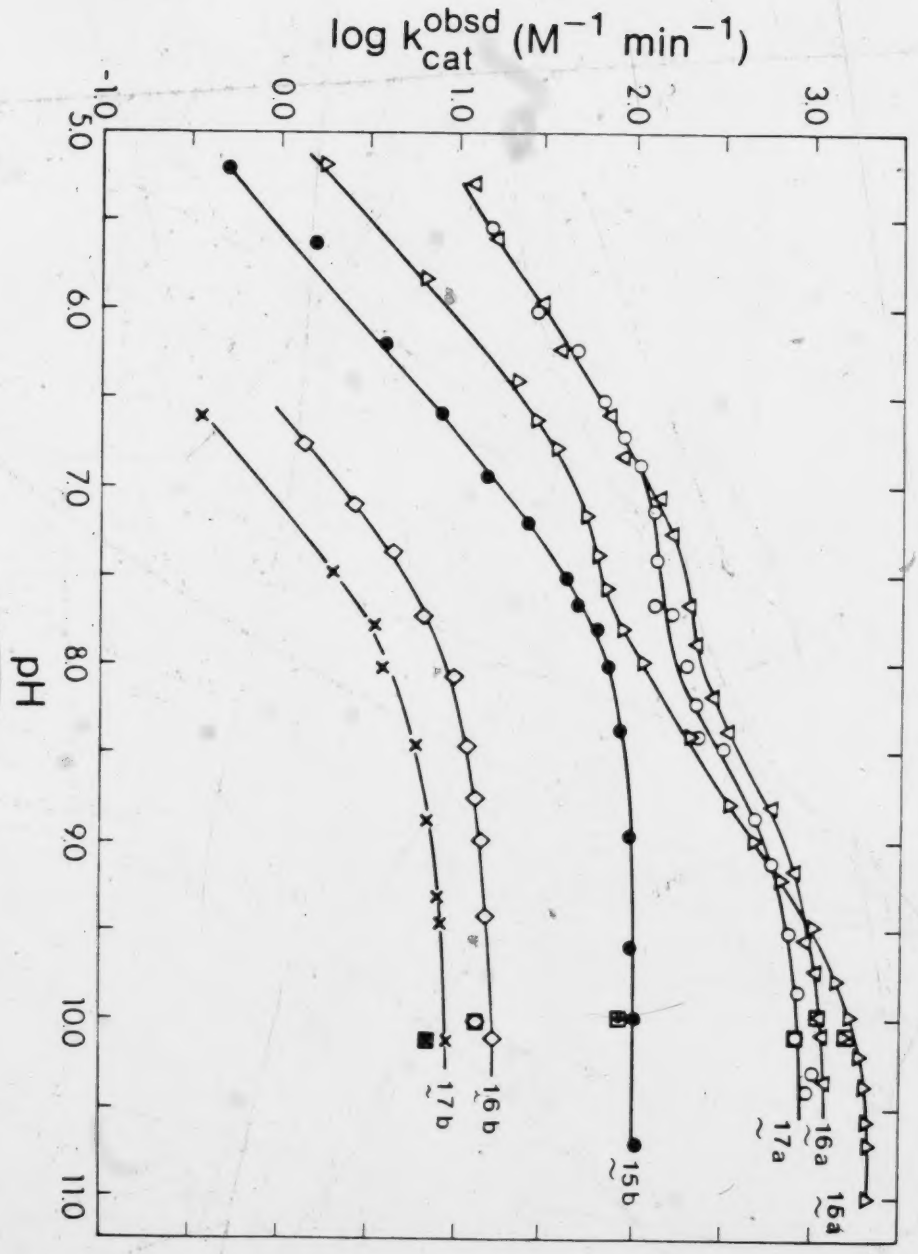
log k_{cat}^{obsd} (M^{-1} min^{-1})
-1.0
0.0
1.0
2.0
3.0
pH
5.0
6.0
7.0
8.0
9.0
10.0
11.0
15b
16a
17a
16b
17b

thiol species (H^+IMSH) was assumed not to be nucleophilic towards PNPA. Nucleophilic attack occurs from the other three microscopic species, IMSH, H^+IMS^-, and IMS^-. In the case of the imidazole compounds **15b-17b** the reaction scheme simplifies to attack on PNPA by neutral imidazole as is shown in Figure 5.

The equation derived from the reaction schemes in Figures 4 and 5 are given in eqn. 23 and 24 respectively. (For the derivation of these kinetic expressions, see Appendix 2.)

$$23.\quad k_{cat} = \frac{(k_1 Ka^{Im} + k_3 Ka^{Im} K_{Zw})[H^+] + k_2 Ka^{Im} Ka^{SH}}{[H^+]^2 + (Ka^{Im} + Ka^{Im} K_{Zw})[H^+] + Ka^{Im} Ka^{SH}}$$

$$24.\quad k_{cat} = \frac{k_1 Ka^{Im}[H^+]}{[H^+]^2 + Ka^{Im}[H^+]}$$

The reaction scheme in Figure 4 can be simplified to a kinetically equivalent scheme having two macroscopic pKa's and not requiring zwitterionic material if one assumes that $K_{Zw} = [H^+IMS^-]/[IMSH] = 0$. In this case, eqn. 23 reduces to eqn. 25.

$$25.\quad k_{cat} = \frac{k_1 Ka^{Im}[H^+] + k_2 Ka^{Im} Ka^{SH}}{[H^+]^2 + Ka^{Im}[H^+] + Ka^{Im} Ka^{SH}}$$

To determine if a zwitterion species is formed and if such a species is nucleophilic towards PNPA, one must determine the magnitude of K_{Zw} and show that k_3 is

Figure 4: Reaction scheme for the attack on PNPA by the model compounds 15a-17a.

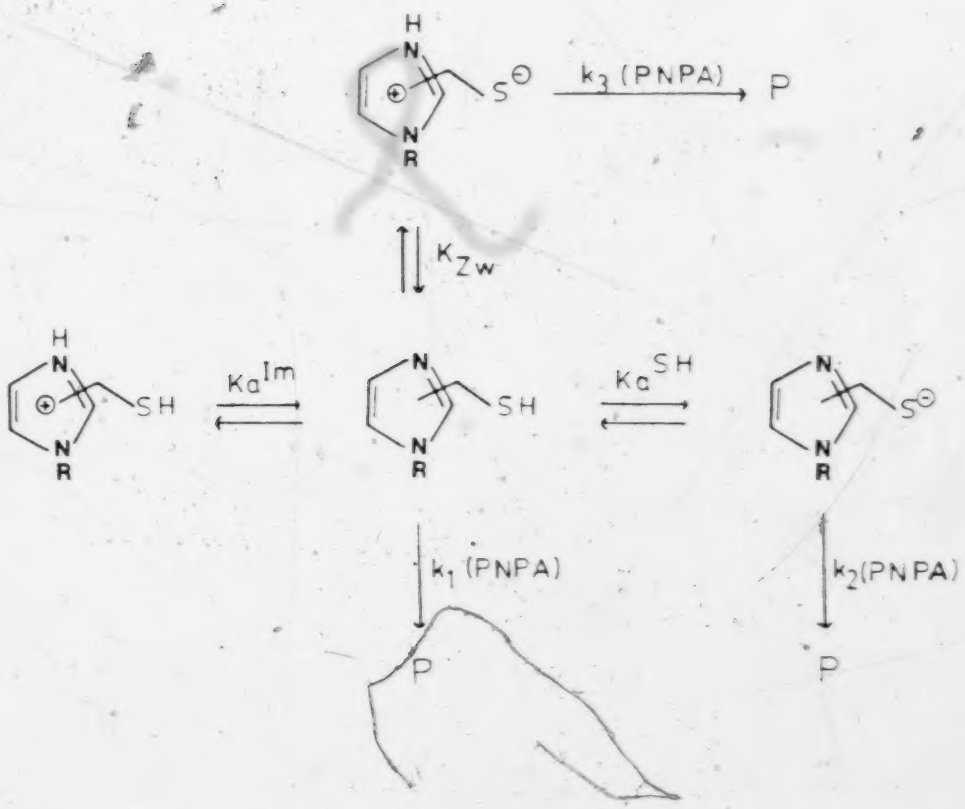

Figure 5: Reaction scheme for the attack on PNPA by the imidazole compounds 15b-17b.

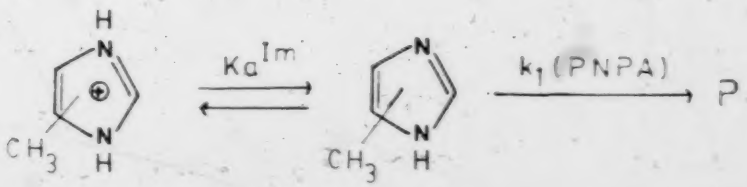

larger than the rate constant (k_1) found for an appropriate comparison imidazole. To calculate K_{Zw}, the microscopic pKa's (as shown in eqn. 11) must be determined since $K_{Zw} = K_1/Ka^{Im}$.

Two methods for determining the macroscopic and microscopic pKa°s were considered and evaluated. One method relied on data from potentiometric titrations while another method relied on data from UV-visible spectra titrations to calculate the pKa's.

(B) pKa Determinations

(1) Potentiometric Titrations

The thiol imidazole compounds **15a-17a** along with their S-benzyl compounds **32-34** were titrated with 0.1 N deoxygenated NaOH under argon at concentrations of 7×10^{-3} to 2×10^{-2} M in water at 25 °C. Analysis of tne titration curve by Simm's Method[56] gave the macroscopic pKa's for each run. (See Appendix 3 for explanation of Simm's method.) The reported pKa's given in Table 7 are the average of at least two determinations.

These macroscopic pKa's are related to the microscopic pKa's by eqn. 26 and 27.

26. $Ka_1 = Ka^{Im} + K_1$

27. $1/Ka_2 = 1/Ka^{SH} + 1/K_3$

However, in order to solve for all the microscopic pKa's one other pKa besides pKa_1 and pKa_2 must be known.

Table 7. Macroscopic pKa's determined by potentiometric titration.[a]

Compound	pKa_1[b]	pKa_2[b]
15a	6.54 ± 0.02	9.54 ± 0.02
16a	6.37 ± 0.02	9.26 ± 0.03
17a	6.31 ± 0.01	8.88 ± 0.02
32	6.57 ± 0.02	-
33	6.96 ± 0.01	-
34	6.83 ± 0.03	-

a. Titrated 7×10^{-3} - 2×10^{-2} M **15a-17a** with 0.1 N NaOH under degassed conditions at 25 °C.

b. Potentiometric pKa's shown are the average of at least two titration runs.

One method of obtaining the third pKa involves the assumption that Ka^{Im} is approximated by that of the corresponding S-benzyl derivative. This assumption has been shown to be reasonable for sulfur-containing compounds.[57] Brown, et al.,[57c] found that the pKa value of S-methylthioglycolic acid at 3.72 was nearly equal to that of the CO_2H unit of thiol glycolic acid at 3.67, giving some justification for the equivalence postulate as applied to SH and SCH_3. Since the inductive effect of the S-benzyl group (σ = 0.25) is approximately the same as the S-methyl group (σ = 0.25) and the SH group (σ = 0.26),[58] it is believed that the equivalence for SH to SCH_3 can be extrapolated to the S-benzyl case.

Using this assumption, the microscopic pKa's were calculated and are given in Table 8.

(2) UV-Visible Spectra Titrations

The UV-Visible absorption spectra of 1×10^{-5} M **15a-17a** between 200 and 400 nm were recorded every 0.2 to 0.5 pH units from pH 3 to 11 in carefully deoxygenated aqueous solutions.

The UV-visible spectra for the three compounds **15a**, **16a** and **17a** are given in Figures 6a, 7a-c and 8a respectively.

For compound **15a**, the maximum UV absorbance changes occur at λ = 208 nm and λ = 240 nm. The 4(5)-methylimidazole compound shows one absorption peak at λ_{max} =

Table 8. Microscopic pKa's based on potentiometric titrations.[a]

Compound	Macroscopic pKa[b]		Microscopic pKa				K_{Zw}
	pKa_1	pKa_2	pK_1	pKa^{Im}[c]	pK_3	pKa^{SH}	
15a	6.54 ±0.01	9.54 ±0.02	7.72 ±0.05	6.57 ±0.02	8.36 ±0.05	9.51 ±0.05	0.07 ±0.01
16a	6.37 ±0.02	9.26 ±0.03	6.50 ±0.05	6.96 ±0.01	9.13 ±0.05	8.67 ±0.05	2.88 ±0.20
17a	6.31 ±0.01	8.88 ±0.02	6.47 ±0.05	6.83 ±0.03	8.75 ±0.05	8.39 ±0.05	2.29 ±0.50

a. Assume pKa^{Im} = pKa of S-benzyl compounds (**32-34**).

b. Average pKa of at least two potentiometric titration runs.

c. Values from at least two potentiometric titrations of S-benzyl compounds.

d. Potentiometric titrations conducted under argon at 25 °C using degassed 0.01 N NaOH to titrate ~1 x 10^{-5} moles of **15a-17a** and **32-34**. Macroscopic pKa's obtained from analysis of titration curve by Simm's method.[56]

e. Errors for pKa_1, pKa_2 and pKa^{Im} are experimental errors from potentiometric titrations while errors in pK_1, pK_3, pKa^{SH} and K_{Zw} are calculated cumulative errors.

Figure 6a: UV-visible spectrum as a function of pH for 4(5)-mercaptomethylimidazole.HCl (15a) (1.335×10^{-4} M at 25 ^{o}C) from pH 4.7 to 11.2.

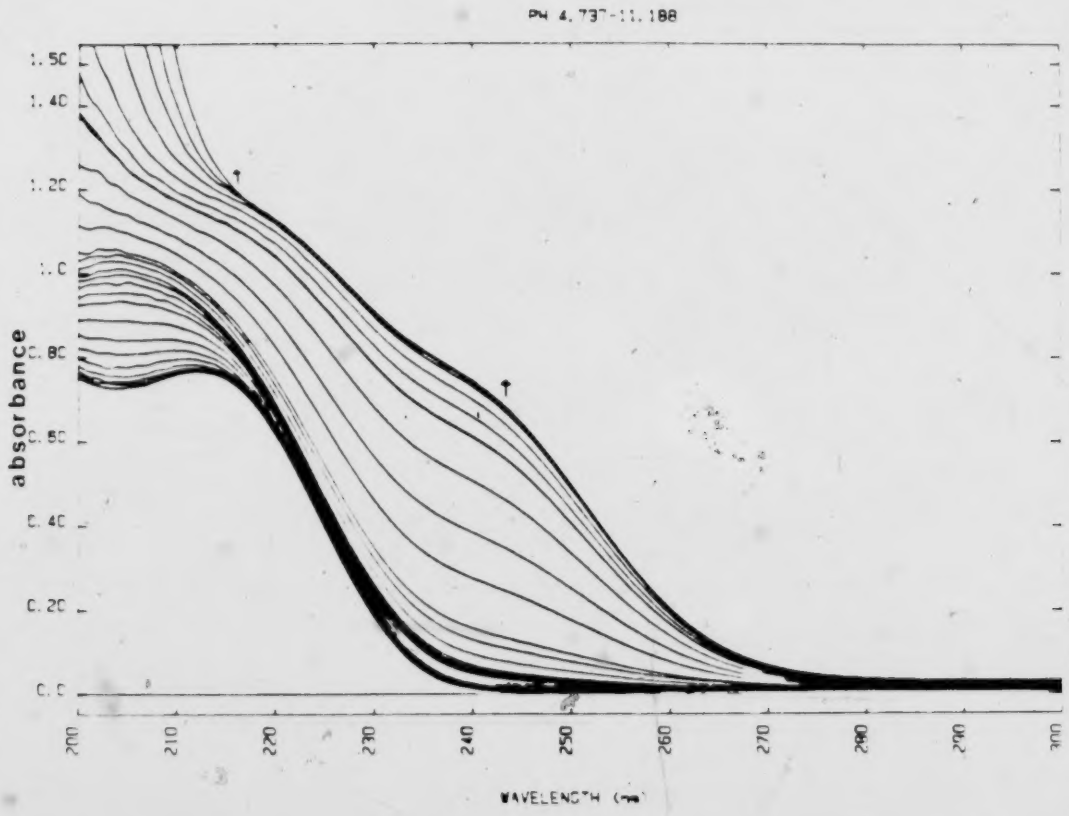

Figure 6b: Plot of absorbance versus pH at λ = 240 nm for 4(5)-mercaptomethylimidazole hydrochloride. (1.335×10^{-4} M at 25 ^{o}C)

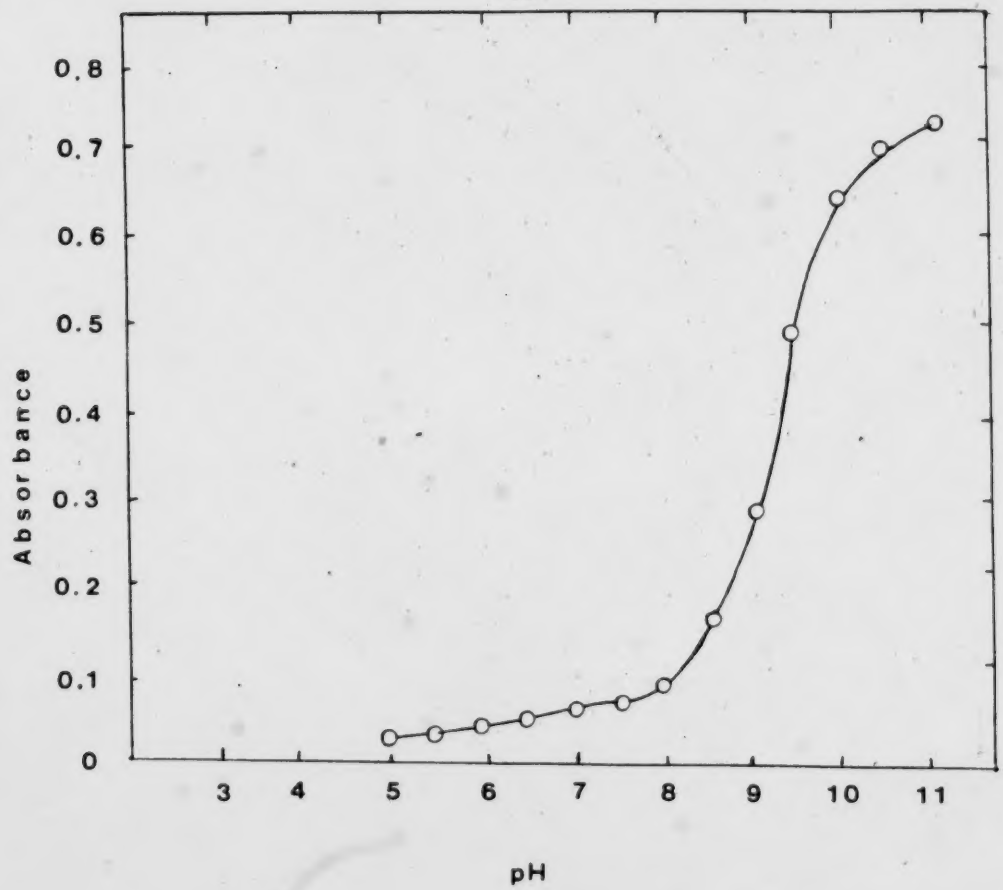

Figure 7a: UV-visible spectrum as a function of pH for N-methyl-2-mercaptomethylimidazole.HCl (16a) (1.09×10^{-4} M at 25 ^{o}C) from pH 3.1 to 6.3.

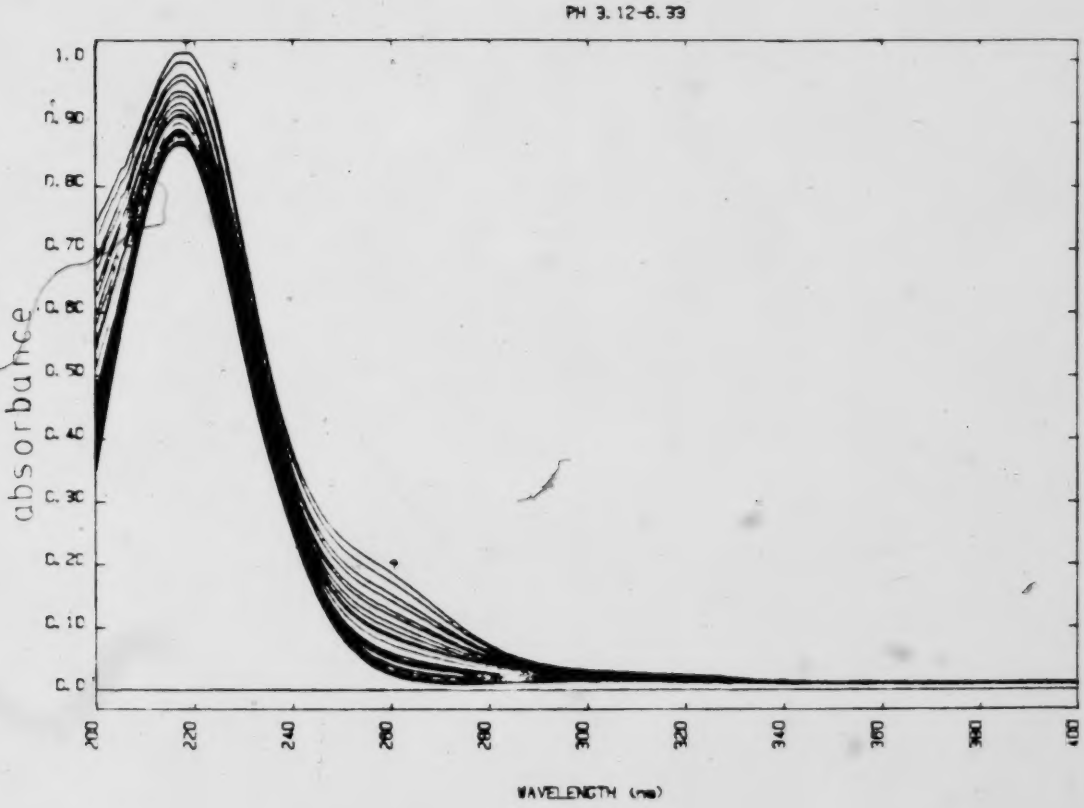

Figure 7b: UV-visible spectrum as a function of pH for N-methyl-2-mercaptomethylimidazole.HCl (16a) (1.09×10^{-4} M at 25 ^{o}C) from pH 6.3 to 8.7.

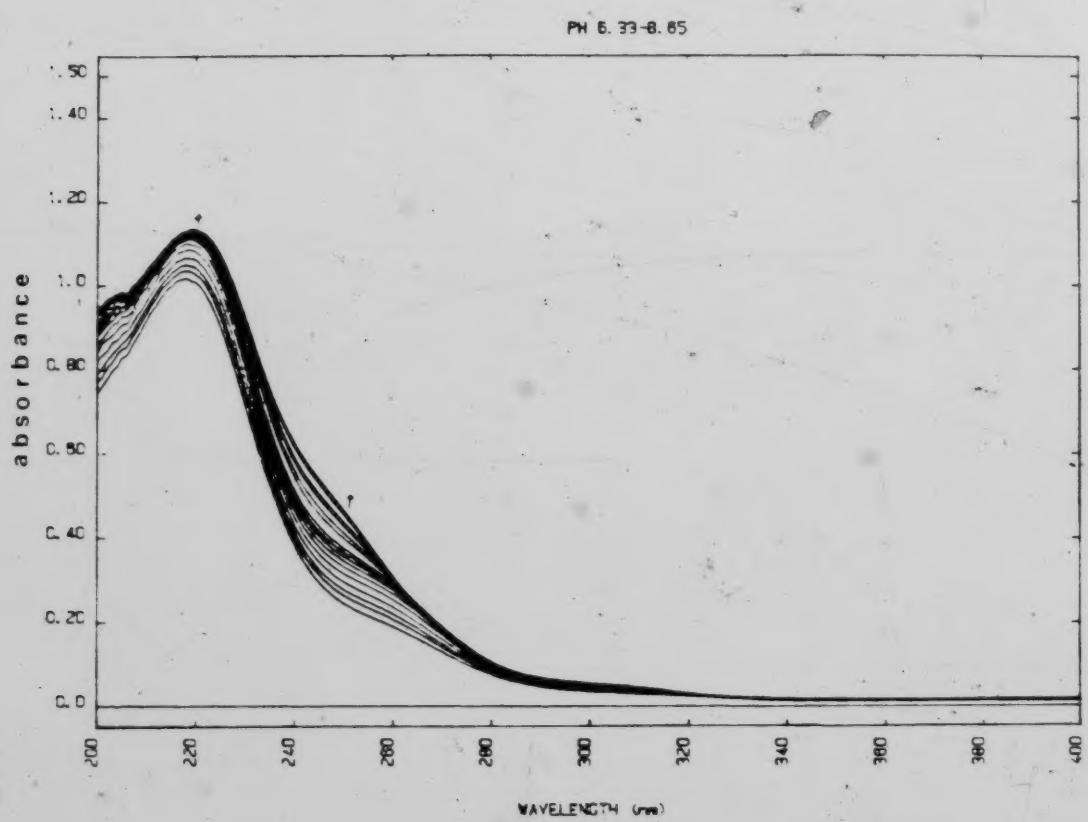

Figure 7c: UV-visible spectrum as a function of pH for N-methyl-2-mercaptomethylimidazole.HCl (16a) (1.09×10^{-4} M at 25 ^{o}C) from pH 8.7 to 11.5.

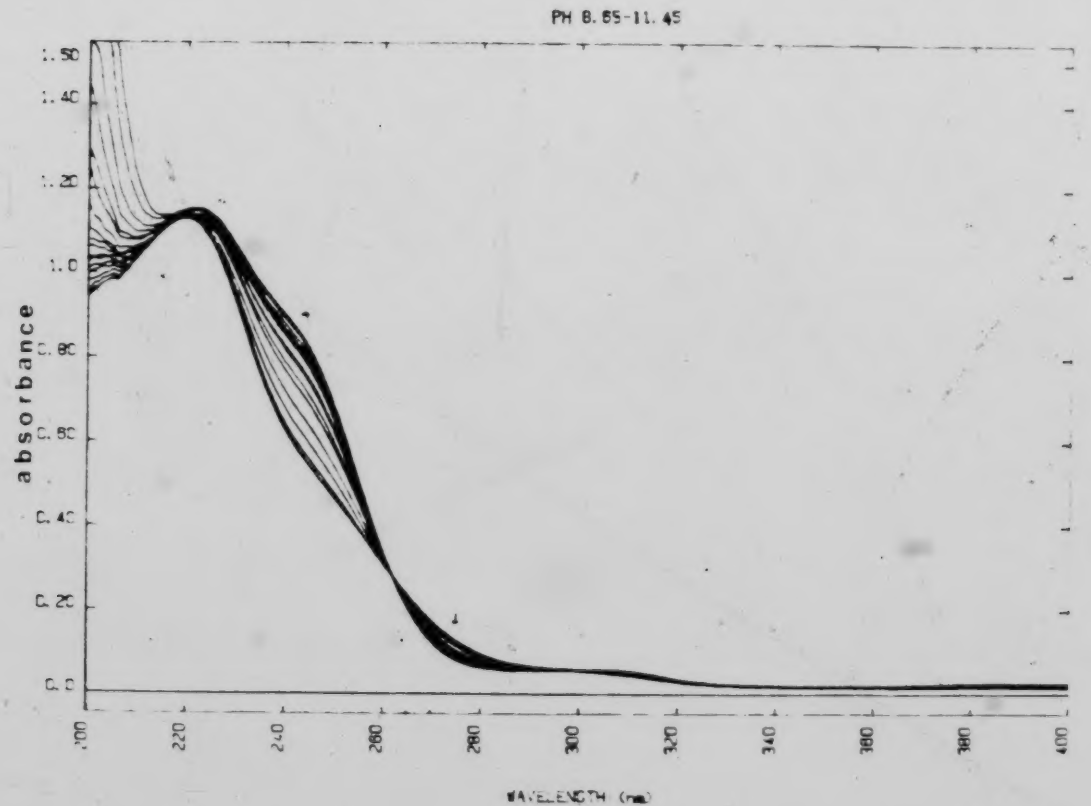

Figure 7d: Plot of absorbance versus pH at λ = 262 nm for N-methyl-2-mercaptomethylimidazole hydrochloride. (1.09×10^{-4} M at 25 ^{o}C)

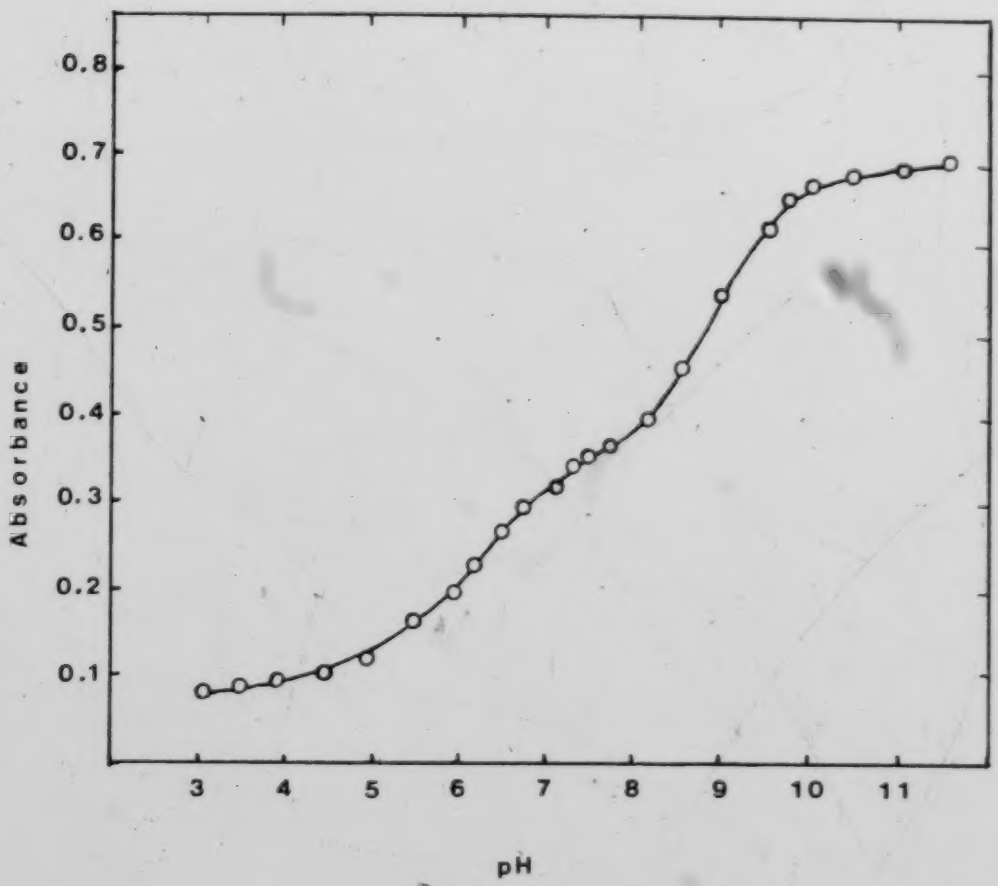

Figure 8a: UV-visible spectrum as a function of pH for 2-mercaptomethylimidazole.HCl (17a) (1.37×10^{-4} M at 25 °C) from pH 3.0 to 11.1.

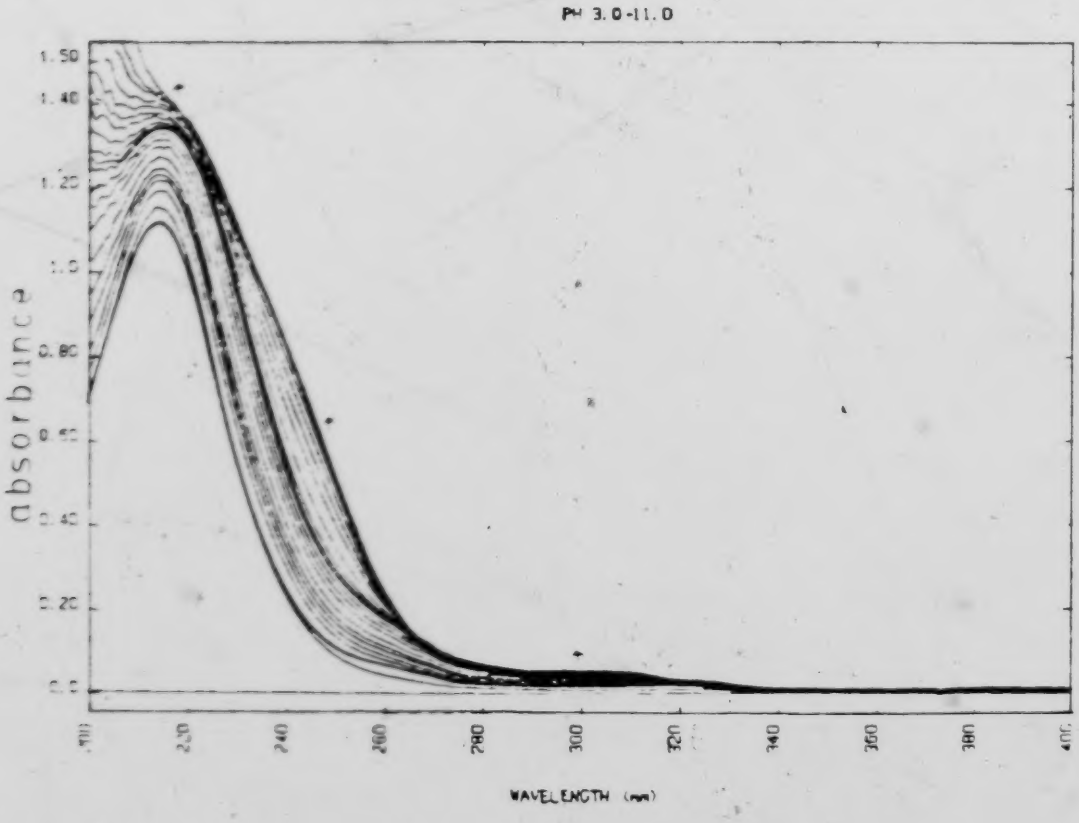

Figure 8b: Plot of absorbance versus pH at λ = 255 nm for 2-mercaptomethylimidazole hydrochloride. (1.37×10^{-4} M at 25 ^{o}C)

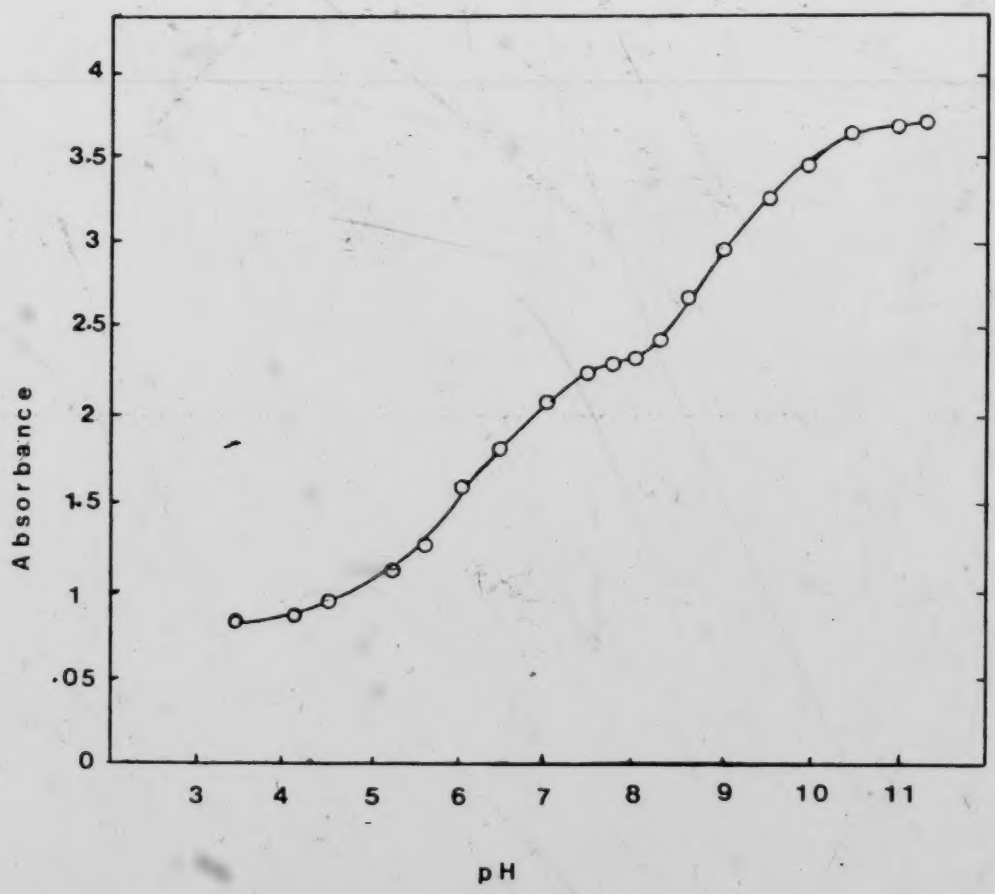

212 nm and there is no absorbance above 245 nm. Thus the absorbance change at 208 nm for **15a** is believed to primarily represent the deprotonation of the imidazole ring as shown in eqn. 28, while that at 240 nm is believed to represent primarily the deprotonation of the thiol to form a thiolate anion as shown in eqn. 29.

28.

29.

For compound **16a** and **17a** the maximum absorbance change for thiolate formation occurred at λ = 250 nm and λ = 255 nm, respectively.

To solve for the microscopic pKa's based on these UV-visible spectral titrations, a method developed by Edsall[59] was used. This method involves the assumption that the individual components IMS^- and H^+IMS^- have the same significant molar absorptivities and that of H^+IMSH and IMSH have molar absorptivities equal to zero at the wavelength followed for these titrations.

Using this assumption, the microscopic pKa's were calculated based on the plot of pM versus α as shown in

Figure 9: Plot of pM versus α for 15a (1.35×10^{-4} M) at λ = 240 nm, 16a (1.09×10^{-4} M) at λ = 260 nm and 17a (1.37×10^{-4} M) at λ = 250 nm. Expanded graph for 15a from α = 0 to 0.05 is shown in the marked square.

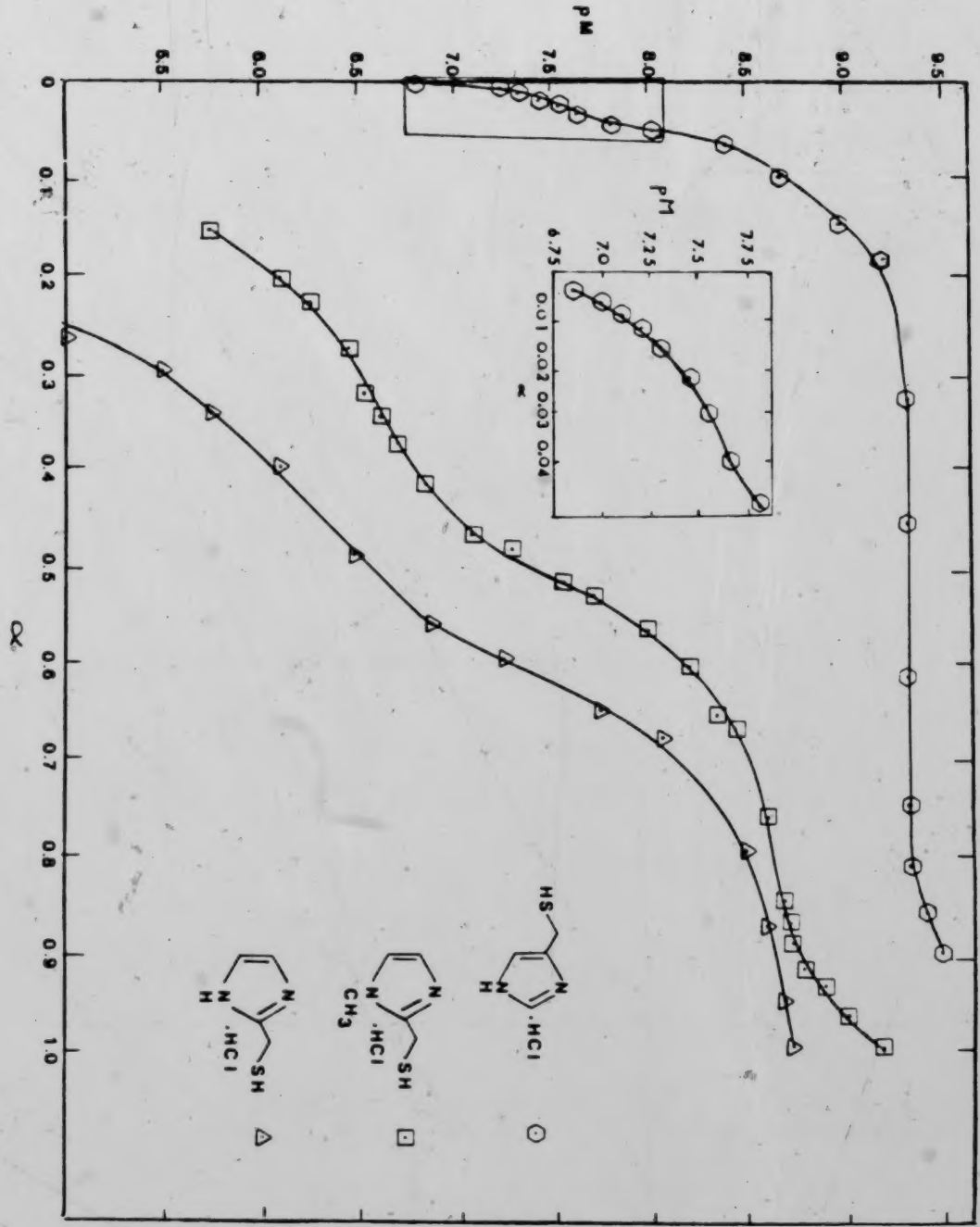
pM
α
pM
α
HS
·HCl
CH3
SH

Figure 9 where pM and α are defined as follows:[59]

30. $$\alpha = \frac{[IMS^-] + [H^+IMS^-]}{[\text{Total Conc. of Species}]} = \mathcal{E}/\mathcal{E}_{max}$$

where $\mathcal{E}$ = molar absorptivity at each pH and $\mathcal{E}_{max}$ = molar absorptivity at pH > 10.

31. $$pM = pH - \frac{\log \alpha}{1 - \alpha}$$

By definition, as $[H^+] \longrightarrow \infty$, $\alpha = 0$ and $pM = pK_1$ and as $[H^+] \longrightarrow 0$, $\alpha = 1$ and $pM = pKa^{SH}$. Once these two constants pK_1 and pKa^{SH} are known, it is possible to solve for pKa^{Im} since at $\alpha = 0.5$, pM = pH and Ka^{Im} is defined as in eqn. 32.

32. $$Ka^{Im} = [H^+]([H^+] - K_1)/(Ka^{SH} - [H^+]).$$

(For a detailed explaination of the above equations, see Appendix 4.)

Calculated values for pM and α for compounds **15a**, **16a**, and **17a** are given in Tables 9, 10 and 11 respectively.

From the plot of pM versus α, the values for the microscopic pKa's were calculated. These values are given in Table 12.

Comparison of the microscopic pKa's calculated from the UV-visible data and those calculated from the potentiometric data, show large differences between the Ka's of 50 % or more. It is believed that the UV-visible

Table 9. Computed values for pM and α from UV-visible titration data of 4(5)-mercaptomethylimidazole hydrochloride (**15a**) at λ = 240 nm.[a]

pH	Absorbance	α [b]	log α 1-α	pM[c]
4.39	0.003	0.004	-2.44	6.83
4.79	0.005	0.006	-2.22	7.01
5.27	0.009	0.011	-1.95	7.22
5.52	0.012	0.016	-1.80	7.32
5.77	0.017	0.021	-1.63	7.43
6.02	0.024	0.029	-1.52	7.54
6.52	0.038	0.048	-1.30	7.82
7.01	0.047	0.052	-1.20	8.21
7.49	0.060	0.075	-1.09	8.58
7.76	0.087	0.108	-0.91	8.67
8.27	0.120	0.150	-0.75	9.02
9.01	0.265	0.331	-0.31	9.32
9.52	0.496	0.620	+0.22	9.31
10.2	0.689	0.861	+0.79	9.43
10.5	0.720	0.900	+0.94	9.52
10.8	0.731	0.916	+1.04	9.73
10.96	0.734	0.917	+1.05	9.91

a. UV-visible titration conducted under argon at 25 °C using deoxygenated 0.1 M NaOH to titrate ~1 x 10^{-5} moles of **15a** in 70 ml of deoxygenated water. Absorbances shown are the average of at least two titration runs.

b. α calculated from $\alpha = Abs./Abs._{max}$ where $Abs._{max} = 0.80$.

c. pM calculated from $pM = pH - \log \alpha / 1 - \alpha$

Table 10. Computed values for pM and α from UV-visible titration data of N-methyl-2-mercaptomethyl-imidazole hydrochloride (**16a**) at λ = 250 nm.[a]

pH	Absorbance	α[b]	log α/1-α	pM[c]
5.01	0.109	0.155	-0.74	5.74
5.50	0.142	0.200	-0.60	6.10
5.71	0.159	0.225	-0.54	6.25
6.21	0.227	0.321	-0.33	6.54
6.47	0.264	0.373	-0.23	6.70
6.72	0.296	0.418	-0.14	6.86
7.13	0.331	0.469	-0.05	7.18
7.59	0.366	0.517	+0.03	7.56
8.08	0.399	0.564	+0.11	8.17
8.65	0.465	0.658	+0.28	8.37
9.12	0.541	0.765	+0.51	8.61
9.42	0.600	0.847	+0.74	8.68
9.65	0.632	0.893	+0.92	8.73
9.84	0.648	0.917	+1.05	8.79
10.0	0.662	0.936	+1.16	8.83
10.5	0.685	0.9689	+1.49	9.01
10.9	0.6904	0.9764	+1.62	9.31

a. UV-visible titration conducted under argon at 25 °C using deoxygenated 0.1 M NaOH to titrate ~1 x 10^{-5} moles of **16a** in 70 ml of deoxygenated water. Absorbances shown are the average of at least two titration runs.

b. α calculated from $\alpha = Abs./Abs._{max}$ where $Abs._{max} = 0.7071$.

c. pM calculated from $pM = pH - \log \alpha / 1 - \alpha$

Table 11. Computed values for pM and α from UV-visible titration data of 2-mercaptomethylimidazole hydrochloride (**17a**) at λ = 255 nm.[a]

pH	Absorbance	α[b]	log α 1-α	pM[c]
3.01	0.062	0.169	-0.69	3.70
3.51	0.083	0.226	-0.53	4.04
4.11	0.085	0.232	-0.52	4.62
4.61	0.101	0.276	-0.42	5.02
5.14	0.114	0.312	-0.34	5.48
5.52	0.128	0.349	-0.27	5.79
6.03	0.157	0.428	-0.13	6.16
6.47	0.179	0.487	-0.02	6.49
7.00	0.205	0.560	+0.11	6.89
7.46	0.219	0.599	+0.17	7.29
8.13	0.238	0.649	+0.27	7.86
8.43	0.246	0.670	+0.31	8.12
9.04	0.291	0.793	+0.58	8.46
9.48	0.321	0.876	+0.85	8.63
10.1	0.344	0.937	+1.17	8.91
10.5	0.355	0.967	+1.47	9.02
11.0	0.362	0.985	+1.82	9.18

a. UV-visible titration conducted under argon at 25 °C using deoxygenated 0.1 M NaOH to titrate ~1 x 10^{-5} moles of **17a** in 70 ml of deoxygenated water. Absorbances shown are the average of at least two titration runs.

b. α calculated from $\alpha = Abs./Abs._{max}$ where $Abs._{max} = 0.3670$.

c. pM calculated from $pM = pH - \log \alpha / 1-\alpha$

Table 12. Microscopic pKa's based on UV-visible titrations.[a]

Compound	Macroscopic pKa[b]		Microscopic pKa[c]			K_{Zw}
	pKa_1	pKa_2	pK_1	pKa^{Im}	pK_3	pKa^{SH}	
15a	5.88 ±0.20	9.33 ±0.30	7.50 ±0.25	5.89 ±0.30	7.69 ±0.60	9.32 ±0.05	0.03 ±0.04
16a	6.23 ±0.35	8.26 ±0.50	6.50 ±0.25	6.57 ±0.50	9.21 ±0.75	8.75 ±0.25	1.17 ±3.00
17a	6.02 ±0.35	8.36 ±0.50	6.20 ±0.25	6.50 ±0.50	8.90 ±0.75	8.60 ±0.25	2.00 ±3.00

a. UV-visible titrations were conducted under argon at 25 °C using degassed 0.1 M NaOH to titrate ~1 x 10^{-5} moles of compound **15a-17a** and the spectra taken from 200 to 400 nm every 0.2 to 0.5 pH units from pH 3 to 11.

b. Values obtained from microscopic pKa's such that $Ka_1 = Ka^{Im} + K_1$ and $Ka_2 = Ka^{SH}Ka_3/(Ka^{SH} + K_3)$.

c. Values obtained from the plot of pM versus α in Figure 9.

d. Errors in pK_1, pKa^{Im} and pKa^{SH} are experimental errors from extrapolating the values from the curve of pM versus α whereas errors in pKa_1, pKa_2 and K_{Zw} are calculated cumulative errors.

microscopic pKa's are inaccurate for several reasons.

One possible source of error is the formation of disulfide during the UV-visible titration sequence. The spectrophotometric titrations require two or more hours to complete, increasing the risk of air oxidation for the compounds. (The potentiometric titrations are completed in 20 minutes or less.) The UV-visible spectra of the disulfide compared with the mercaptan both at 2.92×10^{-5} M is given in Figure 10.

From Figure 10, the absorption due to the imidazole at $\lambda = 220$ nm undergoes a bathochromic shift by 10 nm with a decrease in absorptivity as it is oxidized while the absorption due to the thiolate at $\lambda = 310$ nm undergoes a hypsochromic shift by 10 nm as the mercaptan is oxidized with an increase in absorptivity. Hence, the UV-visible spectra data from 200 to 400 nm would be altered with the oxidation of the mercaptan compound.

The compounds, once titrated with 0.1 M NaOH to pH 11 were back-titrated with 0.1 M HCl to pH 3 to test for reversible behavior. No significant change in UV spectra was observed between the forward and back titration UV-visible spectra curves. Thus, the possibility of disulfide formation did not appear to be the cause for the large error in pKa's.

A more likely source of error in the UV-visible titration method is in the original assumption that the extinction coeffient of the two thiolate species, H^+IMS^-

Figure 10: UV-visible spectrum of N-methyl-2-mercaptomethylimidazole.HCl (**16a**) at 2.92×10^{-5} M in 0.1 M phosphate buffer at pH = 8.0, 37 °C and the spectrum of the final disulfide product after air oxidation for 1 hour.

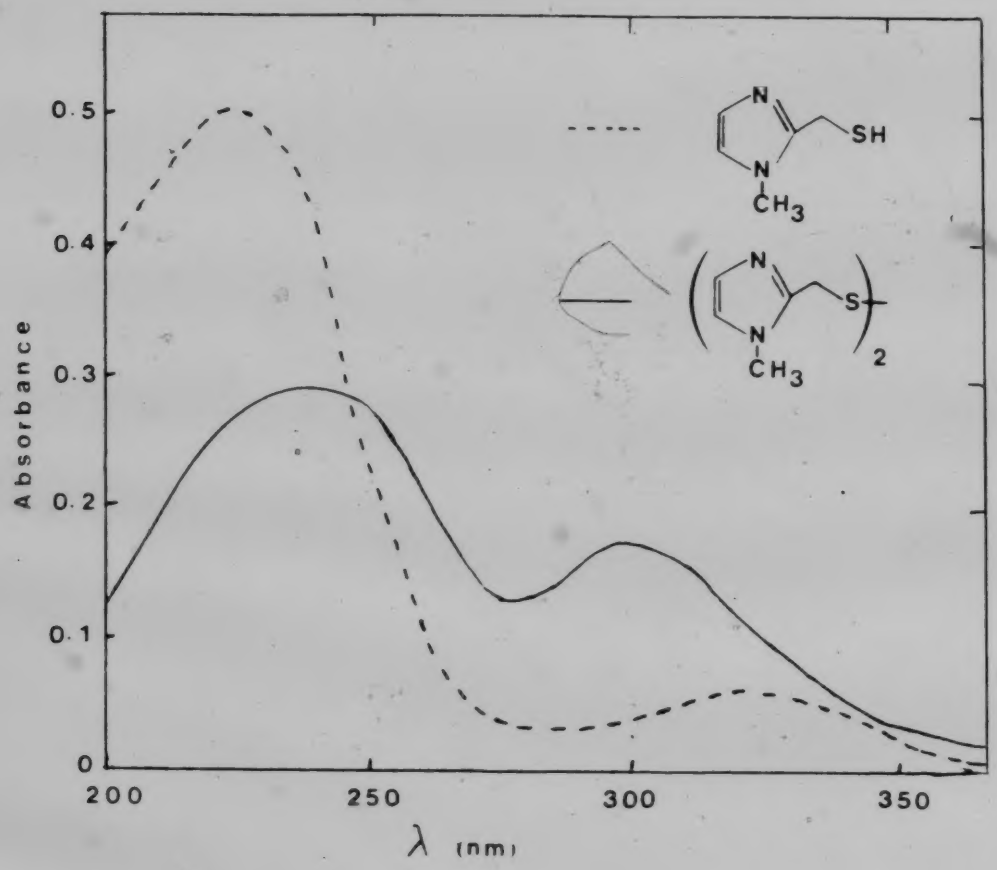

and IMS^- are the same. In the case of the zwitterion, the thiolate anion is in close proximity to the imidazolium ion and H-bonding as well as significant electrostatic interactions may occur, thereby stabilizing this species. The thiolate-imidazole species will not have this stabilizing H-bonding so that it is possible that the extinction coefficients of H^+IMS^- and IMS^- may not be equal. This would make the Edsall method[59] for determining the microscopic pKa's inapplicable for these thiol-imidazole compounds (**15a-17a**).

Another problem in the Edsall method[59] for these compounds is in determining accurately the values for pK_1 and pKa^{SH} at $\alpha = 0$ and 1 respectively from the plot of pM versus α. The values given in the Table have been estimated by locating the inflection points of the plots of pM versus α. This results in large error limits on the microscopic pKa values as shown in the Table 12. The macroscopic pKa's calculated from the potentiometric titration data (Table 8) were calculated by a computer program and are more precise.

In view of the probable inaccuracies in determining the microscopic pKa values by UV-visible absorption spectroscopy, the values determined by the potentiometric titration data were considered to be more accurate and were used to calculate the concentration of each microscopic species at each pH.

These microscopic pKa's from potentiometric data

are believed to be more accurate because they rely on accurate experimental data analyzed by computer and the assumption that Ka^{Im} = Ka of S-benzyl compounds appears to be reasonable.[57,45]

It should be noted, that even if the pKa^{Im} of the thiol-imidazole compounds is different by as much as 0.1 pKa units from the S-benzyl compounds the overall conclusion for the concentration of zwitterion species at neutral pH remains the same with K_{Zw} for **15a** being small (0.27) and K_{Zw} for **16a** and **17a** being larger (3.89 and 3.16 respectively).

(C) Concentration of Zwitterion

From the microscopic pKa's, the concentration of each species I to IV (eqn. 11) over a pH range of 5 to 12 can be calculated as follows.

We define:

$$pKa^{Im} - pH = \log \frac{[I]}{[II]} \; ; \; pK_1 - pH = \log \frac{[I]}{[III]} \; ;$$

$$pKa^{SH} - pH = \log \frac{[II]}{[IV]} \; ; \text{ and } pK_3 - pH = \log \frac{[III]}{[IV]}$$

Using the microscopic pKa's given in Table 8, the concentration of each species at any given pH was calculated for compounds **15a**, **16a** and **17a**. These are given in Tables 13, 14, and 15 respectively. (See Appendix 5 for the computer program used to calculate these concentrations). Plotted in Figures 11, 12, and 13 for compounds **15a**, **16a** and **17a** respectively is the

Table 13. Concentration of species I, II, III and IV for 4(5)-mercaptomethylimidazole hydrochloride as a function of pH.[a]

	Microscopic Concentrations[b] ($M \times 10^{-5}$)			
pH	$[H^+IMSH]$	$[IMSH]$	$[H^+IMS^-]$	$[IMS^-]$
5.0	97.2	2.61	0.19	-
5.5	91.6	7.80	0.55	-
6.0	77.6	20.9	1.47	-
6.5	82.3	44.5	3.15	-
7.0	25.7	69.2	4.89	0.22
7.5	9.80	83.5	5.91	0.82
8.0	3.20	87.8	6.21	2.71
8.5	0.99	84.7	5.91	8.27
9.0	0.26	72.2	5.11	22.3
9.5	0.06	48.7	3.45	47.7
10.0	-	24.0	1.70	74.2
10.5	-	9.22	0.65	90.1
11.0	-	3.12	0.22	96.7
11.5	-	1.01	0.07	98.9
12.0	-	0.32	0.03	99.7

a. $pK_1 = 7.72$, $pKa^{Im} = 6.57$, $pK_3 = 8.36$, $pKa^{SH} = 9.51$

b. Total Concentration of I + II + II + IV = 10^{-3} M.

Figure 11: The fractional amount of each microscopic species of 4(5)-mercaptomethylimidazole.HCl as a function of pH for pKa^{SH} = 9.51 , pK_3 = 8.36, pKa^{Im} = 6.57 and pK_1 = 7.72.

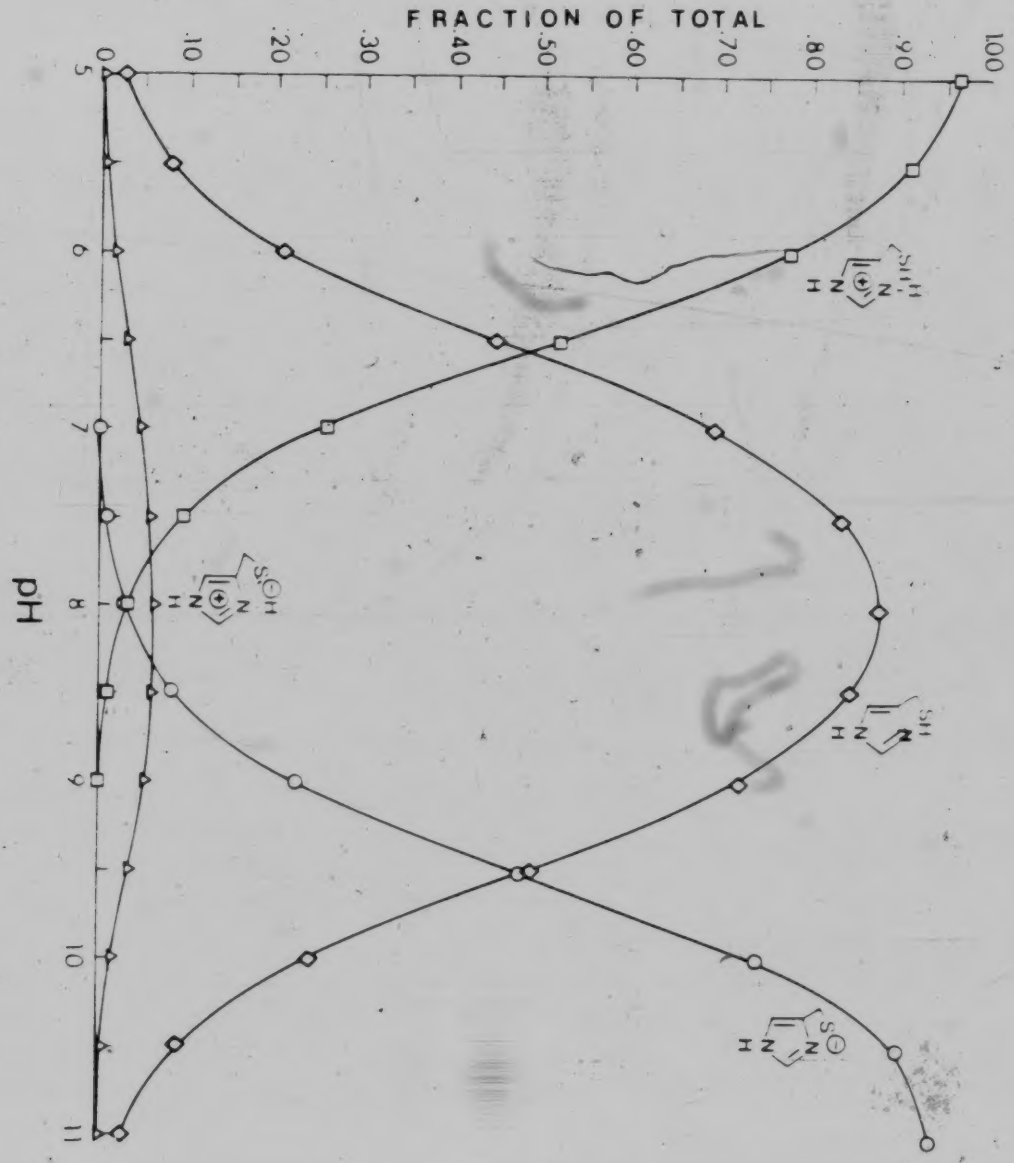

Table 14. Concentration of species I, II, III, and IV for N-methyl-2-mercaptomethylimidazole hydrochloride as a function of pH.[a]

pH	Microscopic Concentrations[b] ($M \times 10^{-5}$)			
	$[H^+IMSH]$	$[IMSH]$	$[H^+IMS^-]$	$[IMS^-]$
5.0	95.9	1.05	3.03	-
5.5	88.2	3.05	8.81	-
6.0	70.1	7.68	22.2	-
6.5	42.5	14.7	42.6	-
7.0	18.9	20.7	59.7	0.44
7.5	6.80	23.6	68.0	1.59
8.0	2.17	23.9	68.8	5.10
8.5	0.63	21.7	62.8	14.7
9.0	0.15	16.6	47.8	35.4
9.5	-	9.39	27.1	63.5
10.0	-	3.95	11.4	84.6
10.5	-	1.39	4.03	94.6
11.0	-	0.45	1.32	98.2
11.5	-	0.15	0.42	99.4
12.0	-	-	0.14	99.8

a. $pK_1 = 6.50$, $pKa^{Im} = 6.96$, $pK_3 = 9.13$, $pKa^{SH} = 8.67$

b. Total Concentration of I + II + III + IV = 10^{-3} M

Figure 12: The fractional amount of each microscopic species of N-methyl-2-mercaptomethylimidazole. HCl as a function of pH for pKa^{SH} = 3.67, pK_3 = 9.13, pKa^{Im} = 6.96 and pK_1 = 6.50.

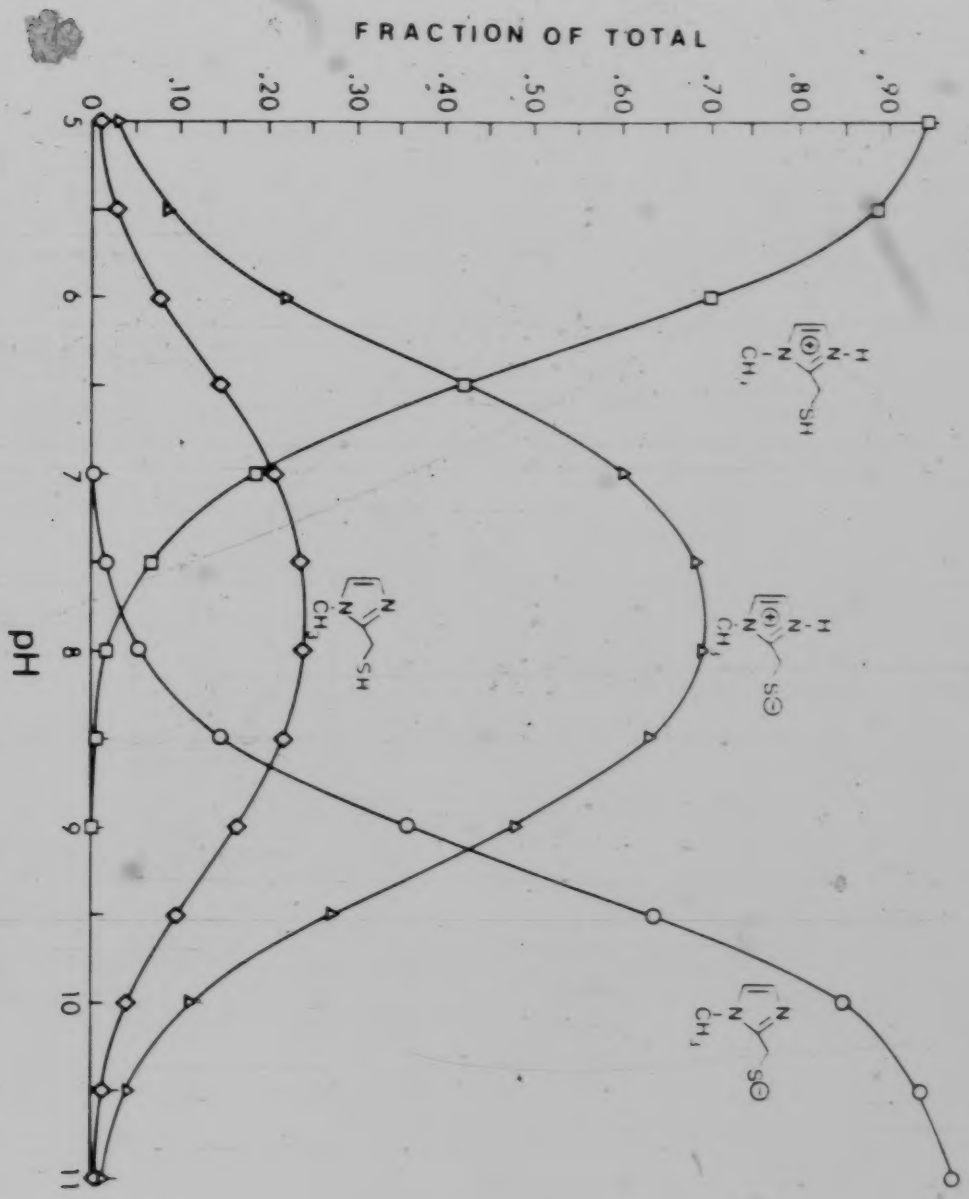

Table 15. Concentration of species I, II, III, and IV for 2-mercaptomethylimidazole hydrochloride as a function of pH.[a]

	Microscopic Concentrations[b] ($M \times 10^{-5}$)			
pH	$[H^+IMSH]$	[IMSH]	$[H^+IMS^-]$	$[IMS^-]$
5.0	95.3	1.41	3.23	-
5.5	86.6	4.05	9.28	-
6.0	67.2	9.94	22.8	-
6.5	39.3	18.4	42.1	0.24
7.0	16.9	24.9	57.2	1.01
7.5	5.88	27.5	63.0	3.55
8.0	1.79	26.6	60.8	10.8
8.5	0.46	21.7	49.8	28.0
9.0	0.09	13.6	31.1	55.3
9.5	-	6.18	14.1	79.6
10.0	-	2.27	5.20	92.5
10.5	-	0.76	1.73	97.5
11.0	-	0.24	0.56	99.2
11.5	-	0.07	0.18	99.7
12.0	-	-	-	99.9

a. $pK_1 = 6.47$, $pKa^{Im} = 6.83$, $pK_3 = 8.75$, $pKa^{SH} = 8.39$

b. Total Concentration of I + II + III + IV = 10^{-3} M.

Figure 13: The fractional amount of each microscopic species of 2-mercaptomethylimidazole.HCl as a function of pH for pKa^{SH} = 8.37, pK_3 = 8.75, pKa^{Im} = 6.83 and pK_4 = 6.47.

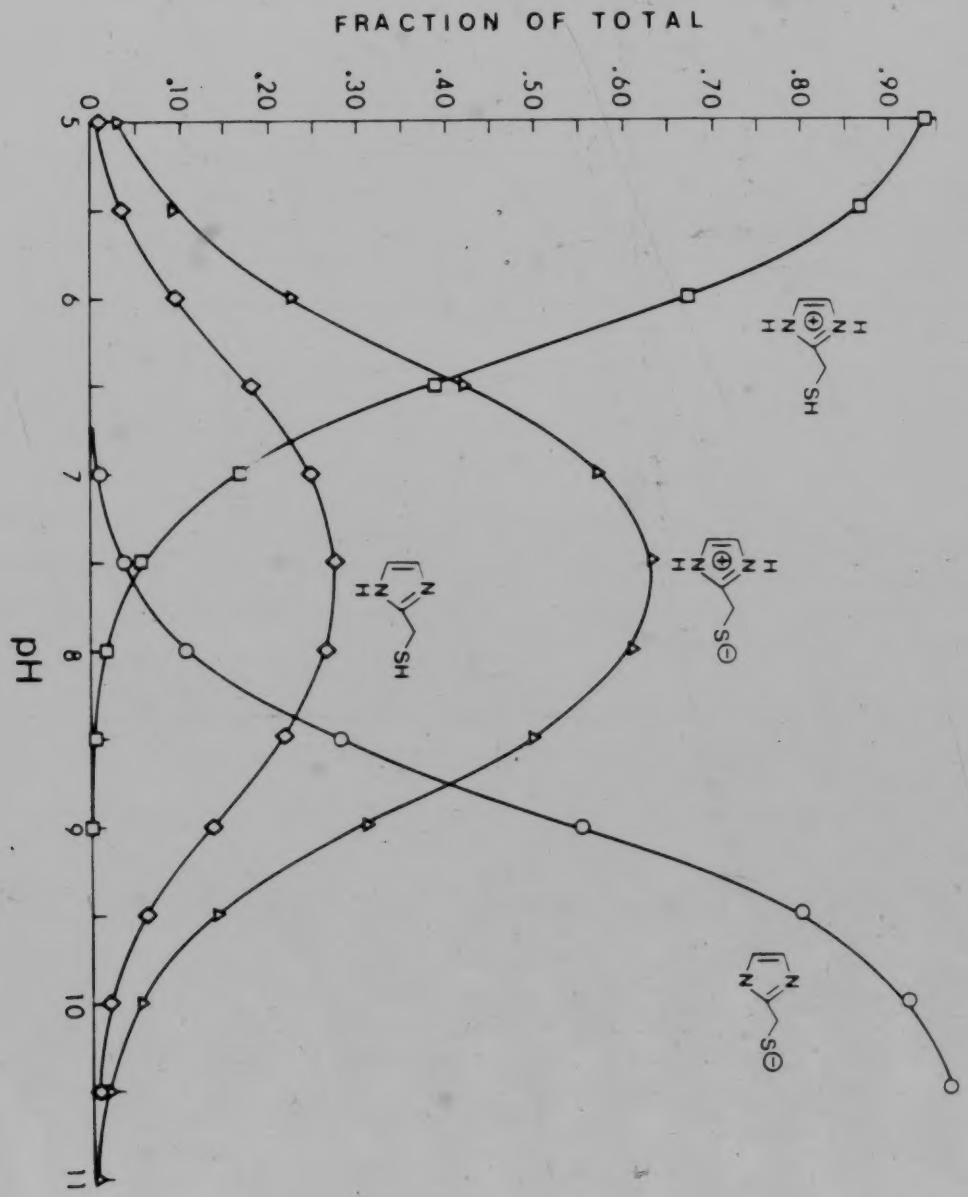

Table 16. Total concentration of thiolate anion as a function of pH.

pH	[III + IV][a] ($M \times 10^{-5}$) 15a[b]	16a[c]	17a[d]
5.0	0.19	3.03	3.23
5.5	0.55	8.81	9.29
6.0	1.48	22.2	22.8
6.5	3.19	42.7	42.3
7.0	5.11	60.3	58.2
7.5	6.72	69.6	66.6
8.0	8.92	73.9	71.6
8.5	14.3	77.6	77.9
9.0	27.5	83.3	86.3
9.5	51.2	90.6	93.8
10.0	75.9	96.1	97.7
10.5	90.7	98.7	99.2
11.0	96.8	99.5	99.7
11.5	98.9	99.9	99.9
12.0	99.7	99.9	99.9

a. Total Concentration of $[IMS^- + H^+IMS^-]$ where I + II + III + IV = 10^{-3} M.

b. $pK_1 = 7.72$, $pKa^{Im} = 6.57$, $pK_3 = 8.36$, $pKa^{SH} = 9.51$

c. $pK_1 = 6.50$, $pKa^{Im} = 6.96$, $pK_3 = 9.13$, $pKa^{SH} = 8.67$

d. $pK_1 = 6.47$, $pKa^{Im} = 6.83$, $pK_3 = 8.75$, $pKa^{SH} = 8.39$

Figure 14: Total thiolate concentration as a function of pH for 4(5)-mercaptomethylimidazole.HCl (15a) ○; N-methyl-2-mercaptomethylimidazole.HCl (16a) □; and 2-mercaptomethylimidazole.HCl (17a) △.

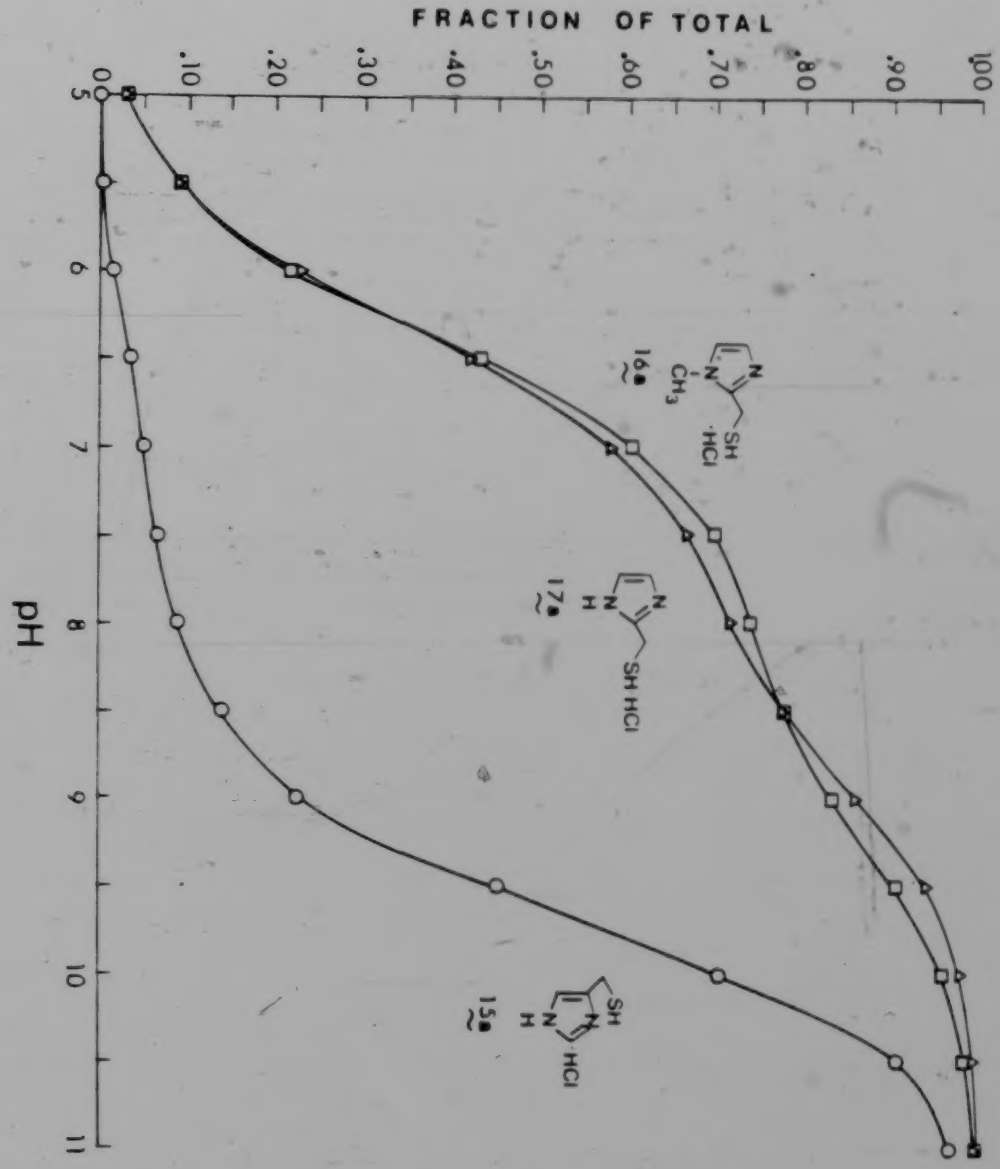

profile for the fraction of each species present as a function of pH. The concentrations of the thiolate species (III + IV) as a function of pH is given in Table 16 and plotted in Figure 14.

The original contention was that when the pKa^{SH} and pKa^{Im} values approached each other ($\triangle pKa < 2$) a substantial amount of zwitterionic material would be present at physiological pH.[45,60] This is reflected nicely in the microscopic pKa's given in Table 8. Note for example that for **15a**, $\triangle pKa, (pKa^{SH}-pKa^{Im}) = 2.94$ and $K_{Zw} = 0.07$. This means that at any pH, only 7% of the neutral species present is attributable to zwitterion. On the other hand, for **16a**, where $pKa^{SH}-pKa^{Im} = 1.7$, $K_{Zw} = 2.88$ this results in most of the neutral species present at any given pH as being in the form of the zwitterion (68% of the total species). A similar result is found for **17a** with $\triangle pKa = 1.92$, $K_{Zw} = 2.29$ and 63% of the total species existing in the zwitterionic form at pH 7.5.

The UV/VIS absorbances of **15a-17a** versus pH as shown in Figures 6b to 8b, also indicates large concentrations of the thiolate ion from pH 6.5-8. The thiolate concentration continues to increase until pH 10.5 at which point the $[RS^-]$ is constant. Although one can qualitatively observe what is most likely to be the H^+IMS^- species, as stated before, one cannot accurately determine its concentration by the UV-visible method.

Having shown that the zwitterionic species is dominant at pH 6.5 to 8 for compounds **16a** and **17a** but not **15a**, it was then necessary to determine if this species was nucleophilically active towards PNPA.

Evidence that the thiolate in the form of the zwitterion is nucleophilically active towards PNPA is shown by comparison of the pH versus log k_{cat} profiles for the **15a,b-17a,b** pairs given in Figure 7. For **15a** which shows only a small amount of zwitterion, H^+IMS^-, present at any given pH (see Figure 11), the observed plateau at pH 7.5 is comparable to that seen for the imidazole compound **15b**. This plateau region for **15a** is considered to be primarily due to nucleophilic attack on PNPA by the unprotonated imidazole. (Bender and Turnquist[55], and several other authors[61] have shown that an unprotonated imidazole can nucleophilically attack PNPA with a $k_{cat} = \sim 0.47\ M^{-1}sec^{-1}$ at 26.2 °C).

The imidazoles **16b** and **17b** are considered to be less nucleophilic than **15b** because of the steric encumberance provided by the 2-substituent.[62] This steric encumberance should also be the case for the thiol imidazoles **16a** and **17a**. However both **16a** and **17a** show plateau regions from pH 7-8 which are 10-15 fold greater in k_{cat} than those seen for their comparison imidazoles. This exalted activity must be the result of attack of the zwitterionic thiolate on PNPA. Note that from Figures 12 and 13, it is the zwitterion that

dominates in this pH range from 7-8.

Strong confirmatory evidence that the zwitterion is nucleophilically active towards PNPA comes from the fact that the plot of total thiolate concentration (III + IV) versus pH in Figure 14 shows a similar curvature to the plot of k_{cat} versus pH in Figure 3. This suggests that the active species for the attack on PNPA throughout the entire pH range are the thiolate species IMS^- and H^+IMS^- Since the former plot shows the same trends as the experimentally derived plot of k_{cat} versus pH, then it is reasonable to conclude that eqn. 23 appears to accurately describe the action of the model compounds **15a**, **16a** and **17a** on PNPA.

The rate constants k_1, k_2 and k_3 were calculated by a non-linear least squares fitting of the k_{cat} versus pH data for **15a-17a** to eqn. 23 using the microscopic pKa^{Im} and pKa^{SH} as well as the K_{Zw} values from Table 8. Separation of the composite term $Ka^{Im}(k_1 + k_3K_{Zw})$ to evaluate k_3 is made by assuming that k_1 for **15a-17a** is approximately the same as that of the corresponding imidazoles **15b-17b.** The rate constants are given in Table 17.

The zwitterionic activity for **16a** and **17a** is substantial as indicated by the large k_3. Jencks and Hupe[34] have shown that the rate constants for acyl transfer from PNPA to thiol anions shows a small sensitivity to thiol basicity with $\beta_{nuc} = 0.27$ for

Table 17. Computed rate constants for the attack of the various ionic forms of **15-17** on PNPA.

Compound	$k_1(M^{-1}min^{-1})$	$k_2(M^{-1}min^{-1})$	$k_3(M^{-1}min^{-1})$
15a[a]	b	2275	c
16a[a]	b	1071	162
17a[a]	b	1179	142
15b[d]	92.5		
16b[d]	7.64		
17b[d]	13.2		

a. Rate constants calculated from eqn. 23 based on pKa's determined from potentiometric titration data:
15a - $pKa^{Im} = 6.54$; $pKa^{SH} = 9.54$; $K_{Zw} = 0.07$
16a - $pKa^{Im} = 6.37$; $pKa^{SH} = 9.26$; $K_{Zw} = 2.88$
17a - $pKa^{Im} = 6.31$; $pKa^{SH} = 8.88$; $K_{Zw} = 2.29$

b. Values for k_1 which represents heterocyclic N attack on PNPA are assumed to be those of the corresponding imidazole.

c. Negligible relative to k_1.

d. Rate constants calculated from eqn. 24 based on pKa's from kinetic data:
15b - $pKa^{Im} = 7.56$; lit. = 7.51[63]
16b - $pKa^{Im} = 7.94$; lit. = 8.00[63]
17b - $pKa^{Im} = 7.64$; lit. = 7.85[63]

e. Cumulative errors resulting from likely deviations in pK values force the errors in k_2 to be 20% and in k_3 to be 5% but do not alter the conclusions presented in text.

rate-limiting attack of basic thiols if pKa(RSH) > pKa(leaving group) and $\beta = 0.84$ if pKa(RSH) < pKa(leaving group). At pKa 7.0 the break in the Bronsted plot occurs. The rate constant k_3 which represents zwitterion attack is smaller than that calculated for thiolate IMS$^-$ attack by an amount corresponding to the reduction of pK_1 versus pKa^{SH}. For example: By definition:

$$\log k_2 - \log k_3 = \beta(\log Ka^{SH} - \log K_1) + C_1 - C_2$$

From Table 8, for compound **16a**, $pKa^{SH} = 8.75$ and $pK_1 = 6.50$. Thus $\triangle k$(rate constant) $= \log^{-1}(0.27(8.75-7.00) + 0.84(7.0-6.50)) = 7.8$ fold lower rate. Experimentally, $\triangle k = k_2/k_3 = 1071/162 = 6.6$ fold lower. For compound **17a**, the $\triangle k$ is calculated to be 6.6 fold lower but experimentally is 8.3 fold lower. Considering, the potential cumulative errors in k_2 and k_3, the $\triangle k$'s are in good agreement.

From the evidence presented for the acylation of the model compounds **15a-17a**, it appears that substantial proportions of zwitterionic material can be present at physiological pH as the pKa^{Im} and pKa^{SH} approach each other. A model (**37**) recently synthesized by J.P. Street has $pKa^{SH} = 3.9$ and $pKa^{Im} = 9.0$.[45]

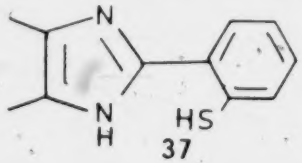

37

In this model (**37**) the pKa's have crossed and one finds that 99.9% zwitterion is present from pH 4 to 9. This is in total agreement with the contention that as the pKa's become only 2 units apart, cooperativity between the imidazole and the thiol(ate) occurs such that the pKa of the imidazole is raised by 2 pKa units and the pKa of the thiol is lowered by 2 pKa units. The pKa of a 2-phenyl-4,5-dimethylimidazole is 7.0 and the pKa of a phenyl thiol is 5.6-6.0. By incorporating these compounds into the model **37**, the pKa of the imidazole and thiol groups have been raised and lowered by 2 pKa units respectively as these groups interact to form a zwitterionic pair.

The evidence from the kinetic rate and titration studies for compounds **16a** and **17a** also indicates for the first time that the zwitterion is capable of nucleophilic attack on PNPA and that a cooperative effect between imidazole and thiol is possible provided that their individual pKa values are closely matched.

The 4(5)-mercaptomethylhydrochloride compound (**15a**·HCl) had been previously studied by Schneider[42]. However, Schneider only followed the reaction profile from pH 6 to 9 and not the more complete pH range from 5 to 11 as was done in this study. Although he obtained pKa values of 9.5 and 6.5 which correspond to the pKa values found in this study, he failed to consider the microscopic species (H^+ImSH, ImSH, H^+ImS^- and ImS^-) and

determine their pKa's. Also, he did not compare his rate of hydrolysis of PNPA catalysed by the imidazole-thiol compound with that of imidazole alone. Had he done so, he would have realized that this particular thiol compound did not react with PNPA at a rate exceeding that of imidazole alone at neutral pH and therefore the thiol(ate) group was not participating significantly. Although Schneider lacked the experimental proof, he did conclude "that cooperation between the imidazole and thiol groups occurs resulting in the concentration of the active catalytic species being greater than that computed on the basis of the pK of the thiol group."[42b] Compounds **16a** and **17a** are believed to be the first model compounds that support this conclusion.

(D) Product Studies

The reaction of equimolar quantities (4×10^{-4} M) of PNPA with **15a-17a** in deoxygenated 0.1 M (μ = 0.3 M) phosphate buffer at pH 7.8 at 25 ^{o}C was followed by monitoring the production of p-nitrophenoxide at 402 nm. The absorbance (after subtracting the blank reaction of PNPA alone) versus time data for these reactions is given in Table 18. The plot of ($1/Abs - 1/Abs_f$) versus time for **15a-17a** is shown in Figure 15.

The slope of the lines of these plots correspond to $-k_{cat}/\epsilon l$ where ϵ = 19054 M^{-1} cm^{-1} for p-nitrophenoxide

Table 18. Absorbance versus time data at λ = 402 nm for the reaction of equimolar quantities of PNPA and **15a-17a** at pH 7.8.[a]

Compound **15a**:

Time (min)	Absorbance (402 nm)	1/Abs	1/Abs - $1/Abs_f$
0	0		
15	0.1	10	7.78
25	0.17	5.88	3.66
35	0.25	4.00	1.78
55	0.35	2.86	0.64
70	0.40	2.50	0.28
100	0.45	2.22	0
130	0.45	2.22	0

Compound **16a**:

Time (min)	Absorbance (402 nm)	1/Abs	1/Abs - $1/Abs_f$
0	0.15	6.66	5.48
15	0.52	1.92	0.74
25	0.57	1.75	0.57
35	0.60	1.62	0.44
55	0.70	1.43	0.25
70	0.75	1.33	0.15
80	0.85	1.18	0
0[b]	0.50	2.00	0.92

Compound **17a**

Time (min)	Absorbance (402 nm)	1/Abs	1/Abs- $1/Abs_f$
0	0.10	10	9.33
15	0.80	1.25	0.58
25	0.90	1.11	0.44
35	1.00	1.00	0.33
55	1.25	0.80	0.13
70	1.50	0.67	0
80	1.50	0.67	0
0[b]	0.68	1.45	0.78

a. Reaction conducted at 25 ^{o}C in 3 ml of degassed 0.1 M (μ=0.3 M) phosphate buffer at pH 7.8 using

4×10^{-4} M PNPA and compound **15a-17a**.

b. Value extrapolated to zero time.

Figure 15: Second-order kinetics plot of $1/Abs - 1/Abs_f$ versus time for the reaction of 4(5)-mercaptomethylimidazole.HCl (15a) ○ ; N-methyl-2-mercaptomethylimidazole.HCl (16a) △ ; and 2-mercaptomethylimidazole.HCl (17a) □ ; with PNPA at equal molar concentrations of 4×10^{-4} M at 25 ^{o}C in pH 7.8, 0.1 M phosphate buffer.

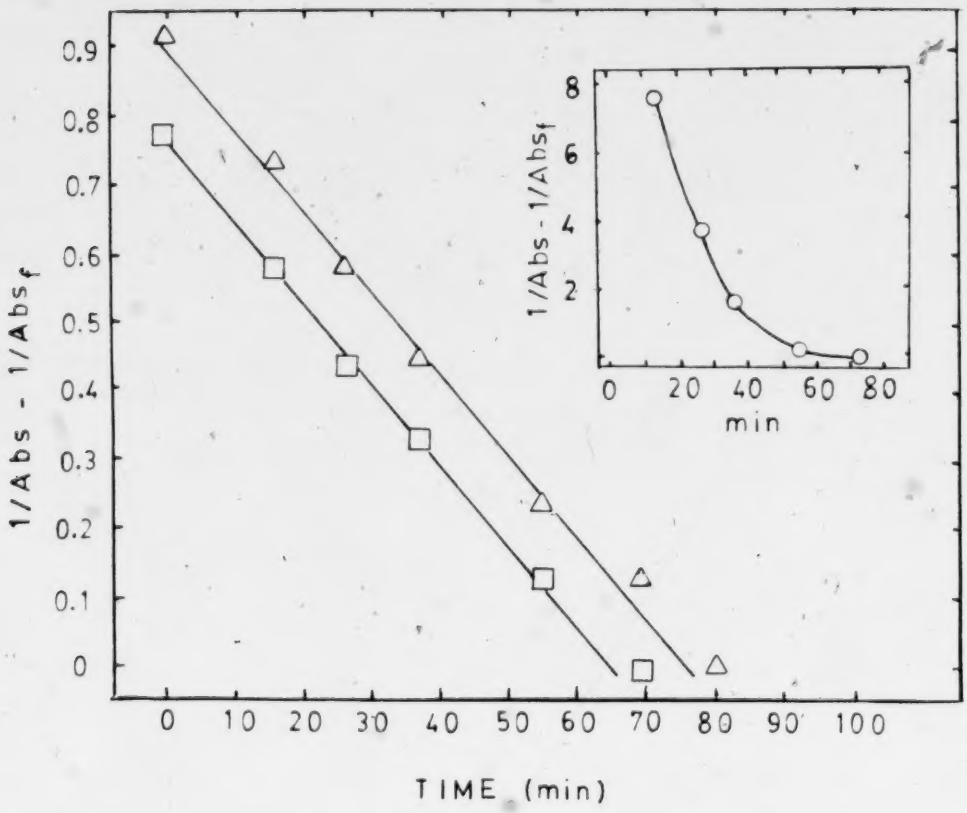

at 403 nm[67] and l = 1 cm. The kinetics observed for the production of the phenoxide for compounds **16a** and **17a** was second order with k_{cat} = 207 ± 50 $M^{-1}min^{-1}$ for **16a** and k_{cat} = 205 ± 65 $M^{-1}min^{-1}$ for **17a** calculated from the slope of the line in Figure 15. When allowances are made for the temperature differences, these constants compare favorable with the second order rate constants found at pH 7.8 at 37.6 °C by the pseudo-first-order method with k_{cat} = 167 $M^{-1}min^{-1}$ for **16a** and k_{cat} = 207 $M^{-1}min^{-1}$ for **17a**. (See Tables 2 and 3 respectively). Such second order kinetics for equal quantities of reactants implies the formation of a relatively stable S-acetyl compound along with p-nitrophenoxide as shown in eqn. 33.

33.

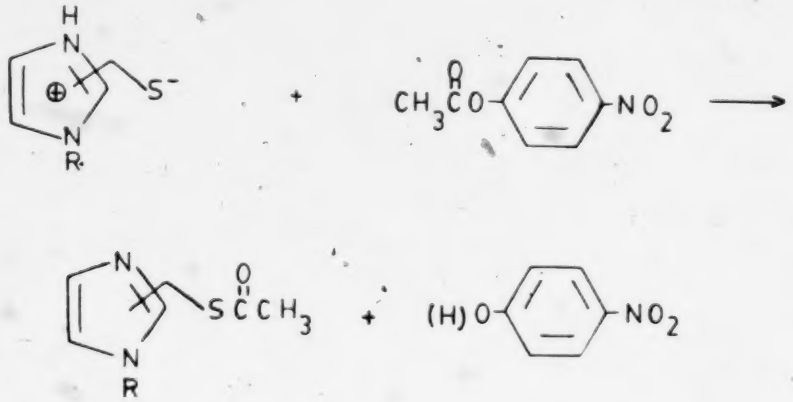

Compound **15a** does not follow second order kinetics as is evidenced by the nonlinearity of the plot of 1/Abs-1/Abs_f versus time in Figure 18. This is expected

as **15a** does not contain any significant amount of zwitterion material and the reaction with PNPA proceeds mainly by nucleophilic attack by the imidazole species (IMSH) on PNPA at pH 7.8. As the imidazole is known to nucleophilically attack PNPA with the formation of a labile N-acyl derivative[55], the reaction of PNPA and **15a** would follow pseudo-first-order kinetics.

Further evidence that an S-acetyl intermediate was formed during the reaction with PNPA was obtained by a ^{1}H-NMR study. Equimolar quantities of PNPA and compound **15a-17a** as its HCl salt were mixed in deoxygenated CD_3OD at room temperature giving a pH < 5. As the reaction proceeded, two methyl acetyl peaks were observed at 2.40 with δ = 0.1 for **15a**, δ = 0.15 for **16a** and δ = 0.2 for **17a** corresponding to the $OCOCH_3$ of PNPA and the $SCOCH_3$ of the S-acetyl intermediate. After a 24 hour period, 10, 10 and 18 % of the S-acetyl compounds of **15a**, **16a** and **17a** respectively were detected, the amounts being judged from the intensities of the $SCOCH_3$ singlets.

A similar experiment was conducted under neutral conditions in which the HCl salts of **15a-17a** were half neutralized with trimethylamine prior to reaction with an equimolar quantity of PNPA in deuterated methanol. At pH 7, **15a** did not show any formation of the methyl peak for $SCOCH_3$, yet after 24 hours, the reaction with PNPA was ~60% complete, this being judged by the

intensity of the $CH_3CO_2CD_3$ peak at δ = 2.05.

Compounds **16a** and **17a** reacted with PNPA to give the S-acetyl intermediate as evidenced by the formation of a strong $SCOCH_3$ peak at δ = 2.38. After 24 hours, the solvolysis of PNPA catalyzed by **16a** and **17a** was 100% complete. (A maximum intensity of the methyl peak due to $CH_3CO_2CD_2$ was observed.)

Under acidic conditions, the compounds exist as the fully protonated species (H^+IMSH) with < 5% as the zwitterionic species (H^+IMS^-). Under these conditions, all the model compounds react through the sulphur to form the S-acetyl intermediate and subsequently solvolyze to form the deuterated methyl acetate.

Under neutral conditions, **15a** exists mainly as the neutral species (IMSH) and nucleophilic attack on PNPA occurs through the imidazole nitrogen resulting in the N-acetyl intermediate. This intermediate immediately solvolyzes to give deuterated methyl acetate and **15a**. No attack through the sulphur to give the S-acetyl intermediate is observed. However, compounds **16a** and **17a** exist largely as zwitterions at neutral pH and attack occurs almost exclusively through the sulphur to give the S-acetyl intermediate. This intermediate solvolyzes over a day to give the deuterated methyl acetate.

The above evidence that an S-acetyl intermediate is formed at neutral pH, clearly defines the attacking

group as the thiolate anion in the zwitterionic form for **16a** and **17a**. Compound **15a** does not form an appreciable amount of zwitterion at any pH and nucleophilic attack on PNPA is mainly by the imidazole.

If the results presented in this thesis can be accurately transposed to the case of the acylation of papain by esters, then it is possible that the active site histidine 159 and cysteine 25 can indeed interact to form a zwitterion-like species. The formation of such electrostatically stabilized ion pairs offers an attractive method of ensuring that substantial concentrations of the nucleophilically active thiolate anion exist in the active site of papain at neutral pH.

(E) Deacylation

For deacylation of the thiol ester intermediate in papain mediated hydrolysis of esters and amides, it has been proposed that histidine imidazole acts as a general base in assisting the delivery of an attacking water molecule to the ester intermediate.[1,36a] This has been supported by a large solvent deuterium isotope effect measured for the enzymatic deacylation reaction.[18,21] As with the acylation studies, no model systems have been able to demonstrate a general base role for an imidazole unit in intramolecularly assisting thiol ester hydrolysis.

The acylated products of **15a**, **16a** and **17a** (38, 39

and **40** respectively) represent the acyl intermediates formed by the hydrolysis of PNPA by **15a-17a.**

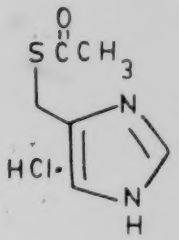

38

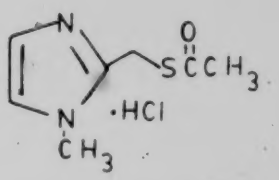

39

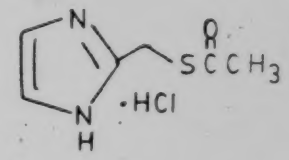

40

With these compounds it should be possible to study the solvolysis of an acyl thiol intermediate similar to the thiol ester intermediates in papain and to determine the involvement of imidazole either as a general base or as a nucleophile in breakdown of the acyl intermediate.

Although the results of the deacylation study are not complete, the evidence found thus far suggests intramolecular general base catalysis of the solvent attack on the thiol ester by imidazole is occurring.[60]

III. EXPERIMENTAL

A. MATERIALS

Sodium acetate, succinic acid, disodium phosphate, boric acid, sodium carbonate, imidazole and N-methyl imidazole were all reagent grade. The *p*-nitrophenyl acetate was recrystallized from Skelly B. Water was triply glass distilled. D_2O, $(CD_3)_2SO$, CD_3OD (Merck, Sharp, Dohme Canada) was 99.7% isotopically pure.

Synthesis

Routine IR, ^{1}H-NMR and mass spectra were recorded on a 7199-Nicolet FT-IR spectrophotometer, a Bruker WP80 (80 MHz) spectrometer and an AE1 MS-50 spectrometer respectively. ^{1}H-NMR spectra are referenced to TMS and IR spectra were obtained as casts.

4(5)-Hydroxymethylimidazole picrate (20)

To a 500 ml metal bomb provided with a magnetic stir bar was added 52 g (0.5 mol) of formamidine acetate,[64] 45 g (0.5 mol) of 1,3-dihydroxyacetone and 450 ml of anhydrous liquid ammonia. The bomb was closed and the mixture stirred at 50-55 ^oC overnight (15-20 hours). The ammonia was then evaporated and the remaining yellow-reddish oil was dissolved in 200 ml boiling water and added to a boiling solution of 85 g of picric acid

in 3 l of water. After treatment with charcoal and filtation, the solution was allowed to cool to room temperature after which 89 g (59% yield) of yellow needles were obtained. m.p. 205-207 °C (lit.[47] m.p. 205-207 °C).

IR(MeOH, cm^{-1}): 3040, 1640, 1620, 1576, 1496, 1335

NMR($(CD_3)_2SO$) δ 9.05(s,1H), 8.63(s,2H), 7.05(s,1H), 4.07(s,2H)

Mass spectrum m/z (rel intensity) 98(M^+,65), 97(100), 91(42), 81(28), 69(48), 62(65)

Exact mass calcd. as the free base $C_4H_6N_2O$: 98.0461; found, 98.0476

Anal. calcd. for $C_{10}H_9N_5O_8$: C,86.69; H,2.77; N,21.41; O,39.13. Found: C,36.96; H,2.69; N,21.30; O,39.05

Formamidine acetate (**18**)

Formamidine acetate was prepared according to the procedure by Taylor, et al.,[64] in 70% yield.

m.p. 160-2 °C (lit.[64] m.p. 162-164 °C)

NMR($(CD_3)_2SO$) δ 8.90(broad,4H), 7.75(s,1H), 1.75(s,3H)

Mass spectrum m/z (rel intensity) 60(34), 45(66), 43(100)

4(5)-Hydroxymethylimidazole hydrochloride (**21**)

To a 2 l flask was added 72 ml (0.8 mol) of 37% hydrochloric acid, 200 ml of water and 400 ml of benzene. This was immersed in a water bath at 80 °C and

72 g (0.26 mol) of 4(5)-hydroxymethylimidazole picrate was added to the stirring solution. The benzene layer was then decanted and the aqueous layer extracted five times with 300 ml portions of benzene. After treatment of the water layer with Norite and filtation, the water was evaporated under vacuum to obtain yellow crystals. Recrystallization from ethanol-ether gave 27 g (93% yield) of white crystals. m.p. 107-109 °C (lit.[48] m.p. 107-109°C)

IR(MeOH, cm^{-1}): 3100, 1608, 1460, 1040, 830, 615

NMR(CD_3OD) δ8.95(s,1H), 7.50(s,1h), 4.75(s,2H)

Mass spectrum m/z (rel intensity) 98(M^+,64), 97(100)

Exact mass calcd. as the free base $C_4H_6N_2O$: 98.0481; found, 98.0475

Anal. calcd. for $C_4H_7N_2OCl$: C,35.81; H,5.26; N,20.89; O,11.93; Cl,26.16 Found: C,35.89; H,5.25; N,21.06; O,11.94; Cl,25.86

N-Methyl-imidazole-2-carboxaldehyde (24)

To a 2 l 3-neck flask containing a solution of 550 ml dry THF and 27 ml (0.34 mol) of N-methylimidazole under N_2 at -40 °C was added via syringe 0.37 mol of n-BuLi in hexane. This was then stirred for 40 minutes at -40 °C after which time 40 ml (0.52 mol) of dry redistilled dimethylformamide was slowly added and the mixture left to warm to room temperature. After 16-20 h, 550 ml of ether was added and the reaction mixture

extracted with 1.5 N HCl (5x200 ml). The acid extracts were neutralized to pH 7.6 with solid $NaHCO_3$ and this solution was extracted with CH_2Cl_2 (5x200 ml). The organic extracts were dried over Na_2SO_4, filtered and the solvent removed under vacuum. The remaining liquid was distilled (58 °C at 0.250 torr) giving 31 g (83% yield) of crystalline solid. m.p. 33-34 °C s.t. (lit.[49] m.p. 32-34 °C s.t)

IR($CHCl_3$, cm^{-1}): 1685 (C=O)

NMR($CDCl_3$) δ 9.80(s,1H), 7.25(s,1H), 7.20(s,1H), 4.05(s,3H)

Mass spectrum m/z (rel intensity) 110(M^+,100), 109(15), 82(56), 81(39)

Exact mass calcd. for $C_5H_6N_2O$: 110.0480; found 110.0473

Anal. calcd for $C_5H_6N_2O$: C,54.52; H,5.49; N,25.45; O,14.55. Found: C,54.57; H,5.46; N,25.16; O,14.81

N-(1,1-diethoxymethyl)imidazole (**25**)

N-(1,1-diethoxymethyl)imidazole was prepared according to the method of Brown and Curtis[50a] in 76% yield. b.p. 79 °C at 0.35 torr (lit.[50a] b.p. 79.3 °C at 0.35 torr)

NMR($CDCl_3$) δ 7.65(s,1H), 7.05(m,2H), 6.02(s,1H), 3.60(q,4H) 1.25(t,6H)

Imidazole-2-carboxaldehyde (26)

To a 2 l 3-neck round bottom flask was added 500 ml dry THF and 85 g (0.50 mol) of N-(1,1-diethoxymethyl)-imidazole. To this cooled solution (-55 °C) was added 0.55 mol of n-BuLi in hexane and the resulting pale orange solution was stirred for 40 minutes at -40 °C. Then 60 ml (0.75 mol) of dried, distilled dimethylformamide was added slowly and the solution left to warm to room temperature. After 16-20 h, 500 ml of ether was added and the reaction mixture extracted with 1.5 N HCl. The acid extracts were adjusted to pH 7.6 with solid $NaHCO_3$ at which point the aldehyde precipitated from the solution. The water layer was filtered to yield 27 g of crude product. Evaporation of the water layer under vacuum gave a furthur 9 g of crude product. (m.p. 200-205 °C) Sublimation of the crude product gave 35 g (76% yield) of white crystals. m.p. 206-207 °C sealed tube (lit.[49] m.p. 195 °C)

IR($CHCl_3$-MeOH, cm^{-1}): 1635 (C=O)

NMR($(CD_3)_2SO$) δ 9.70(s,1H), 7.40(s,2H)

Mass spectrum m/z (rel intensity) 96(M^+,100), 68(54)

Exact mass calcd. for $C_4H_4N_2O$: 96.0324; found 96.0324

Anal. calcd. for $C_4H_4N_2O$: C,49.98; H,4.20; N,29.16; O,16.65 Found: C,49.95; H,4.13; N,28.88; O,17.04

N-Methyl-2-hydroxymethylimidazole (27)

To a solution of 4.8 g (0.29 mol) of N-methyl-imidazole-2-carboxaldehyde in 80 ml dry MeOH cooled to 0 °C was added 2.5 g (0.44 mol) of sodium borohydride in small portions. The reaction mixture was slowly warmed to room temperature and stirred overnight. After 16-20 h, the reaction was quenched with 10 ml of water and the solvent removed under vacuum. The product was extracted from the borate salts with hot chloroform and the chloroform extracts dried over Na_2SO_4. Removal of the chloroform under vacuum left 4.0 g (82% yield) of a white crystalline solid. m.p. 108-110 °C (lit.[52] m.p. 114 °C)

IR($CHCl_3$, cm^{-1}): 3185-3145 (OH)

NMR($CDCL_3$) δ 6.85(m,2H), 6.60(broad,1H), 4.65(s,2H), 3.70(s,3H)

Mass spectrum m/z (rel intensity) 112(M^+,100), 95(30)

Exact mass calcd. for $C_5H_8N_2O$: 112.0637; found 112.0630

Anal. calcd. for $C_5H_8N_2O$: C,53.54; H,7.19; N,24.99; O,14.28 Found: C,53.21; H,7.13; N,24.88; O,14.78

2-Hydroxymethylimidazole (28)

This was prepared following the procedure as for N-methyl-2-hydroxymethylimidazole except extraction of the crude product from the reaction mixture required continous extraction for 90-115 h with a 4:1:1 mixture

of ether:chloroform:ethanol. Removal of the solvent and recrystallization of the crude product from ethanol resulted in 14 g (43% yield) of white crystals.

m.p. 112-114 °C (lit.[49] m.p. 114 °C, lit.[53a] m.p. 112 °C)

IR($CHCl_3$-MeOH, cm^{-1}): 3080 (OH)

NMR($(CD_3)_2SO$) δ 6.90(s,2H), 4.45(s,2H)

Mass spectrum m/z (rel intensity) 98(M^+,100), 97(35), 81(26)

Exact mass calcd. for $C_4H_4N_2O$: 98.0481; found 98.0478

General Procedure for Preparation of Chloromethylimidazole Hydrochlorides

To a 100 ml flask was placed 30-40 ml of freshly distilled thionyl chloride. In small portions 0.2-0.5 mole of the hydroxymethylimidazole was added. The solution was heated to 55 °C and stirred for 30 minutes. The excess thionyl chloride was removed under vacuum below 60 °C. The remaining solid was washed with ether and recrystallized from ethanol-ether.

4(5)-Chloromethylimidazole hydrochloride (**29**)

Yield 98%, m.p. 142-144 °C (lit.[53c] m.p. 144 °C)

IR(KBr, cm^{-1}) 3140, 1610, 1460, 1420

NMR($(CD_3)_2SO$) δ 9.26(s,1H), 7.90(s,1H), 5.00(s,2H)

Mass spectrum m/z (rel intensity) 116(M^+,22), 81(100)

Exact mass calcd. as the free base $C_4H_6N_2Cl$: 116.0143; found 116.0144

Anal. calcd. for $C_4H_6N_2Cl_2$: C,31.58; H,3.98; N,18.43; Cl,46.04. found: C,31.38; H,3.92; N,18.63; Cl,46.16

N-Methyl-2-chloromethylimidazole hydrochloride (**30**)

Yield 92% m.p. 175-177 °C (lit.[53b] m.p. 175-177 °C)

IR(MeOH, cm^{-1}) 3109, 2995, 780, 755, 665, 625

NMR($(CD_3)_2SO$) δ 7.90(d,1H), 7.75(d,1H), 5.30(s,2H), 3.95(s,3H)

Mass spectrum m/z (rel intensity) 130(M^+,20), 95(100)

Exact mass calcd. as the free base $C_5H_7N_2Cl$: 130.0302; found 130.0297

2-Chloromethylimidazole hydrochloride (**31**)

Yield 71%, m.p. 151-153 °C

IR($CHCl_3$, cm^{-1}): 3400, 3126, 1610, 1430, 1310, 897, 795, 727

NMR(CD_3OD) δ 7.65(s,2H), 5.10(s,2H)

Mass spectrum m/z (rel intensity) 116(M^+,23), 81(100), 54(32)

Exact mass calcd. as the free base $C_4H_5N_2Cl$: 116.0143; found 116.0143

General Procedure for the Preparation of (Benzylmercaptomethyl)imidazole Hydrochlorides

To a solution consisting of 100 ml of 1.3 N sodium methoxide in methanol, 70 ml dry ethanol and 2.0 equivalents of benzyl mercaptan held at reflux was added through the reflux condenser a solution of 0.06-0.10 mole of chloromethylimidazole hydrochloride in 70 ml of ethanol. After 16-20 h at reflux, the solution was acidified to pH 1.0 with 20% ethanolic HCl and the salts removed by filtration. The solvent was reduced to 60 ml under vacuum and 120-150 ml of water added. The excess benzyl mercaptan was extracted with ether and the remaining aqueous layer reduced under vacuum to a yellow oil. If possible, the oil was crystallized from ethanol-ether.

4(5)-(Benzylmercaptomethyl)imidazole hydrochloride (**32**)

Yield 68% m.p. 138-143 °C (lit.[65] m.p. 143-144 °C)
IR($CHCl_3$, cm^{-1}) 3087, 2964, 2616, 2538, 702 cm^{-1}
NMR(CD_3OD) δ 8.80(s,1H), 7.55(s,6H), 3.78(s,4H)
Mass spectrum m/z (rel intensity) 204(M^+,9), 113(3), 91(28), 82(100), 81(74)
Exact mass calcd. as the free base $C_{11}H_{12}N_2S$: 204.0722; found 204.0720

N-Methyl-2-(benzylmercaptomethyl)imidazole hydrochloride (**33**)

Yield 46% m.p. 155-157 °C

IR($CHCl_3$, cm^{-1}): 3120, 2897, 2650, 1597, 1287, 712, 703

NMR(CD_3OD) δ 7.25(m,7H), 4.10(s,2H), 3.90(s,2H), 3.75(s,3H)

Mass spectrum m/z (rel intensity) 96(100%), 95(37%)

Exact mass calcd. as the free base $C_{12}H_{14}N_2S$: 218.0879; found 217.9946

Anal. Calcd. for $C_{12}H_{15}N_2SCl$: C,56.69; H,5.90; N,11.02; S,12.60; Cl,13.78 found: C,56.45; H,5.98; N,10.91; S,12.60; Cl,14.06.

2-(Benzylmercaptomethyl)imidazole hydrochloride (**34**)

Yield 96% oil

IR($CHCl_3$, cm^{-1}): 3039, 2822, 2687, 2550, 1610, 765, 704

NMR(CD_3OD) δ 7.30(s,2H), 7.25(s,5H), 4.0(s,2H), 3.85(s,2H)

Mass spectrum m/z (rel intensity) 204(M^+,0.2), 91(22), 82(100)

Exact mass calcd. as the free base $C_{11}H_{12}N_2S$: 204.0722; found 204.0707

General Procedure for Preparation of Mercaptomethyl-imidazole Hydrochloride

To a 1 l flask under an atmosphere of N_2 was added 0.025 mol of the (benzylmercaptomethyl)imidazole hydrochloride in 300 ml liquid anhydrous ammonia (-33 ^{o}C). To this was added in small portions 3 equivalents of sodium metal until a blue colour persisted. The reaction mixture was stirred for 30-40 minutes then quenched with solid ammonium chloride. The ammonia was allowed to evaporate under a nitrogen flow. The remaining solid was dissolved in 200 ml dry ethanol and made acidic with 20% ethanolic HCl (120 ml). The solution was filtered and the solvent reduced to 30 ml under vacuum. The solution was filtered again and then all the solvent was removed. The final mercaptan product was recrystallized 2-3 times from ethanolic HCl which was deoxygenated by bubbling argon through the solution for 4 hours prior to use. The percentage of free thiol was determined by titration with iodine in ethanolic solution as described by Harnish and Tarbell.[66] The product was kept under a vacuum and was stable towards oxidation for periods of 3 to 4 weeks.

Reduction of the Disulfide

The disulfide of the three mercaptan compounds could be reduced to their respective mercaptans using tributylphosphine. In a typical experiment, 0.002 moles

of the disulfide of 4(5)-mercaptomethylimidazole hydrochloride was placed in a 25 ml round-bottom flask and septum-sealed. After flushing with argon for 15 minutes, 5 ml of deoxygenated methanolic HCl was added to the flask via syringe and the disulfide dissolved. 1 ml of tributylphosphine was then added via syringe and the mixture stirred at room temperature for 20 min. 10 ml of deoxygenated 0.1 N HCl was added and the unreacted tributylphosphine and tributylphosphine oxide extracted with chloroform (4x10 ml) under argon via syringe. The remaining aqueous layer was evaporated under vacuum and the crude solid recrystallized from deoxygenated ethanolic HCl and ether to give pure mercaptan. Yields >85%.

4(5)-Mercaptomethylimidazole hydrochloride (**15a**)

Yield 51% m.p. 119-121 °C (lit.[39d] m.p. 119-120 °C)

IR(KBr, cm^{-1}): 3830, 3106. 2597, 2352, 1614, 821, 622

NMR($(CD_3)_2SO$) δ 12.0(broad,2H), 9.04(d,1H), 7.48(d,1H), 3.80(d,2H), 3.54(t,1H)

Mass spectrum m/z (rel intensity) 114(M^+,59), 81(100)

Exact mass calcd. as the free base $C_4H_6N_2S$: 114.0253; found 114.0252

Anal. calcd. for $C_4H_6N_2S.HCl$: C,32.0; H,4.70; N,18.67; S,21.31; Cl,23.31. Found: C,31.73;

H,4.72; N,18.41; S,21.56; Cl,23.27

I_2 titration: 99.3 + 0.5%

N-Methyl-2-mercaptomethylimidazole hydrochloride (16a)

Yield 59% m.p. 114-118 °C

IR(KBr, cm^{-1}): 3425, 3152, 1589, 1298, 1101, 782, 642

NMR($(CD_3)_2SO$) δ 7.6(m,2H), 4.1(s,2H), 3.80(s,4H)

Mass spectrum m/z (rel intensity) 128(M^+,100), 95(79), 83(18)

Exact mass calcd as the free base $C_5H_8N_2S$: 128.0409; found 128.0409

Anal. calcd. for $C_5H_8N_2S.HCl$: C,36.58; H,5.53; N, 17.08; S,19.49; Cl,21.32. Found: C,36.18; H,5.51; N,16.99; S,19.2; Cl,21.2

I_2 titration: 98.6 + 0.5%

2-Mercaptomethylimidazole hydrochloride (17a)

Yield 60% m.p. 77-85 °C Unable to recrystallize product due to the presence of 10-15% disulfide

IR(KBr, cm^{-1}): 3481, 3125, 1611, 1080, 856, 761

NMR($(CD_3)_2SO$) δ 7.55(s,2H), 4.0(broad,3H)

Mass spectrum m/z (rel. intensity) 114(M^+,100), 81(98), 69(16)

Exact mass calcd. as the free base $C_4H_6N_2S$: 114.0253; found 114.0250

I_2 titration: 85-90% (15-10% disulfide)

Satifactory microanalyses could not be obtained due to extreme ease of oxidation to disulfide.

B. BUFFERS

Oxygen-acid buffers (acetate, succinate, phosphate, borate and carbonate) were prepared to 0.1 M, u=0.3 M (KCl) in triply distilled water except for the buffer used in the following D_2O experiments.

D_2O Experiment

Matching 0.1 M, u=0.3 M carbonate buffers were prepared in water and 99.7% D_2O. pD was determined by adding +0.4 units to the meter reading. These buffers correspond to the points at pH 10.0 and 10.1 in Figure 3.

C. KINETICS

All kinetic studies were done using a Cary 210 UV-VIS spectrophotometer equipped with a cell programmer, a wavelength programmer and a timer accessory. The equipment was interfaced to a computer for data collection and processing. Temperature was maintained at 37.6 ± 0.3 ^{o}C by means of an external Colora Model NB-ELE circulating water bath.

Acetate buffer was used from pH 5.0 to 5.5, succinate from 5.6 to 6.5, phosphate from 6.7 to 7.7, borate from 8.0 to 9.5 and carbonate from 9.7 to 11.0.

All buffers were deoxygenated by bubbling argon through the solution for 4 to 16 h. Then 3 ml of the

buffer was transferred via syringe to argon flushed septum-sealed 1 cm quartz cells via syringe and allowed to equilibrate at 37.6 ^{o}C in the spectrophotometer for 20 minutes prior to initiation of a run. Stock solutions of **15a-17a** were prepared in deoxygenated 0.1 N HCl by carefully deoxygenating 1 ml volumetric flasks containing $1x10^{-4}$ moles of mercaptan and transferring the deoxygenated HCl via syringe to these flasks. The concentration of the stock solutions of **17a** were corrected to account for a purity of 85% mercaptan since iodometric titration showed 15% oxidation had occurred. The stock solutions of **15a** and **16a** did not require correction factors as each compound's purity was 99%. These solutions were frozen when stored between runs and periodically replaced.

For the acylation kinetic studies, 5 ul of a stock solution of $2.6x10^{-2}$ M p-nitrophenylacetate in ethanol solvent was first injected into 3 ml of buffer in the quartz cell. Reactions were initiated by injecting a 10-100 fold excess of the thiol **15a-17a** into the cuvette. The rate of reaction of p-nitrophenylacetate was followed by observing the rate of appearance of p-nitrophenoxide at 400 nm.

Observed pseudo-first order rate constants (k_{obs}) for the acylation studies were obtained by fitting the absorbance versus time data to a standard exponetial equation via a non-linear least squares program.

Second order rate constants for acylation were calculated from the slope of k_{obs} versus [imidazole-thiol]. These results are given in Tables 1-6.

The presence of buffer catalysis for the acylation process was tested for by using 0.05, 0.1, and 0.3 M borate buffers at pH 7.8, 9.0 or 10.0. No buffer catalysis was observed.

pH was determined using a separate glass and saturated calomel electrodes (Fisher model) and a Fisher Model 825 MP meter standardized at pH 4.0, 7.0, and 10.0 using standard buffer solutions (Fisher). pH measurements of all reaction mixtures were taken before and after every kinetic run. No deviations greater than 0.03 units were found.

D. UV TITRATIONS

UV spectra from 200 to 400 nm were taken of 1×10^{-5} mole of **15a-17a** at various pH's using a Hewlett Packard 8450A Diode Array UV/VIS spectrophotometer with built in microprocessor. The temperature of the cells were maintained at 25 ^{o}C using a Hewlett Packard 8900A Temperature controller and the spectra plotted with a Hewlett Packard 7470A plotter.

A specially designed 1 cm quartz cuvette capable of holding 90 ml of solution under deoxygenated conditions and constant pH monitoring was made for this study. (See Appendix 6)

The cuvette containing 1.0-1.5 mg of the mercaptan was flushed with argon at 25 ^{o}C for 1 hour. 80 ml of pH 3 aqueous HCl (deoxygenated with argon for 16 h) was added to the cuvette via syringe and the solution titrated with 0.1 N NaOH added gradually via syringe. At every 0.2 to 0.5 pH units, the UV spectrum from 200 to 400 nm was recorded and stored in the computer. Analysis of the UV absorbance change by Edsall's method[59] at λ = 240 nm for **15a**, λ =262 for **16a** and λ =255 for **17a** versus pH gave the microscopic pKa's for these compounds. (See Appendix 4)

E. POTENTIOMETRIC TITRATIONS

The titrations were performed in a 4 cm^3 jacketed cell kept at room temperature and under a constant flow of argon bubbled through a solution of barium hydroxide to remove carbon dioxide and oxygen. The pH was measured using a Radiometer TTT2 titrator and PHA 943B titrator module in conjunction with a Radiometer 6K2402B combination electrode. The pH was recorded as a function of added deoxygenated 0.0100 N NaOH delivered by a Radiometer ABU12 autoburette, on a Radiometer SBR 3 titragraph.

A 5 ml stock solution containing 6 mg of **15a-17a** or 25 mg of the benzylated compounds was made in 0.002 N HCl and 1.0 ml aliquots of these solutions were added to 5 ml of deoxygenated distilled water in the jacket cell

and the titration begun. Analysis of the data by a computer version of the Simm's Method[56] (Appendix 3) gave the pKa's for each run. Reported pKa's are the average of at least two determinations.

F. PRODUCT STUDIES

(a) Second-Order Kinetics

To a deoxygenated (1 h under argon) 1 cm quartz cell containing 1.2×10^{-6} moles of compound **15a-16a** was added via syringe 3 ml of deoxygenated (16 h under argon) 0.1 M phosphate buffer (μ = 0.3 M) at pH 7.8. The reaction was initiated by injecting 45 μl of 2.62×10^{-2} M solution of PNPA (1.2×10^{-6} moles) and was monitored by following the production of p-nitrophenoxide at 402 nm over time. The absorbance versus time data is given in Table 18. The data was analyzed for second order kinetics.

(b) ^{1}H-NMR Study

To a deoxygenated (1 h with argon) NMR tube containing an equimolar quantity (7×10^{-5} mole) of **15a-17a** and PNPA was added via syringe 0.5 ml of deoxygenated (4 h under argon) CD_3OD. The ^{1}H-NMR spectra of this acidic reaction mixture were taken at t= 0, 24 and 288 hours. The formation of the S-acetyl compound was monitored by observing the peak for $SCOCH_3$ at δ = 2.35, 2.45 and 2.45 for **15a**, **16a** and **17a**, respectively. As the reaction proceeded, the $SCOCH_3$ peak increased while

the $OCOCH_3$ for PNPA at $\delta = 2.40$ decreased.

A similar experiment was conducted under neutral conditions. To a 1 ml deoxygenated flask containing 7×10^{-5} mole of **15a-17a** was added 0.5 ml of deoxygenated deuterated methanol and 7×10^{-5} mole of trimethylamine which neutralized the imidazole. This solution was then added to a deoxygenated NMR tube containing equimolar PNPA. The ^1H-NMR spectra of this neutral reaction mixture were taken at t = 2.5 and 24 hours. The $SCOCH_3$ peak for the S-acetyl intermediate was observed for compounds **16a** and **17a** but not **15a**.

BIBLIOGRAPHY

1. (a) A.N. Glazer and E.L. Smith in "The Enzymes", P.D. Boyer, Ed. Vol. III, Third Ed., Academic Press, New York, 1971, pp. 502-546.
   (b) L.Polgar, **Int. J. Biochem.**, 8, 171 (1977).
   (c) C.J. Drenth, **Recueil des Travaux Chemiques des Pays-Bas**, 99, 185 (1980).
2. (a) R.C. Wong and I.E. Liener, **Bioc. Biop. Res. Com.**, 17, 470 (1964)
   (b) S.S. Husain and G. Lowe, **Chem. Commun.**, 1397 (1968)
   (c) J.N. Tsunada and K.T. Yasunobu, **J. Biol. Chem.**, 240, 4610 (1966).
   (d) M. Castaneda-Agulto, A. Hernandez, F. Loaeza and W. Salazar, **J. Biol. Chem.**, 159, 751 (1945)
   (e) D.C. Carpenter and F.E. Lovelace, **J. Am. Chem. Soc.**, 65, 2364 (1943).
   (f) F.G. Lennox and W.J. Ellis, **Biochem. J.**, 39, 465 (1945).
   (g) E.N. Baker, **J. Mol. Biol.**, 115, 263, (1977).
3. (a) W.N. Mitchell and W.F. Harrington, in "The Enzymes", P.D. Boyer, Ed., Vol. III, Third Ed., Academic Press, New York, 1971, pp. 699-719.
   (b) T.Y. Liu and S.D. Elliot, **ibid.**, pp. 609-649
4. The first report of the consequences of the organism manufacturing clostripain were those of

M. Weinberg and P. Sequin, **Compt. Rend.**, 163, 449 (1916) on the basis of wound cultures taken from victims of gas gangrene.

5. (a) E.L. Smith, J.R. Kimmel, D.M. Brown and E.O.P. Thompson, **J. Biol. Chem.**, 215, 57 (1955).

(b) J.B. Howard and A.N. Glazer, **J. Biol. Chem.** 242, 5715 (1967).

(c) A.N. Glazer, A.O. Borel, J.B. Howard and D.M. Brown **J. Biol. Chem.**, 244, 3583 (1969).

6. (a) Commercial meat tenderizing agents list papain as their active ingredients.

(b) A well known Mexican women's tonic consists of papaya skin rubbed over the face to give a "youthful fresh appearance", see M. Briskin and L.S. Briskin in "Make your own Cosmetics", Dell Publishing Co., 1971, p. 63.

(c) S.J. Taussig, M.M. Yokoyama, A. Chinen, K. Onari, M. Yamakido, and Y. Nishimoto, Hiroshima, **J. Med. Sci.**, 24, 185 (1975): Bromelain, A proteolytic enzyme; its clinical applications, a review.

(d) G. Reed in "Enzymes in Food Processing", Academic Press, New York, 1966, pp 123-405.

7. J.R. Kimmel and E.L. Smith, **J. Biol. Chem.**, 207, 515 (1954)

8. (a) J. Drenth, J.N. Jansonius, R. Koekoek and B.G. Wolthers in "The Enzymes", P.D. Boyer, Ed., Vol. III, Academic Press, New York, 1971, pp. 485-499.

(b) J. Drenth, J.N. Jansonius and B.G. Wolthers, **J. Molec. Biol.**, 24, 449 (1967).

(c) J. Drenth, J.N. Jansonius, R. Koekoeck, H.M. Swen and B.G. Wothers, **Nature**, London 218, 929 (1968).

(d) J. Drenth, K.H. Kalk and H.M. Swen, **Biochemistry**, 15, 3731 (1976).

9. (a) J.R. Kimmel, H.J. Rogers, and E.L. Smith, **J. Biol. Chem.**, 240, 266 (1965).

(b) M.A. McDowall and E.L. Smith, **J. Biol. Chem.**, 240, 281 (1965).

(c) A. Light, R. Frater, J.R. Kimmel, and E.L. Smith **Proc. Natl. Acad. Sci. U.S.**, 52, 1276 (1964).

(d) R.E.J. Mitchel, I.M. Chaiken and E.L. Smith, **J. Biol. Chem.**, 245, 3485 (1970).

(e) S.S. Husain and G. Lowe, **Biochem. J.**, 114, 279 (1969); 116, 689 (1970).

10. A. Stockell and E.L. Smith, **J. Biol. Chem.**, 227, 1 (1957).

11. (a) J. Weisz, **Chem. Ind.** (London), 15, 685 (1937).

(b) I.B. Wilson, F. Bergmann and D. Nachmansohn, **J. Biol Chem.**, 186, 781 (1950).

12. E.L. Smith, B.J. Finkel and A. Stockell, **Dis. Faraday Soc.**, 20, 96 (1955).

13. E.L. Smith and M.J. Parker, **J. Biol. Chem.**, 233, 1387 (1958).

14. (a) S.A. Bernhard and H. Gutfreund, **Biochem. J.**, 63, 61 (1956).

(b) B.R. Hammond and H. Gutfreund, **ibid**, 72, 349 (1959).

15. G.R. Schonbaum and M.L. Bender, **J. Am. Chem. Soc.**, 82, 1900 (1960).

16. (a) G. Lowe and A. Williams, **Biochem. J.**, 96, 189 (1965).

(b) A.C. Storer, W.F. Murphy and P.R. Carey, **J. Biol. Chem.**, 254, 3163 (1979).

17. K. Brocklehurst, E.M. Cook and C.W. Wharton, **Chem. Comm.**, 1185 (1967).

18. (a) L.J. Brubacker and M.L. Bender, **J. Am. Chem. Soc.**, 88, 5871 (1960).

(b) **ibid., idem.**, 86, 5333 (1964).

(c) M. Smolarsky, **Isr. J. Chem.**, 12, 615 (1974).

19. A.I. Scott, J.P.G. Malthouse, M.P. Gamcsik, A.S.F. Boyd, and N.E. MacKenzie, **J. Am. Chem. Soc.**, 104, 6811 (1982).

20. A.I. Scott, J.P.G. Malthouse, M.P. Gamcsik, W.A. Prinrose, N.E. MacKenzie, A.S.F. Boyd, and R.A. Russell, **J. Am. Chem. Soc.**, 105, 6324 (1983).

21. (a) J.R. Whitaker and M.L. Bender, **J. Am. Chem. Soc.**, 87, 2728 (1965).

(b) V.I. Zannis and J.F. Kirsch, **Biochemistry**, 17, 2669 (1978).

22. C.D. Hubbard and J.F. Kirsch, **Biochemistry**, 11, 2483 (1972)

23. (a) G. Lowe, reported in **Phil. Trans. Roy. Soc. London**, 257, 237 (1970).
(b) P.M. Hinkle and J.F. Kirsch, **Biochemistry**, 9, 4633 (1970).

24. (a) S.D. Lewis, F.W. Johnson and J. Shafer, **Biochemistry**, 15, 5009 (1976).
(b) L. Polgar, **Eur. J. Biochem.**, 71, 563, (1976).

25. B.J. Finkle and E.L. Smith, **J. Biol. Chem.**, 230, 669 (1958).

26. S.S. Husain and G. Lowe, **Biochem. J.**, 108, 855, 861 (1968).

27. K. Morihara and K. Nagami, **J. Biochem.** (Tokyo), 65, 321 (1969).

28. (a) R.B. Perfette, C.F. Anderson and P.L. Hall, **Biochemistry**, 15, 1735 (1976).
(b) H.G. Loffler and F. Schneider, **F.E.B.S. Lett.**, 45, 79 (1974).

29. L. Polgar, **Eur. J. Biochem.**, 33, 104 (1973).

30. (a) G. Lowe and Y. Yuthavong, **Biochem. J.**, 124, 117 (1971).
(b) M.H. O'Leary, M. Urberg and A.P. Young, **Biochemistry**, 13, 2077 (1974).

31. (a) H. Lindley, **Biochem. J.**, 74, 577 (1960).
(b) J.R. Whittaker, **J. Am. Chem. Soc.**, 84, 1900 (1960).

(c) J.W. Ogilvie, J.T. Tildon and B.S. Strauch, **Biochemistry**, 3, 754 (1964).

(d) A.R. Fersht, **J. Am. Chem. Soc.**, 93, 3504 (1971).

(e) G.E. Lienhard and W.P. Jencks, **J. Am. Chem. Soc.**, 88, 3982 (1966).

32. L. Polgar, **F.E.B.S. Lett.**, 47, 15 (1974).

33. (a) G. Lowe, **Tetrahedron**, 32, 291 (1976).

(b) M.R. Bendall and G. Lowe, **Eur. J. Biochem.**, 65, 481, 483 (1976).

(c) J. Drenth, K.H. Kalk and H.M. Swen, **Biochemistry**, 15, 3731 (1976).

34. D.J. Hupe and W.P. Jencks, **J. Am. Chem. Soc.**, 99, 451 (1977).

35. F.A. Johnson, S.D. Lewis and J.A. Shafer, **Biochemistry**, 20, 44 (1981).

36. (a) K.J. Angelides and A.L Fink, **Biochemistry**, 17, 2659 (1978).

(b) **ibid., idem.**, 18, 2355 (1979).

(c) A.L. Fink and K.J. Angelides, **Biochemistry**, 15, 5287 (1976).

(d) J.D. Roberts and K. Kanamori, **Proc. Natl. Acad. Sci., U.S.A.**, 77, 3095 (1980).

37. (a) K. Brocklehurst, B.S. Baines and M.P.J. Kierston, **Top. Enzyme Ferment. Biotechnol.**, 5, 262 (1981).

(b) K. Brocklehurst and J.P.G. Malthouse, **Biochem. J.**, 159, 221 (1976).

(c) K. Brocklehurst, S.M. Mushiri, G. Patel and F. Willenbrock, **Biochem. J.**, 201, 101 (1982).

(d) K. Brocklehurst and J.P.G. Malthouse, **Biochem. J.** 191, 707 (1980).

(e) K. Brocklehurst and M. Shipton, **Biochem. J.**, 171, 385 (1978).

(f) K. Brocklehurst, S.J.F. Willenbrock and E. Salih, **Biochem. J.**, 211, 701 (1983).

(g) K. Brocklehurst, T. Stuckbury and J.P.G. Malthouse, **Biochem. J.**, 183, 233 (1979).

(h) K. Brocklehurst, S.M. Mushiri, G. Patel and F. Willenbrock, **Biochem. J.**, 209, 873 (1983).

38. F.A. Johnson, S.D. Lewis and J.A. Shafer, **Biochemistry**, 15, 5009 (1976).

39. (a) F. Schneider, E. Schaich and H. Wenck, Hoppe-Seyler's Z. **Physiol. Chem.**, 349, 1525 (1968).

(b) F. Schneider and H. Wenck, **ibid**, 350, 1653 (1969).

(c) F. Schneider and H. Wenck, **ibid**, 350, 1521 (1969).

(d) F. Schneider, **ibid**, 348, 1034 (1967).

(e) D. Petz and F. Schneider, Z. **Naturforsch**, 31, 534 (1976).

40. D.J. Creighton and D.J. Schamp, **F.E.B.S. Lett.**, 110, 313 (1980).

41. (a) P. Lochon and J. Schoenleber, **Tetrahedron**, 32, 2023 (1976).

(b) J. Schoenleber and P. Lochon, **C.R. Acad. Sci. Ser. C.** 278, 1243 (1974).

42. C.G. Overberger, T.J. Pacansky, J.Lee, T. St. Pierre and S. Yaroslavsky, **J. Polymer Sci.**, Symposium, 46, 204 (1974).

43. I.M. Klotz, M.J. Heller and J.A. Walder, **J. Am. Chem. Soc.**, 99, 2780 (1977).

44. R.S. McDonald, P. Patterson and A. Stevens-Walley, **Can. J. Chem.**, 61, 1846 (1983).
Soc., 97, 1193 (1975).

45. J.P. Street and R.S. Brown, To be Published.

46. (a) W.P. Jencks and J. Carriuolo, **J. Biol. Chem.**, 234, 1280 (1959).

(b) **idem., ibid.**, 234, 1272 (1959).

(c) W. Palaitis and E.R. Thorton, **J. Am. Chem. Soc.**, 97, 1193 (1975).

(d) K. Hofmann in "The Chemistry of Heterocylic Compounds, Imidazole and its Derivatives", Interscience Publishers, Inc., New York, 1953 pp. 3-32.

47. W. Schunack, **Arch. Pharmaz.**, 307, 46, (1974).

48. J.R. Totter and W.J. Darby, **Org. Syn.**, 24, 64 (1964).

49. P.E. Iversen and H. Lund, **Acta. Chemica. Scand.**, 20, 2649 (1966).

50. (a) R.S. Brown and N. Curtis, **J. Org. Chem.**, 45, 4053 (1980).

(b) R.S. Brown and J.G. Ulan, **J. Am. Chem. Soc.**, 105, 2382 (1983).

51. (a) C.C. Tang, D. Davalian, P. Huang and R. Breslow, **J. Am. Chem. Soc.**, 100, 3918 (1978).

(b) R.S. Brown and J. Huguet, **Can. J. Chem.**, 58, 889 (1980).

(c) A.M. Roe, **J. Chem. Soc.**, 2195 (1963).

(d) S. Sakakibara and T. Fujii, **Bull. Chem. Soc. Jap.**, 42, 1466 (1969).

(e) J.M. van der Eijk, R.M. Nolte and J.W. Zwikker, **J. Org. Chem.**, 45, 547 (1980).

52. P.C. Jocelyn, **J. Chem. Soc.**, 3305 (1957).

53. (a) R.G. Jones, **J. Am. Chem. Soc.**, 71, 383 (1949).

(b) G.J. Durant, M.E. Foottit, C.R. Garrellin, J.M. Loynes, E.S. Pepper and A.M. Roe, **Chem. Commun.**, 2, 108 (1968).

(c) R.A. Turner, C.F. Huebner and C.R. Scholz, **J. Am. Chem. Soc.**, 71, 2801 (1949).

54. R. Humphrey, and J. Hawkins, **Anal. Chem.**, 36, 1812 (1964).

55. M.L. Bender and B.W. Turnquist, **J. Am. Chem. Soc.**, 79, 1652 (1956).

56. H.S. Simms, **J. Am. Chem. Soc.**, 48, 1239 (1926).

57. (a) L. Ebert, **Z. Physik. Chem.**, 121, 385 (1926).

(b) R. Wegscheider, **Monatshefte f. Chem.**, 16, 153 (1895), 23, 287 (1902).

(c) H.C. Brown, D.H. McDaniel and O. Hafliger in "Determination of Organic Structures by Physical Methods", E.A. Braude, F.C. Nachod, Eds.; Academic Press: New York, 1955, pp 620, 632-634.

58. M. Charton, **J. Org. Chem.**, 29, 1222 (1964).

59. (a) J.T. Edsall, R.B. Martin and B.R. Hollingworth, **Proc. Nat. Acad. Sci. U.S.A.**, 44, 505 (1958).

(b) R.E. Benesch, and R. Benesch, **J. Am. Chem. Soc.** 77, 5877 (1955).

(c) J.T. Edsall, and M.H. Blanchard, **J. Am. Chem. Soc.**, 55, 2337 (1933).

(d) Ho-Leung Fung and L. Cheng, **J. Chem. Ed.**, 51, 106 (1974).

60. R.S. Brown and K.I. Skorey, To be Published.

61. (a) T.H. Fife, R.J. Bombery and B.R. DeMark, **J. Am Chem. Soc.**, 100, 5500 (1978).

(b) T.C. Bruice and J.M. Sturtevant, **J. Am. Chem. Soc.**, 81, 2860 (1959).

62. M.L. Bender in "Catalysis and Enzyme Action", McGraw-Hill, New York, 1973.

63. D.D. Perrin. "Dissociation Constants of Organic Bases in Aqueous Solution", Butterworths: London, 1965.

64. A.H. Blatt (Ed), **Organic Synthesis** coll. vol. 5, John Wiley, London, 582 (1960).

65. J.L. Kelley, E.W. McLean, C.A. Miller, **J. Pharm. Sci.**, 70, 341 (1981).

66. D.P. Harnish and D.S. Tarbell, **Anal. Chem.**, 21, 968 (1949).

67. L. Skulski and T. Urbanski, **Roczniki Chemji**, 34, 1033 (1960).

APPENDIX 1: Non-Linear Least Squares Program

The software package was supplied by Varian and Associates Co. a brief description of the storage program and calculation program is given below.

Master Kinetic Storage Program

The Varian Cary 210 UV/VIS spectrophotometer Master Kinetic Storage Program collects, displays and stores spectral information (absorbance versus time) derived from kinetic runs.

Advanced Order Kinetics Calculation Program

This is an auxiliary software program intended to calculate the stored data either as zero, first or second order kinetics to give rate equations which will fit the raw kinetic data. The calculated curve can be graphically displayed with the raw data and the curve fitting parameters presented.

In the case of first order processing, the data is fitted to:

$$Abs_t = Abs_{inf} + (Abs_0 - Abs_{inf}) \times e^{-kt}$$

which is expanded into a Taylor series and solved by linear regression.

APPENDIX 2: Derivation of Kinetic Expressions for Figures 4 and 5.

Consider the following reaction scheme:

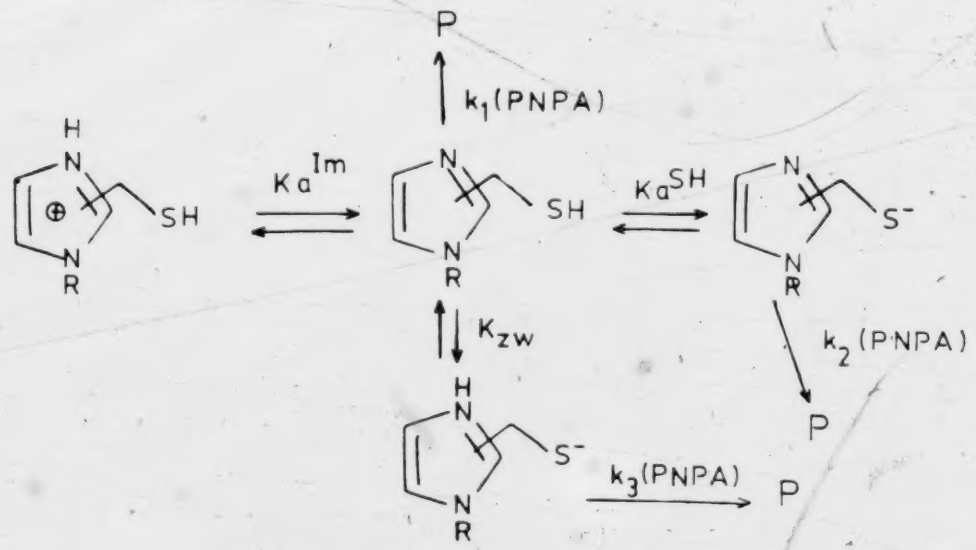

The equilibrium constants are defined as follows:

1. $Ka^{Im} = \frac{[IMSH][H^+]}{[H^+IMSH]}$ 2. $Ka^{SH} = \frac{[IMS^-][H^+]}{[IMSH]}$

3. $K_{Zw} = \frac{[H^+IMS^-]}{[IMSH]}$

The rate expression is:

4. $v = k_{cat}[IM_T] = k_1 x frac[IMSH] + k_2 x frac[IMS^-] + k_3 x frac[H^+IMS^-]$

Using eqns. 1 and 3 it can be shown that:

5. $[IMSH] = Ka^{Im}[H^+][IM_T]/X$

6. $[IMS^-] = Ka^{Im}Ka^{SH}[IM_T]/X$

7. $[H^+IMS^-] = Ka^{Im}K_{Zw}[H^+][IM_T]/X$

8. $[H^+IMSH] = [H^+]^2[IM_T]/X$

where $X = [H^+]^2 + Ka^{Im}K_{Zw}[H^+] + Ka^{Im}[H^+] + Ka^{Im}Ka^{SH}$

and $[IM_T] = [IMSH] + [IMS^-] + [H^+IMS^-] + [H^+IMSH]$

Using eqns. 5 to 8 and plugging into eqn. 4 the second order rate constant becomes:

$$k_{cat} = \frac{k_1Ka^{Im}[H^+] + k_2Ka^{Im}Ka^{SH} + k_3Ka^{Im}K_{Zw}[H^+]}{[H^+]^2 + Ka^{Im}K_{Zw}[H^+] + Ka^{Im}[H^+] + Ka^{Im}Ka^{SH}}$$

In the case of only one pKa as in the scheme shown below:

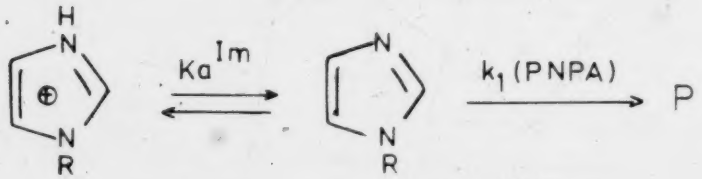

where $Ka^{Im} = [IM]/[H^+IM]$

The rate expression becomes:

$$v = k_{obs}[IM_T] = k_1 xfrac[IM]$$

Using the equilibrium constant, then:

$$k_{obs} = \frac{k_1Ka^{Im}}{Ka^{Im} + [H^+]}$$

APPENDIX 3: Simm's Method to Determine the pKa by Potentiometric Titration [56]

Let L be an organic base, then:

$$L + H \longrightarrow LH$$

$$LH + H \longrightarrow LH_2$$

$$LH_2 + H \longrightarrow LH_3$$

and $Ka_1 = \frac{[L][H]}{[LH]}$, $Ka_2 = \frac{[LH][H]}{[LH_2]}$, $Ka_3 = \frac{[LH_2][H]}{[LH_3]}$

Define:

$$n_H = \frac{[LH] + 2[LH_2] + 3[LH_3]}{[L] + [LH] + [LH_2] + [LH_3]}$$

If the pKa's are different enough, then when $pH = pKa_1$:

$[L] = [LH]$ and $[LH_2]$, $[LH_3] << [LH]$ and

$$n_H = \frac{[LH]}{[L] + [LH]} = 0.5$$

Similary, when $pH = pKa_2$, then $[LH] = [LH_2]$, and $[L], [LH_3] << [LH]$

$$n_H = \frac{[LH] + 2[LH_2]}{[LH] + [LH_2]} = 1.5$$

And when $pH = pKa_3$, then $[LH_2] = [LH_3]$, and $[L], [LH] << [LH_2]$

$$n_H = \frac{2[LH_2] + 3[LH_3]}{[LH_2] + [LH_3]} = 2.5$$

Thus the final equation becomes:

$$n_H = \frac{[H]_T - [H] - [OH^-]added + Kw/[H]}{[L]_T} = Cs/[L]_T$$

where $[H]_T$ = total concentration of acid at beginning

$[H]$ = pH measured

$[L]_T$ = total organic base added

Kw = dissociation constant of water = 1.66×10^{-14}

APPENDIX 4: Determination of Microscopic Dissociation Constants using UV Spectrophotometric Titration Data.

The following method was developed by Edsall, et al.[58] in 1958. Edsall developed equations to calculate values of the micro-constants from spectral data when the macro-constants are also unknown.

They based their equations on the equilibria described below:

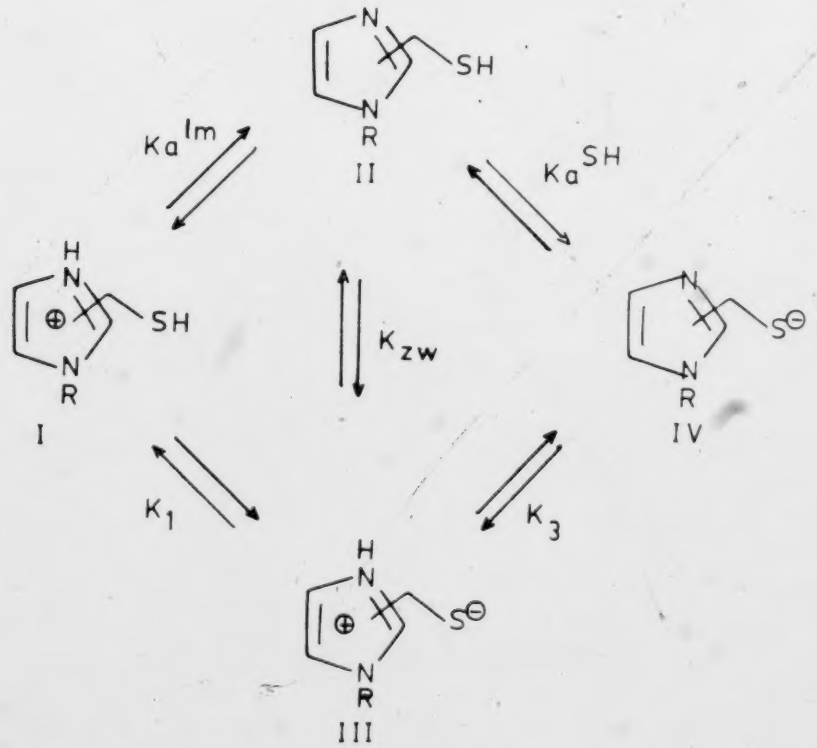

where $K_1 = \frac{[H^+IMS^-][H^+]}{[H^+IMSH]}$, $\quad Ka^{Im} = \frac{[IMSH][H^+]}{[H^+IMSH]}$

$K_3 = \frac{[IMS^-][H^+]}{[H^+IMS^-]}$, $\quad Ka^{SH} = \frac{[IMS^-][H^+]}{[IMSH]}$

In their derivation they assumed that species H^+IMS^- and IMS^- have the same molar absorptivity different from the absorptivitites of H^+IMSH and IMSH. The absorptivity of the latter were assumed equal to zero at the wavelength followed for the titration. They defined:

α = Concentration of all molecules with SH ionized / Concentration of all molecular species

$$\alpha = \frac{[H^+IMS^-] + [IMS^-]}{[H^+IMSH] + [H^+IMS^-] + [IMSH] + [IMS^-]}$$

Using the equilibrium constants, then:

1. $[IMSH] = Ka^{Im}[H^+][IM_T]/X$
2. $[IMS^-] = Ka^{Im}Ka^{SH}[IM_T]/X$
3. $[H^+IMS^-] = Ka^{Im}K_{Zw}[H^+][IM_T]/X$
4. $[H^+IMSH] = [H^+]^2[IM_T]/X$

where $X = [H^+]^2 + Ka^{Im}K_{Zw}[H^+] + Ka^{Im}[H^+] + Ka^{Im}Ka^{SH}$

and $[IM_T] = [IMSH] + [IMS^-] + [H^+IMS^-] + [H^+IMSH]$

From eqns. 1 to 4, it can be shown that:

5. $$\alpha = \frac{K_1[H^+] + Ka^{Im}Ka^{SH}}{[H^+]^2 + (Ka^{Im} + K_1)[H^+] + Ka^{Im}Ka^{SH}}$$

The authors then defined a new term M to be:

6. $$M = \frac{[H^+]}{1 - \alpha} = \frac{K_1[H^+] + Ka^{Im}Ka^{SH}}{[H^+] + Ka^{Im}}$$

7. $$pM = pH - \log\frac{\alpha}{1 - \alpha} = -\frac{\log K_1[H^+] + Ka^{Im}Ka^{SH}}{[H^+] + Ka^{Im}}$$

From equation 5, it can be seen that as $[H^+]$ approaches ∞ α approaches $K_1/[H^+] = 0$. Thus $pM = pK_1$ at $\alpha = 0$. Similarly, when $[H^+]$ approaches 0, α approaches 1. Thus $pM = pKa^{SH}$ at $\alpha = 1$. At $\alpha = 0.5$, $pM = pH$ and $Ka^{Im} = [H^+]([H^+] - K_1)/Ka^{SH} - [H^+]$.

From a plot of pM versus α, one can obtain K_1, Ka^{SH} and Ka^{Im}. The fourth Ka can then be calculated as: $K_3 = Ka^{Im}Ka^{SH}/K_1$.

APPENDIX 5: Determination of the Concentration of each species I, II, III, and IV as a function of pH.

Consider the scheme below:

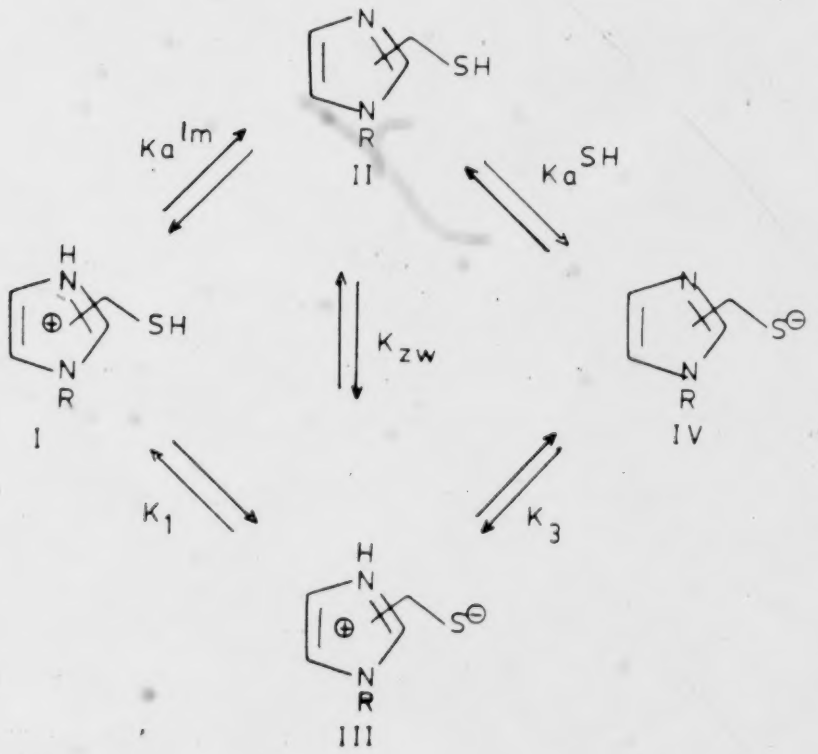

The equilibrium constants are defined as follows:

1. $Ka^{Im} = \frac{[IMSH][H^+]}{[H^+IMSH]}$ 2. $Ka^{SH} = \frac{[IMS^-][H^+]}{[IMSH]}$

3. $K_{Zw} = \frac{[H^+IMS^-]}{[IMSH]}$ 4. $K_1 = \frac{[H^+IMS^-][H^+]}{[H^+IMSH]}$

Thus, using eqns. 1 to 3 , one can defined:

$pK_1 - pH = \log I/III$; $pKa^{Im} - pH = \log I/II$;

$pK_3 - pH = \log III/IV$; $pKa^{SH} - pH = \log II/IV$

Define the total concentration of species I + II + III + IV

as 10^{-3} M. Then by definition:

$$\text{fraction of I} = \frac{[H^+IMSH]}{10^{-3}} = 1/(1 + K_1/[H^+] + K_3/[H^+] + Ka^{Im}Ka^{SH}/[H^+]^2)$$

$$\text{fraction of II} = \frac{[IMSH]}{10^{-3}} = 1/(1 + [H^+]/K_1 + Ka^{Im}/K_1 + [H^+]/Ka^{SH})$$

$$\text{fraction of III} = \frac{[H^+IMS^-]}{10^{-3}} = 1/(1 + [H^+]/K_1 + Ka^{Im}/K_1 + [H^+]/K_3)$$

$$\text{fraction of IV} = \frac{[IMS^-]}{10^{-3}} = 1/(1 + [H^+]^2/K_1K_3 + [H^+]/Ka^{SH} [H^+]/K_3)$$

A basic program was written to calculate the concentration of each species. This is given below:

```
1   OPEN 1,4;OPEN 2,4;OPEN3,4;OPEN 4,4; OPEN 5,4
2   OPEN 6,4; OPEN 7,4
3   DIM R(100), T(100), W(100), Y(100), Z(100),
    V(100)
4   PRINT "INPUT PKa1"
5   INPUT C1
6   PRINT "INPUT PKa2"
7   INPUT C2
8   PRINT "INPUT PKa3"
9   INPUT C3
10  PRINT "INPUT PKa4"
11  INPUT C4
15  INPUT "NUMBER OF DATA POINTS";N
20  PRINT "pH="
25  FOR I=1 TO N
30  INPUT R(I)
35  NEXT
40  FOR S1=1 TO N
45  A=10**(C1-R(S1))
50  B=10**(C2-R(S1))
55  D=10**(C3-R(S1))
60  E=10**(C4-R(S1))
65  M = 1E-3
70  HIMSH=(M)/(1+1/A+1/B+1/(B*E))
75  T(S1)=HIMSH
80  IMSH=(M)/(1+B+B/A+1/E)
85  W(S1)=IMSH
90  HIMS=(M)/(1+A+A/B+1/D)
95  Y(S1)=HIMS
100 IMS=(M)/(1+A*D+E+D)
```

```
105 Z(S1)=IMS
110 THIOLATE=IMS + HIMS
115 V(S1)=THIOLATE
120 NEXT
125 PRINTΔ1,"MICRO CONCENTRATIONS"
130 PRINTΔ2,"CONC. OF HIMSH";"       H+"
135 FOR X=1 TO N
140 PRINTΔ2,T(X),R(X)
145 NEXT
150 PRINTΔ3,"CONC. OF IMSH";"        H+"
155 FOR X = 1 TO N
160 PRINTΔ3,W(X),R(X)
165 NEXT
170 PRINTΔ4, "CONC. OF HIMS";"       H+"
175 FOR X = 1 TO N
180 PRINTΔ4,Y(X),R(X)
185 NEXT
190 PRINTΔ5,"CONC. OF IMS";"         H+"
195 FOR X = 1 TO N
200 PRINTΔ5, Z(X), R(X)
205 NEXT X
210 PRINTΔ6,:TOTAL IMS + HIMS";"     H+"
215 FOR X = 1 RO N
220 PRINTΔ6,V(X),R(X)
225 NEXT X
230 PRINTΔ7,"PKa1   PKa2   PKa3   PKa4"
235 PRINTΔ7,C1,C2,C3,C4
240 CLOSE 1;CLOSE 2;CLOSE 3; CLOSE 4; CLOSE 5;
    CLOSE 6;CLOSE 7
```

Note: * - multiply
** - to the power of

Appendix 6: Diagram of Specially-Designed Quartz Cell for UV-Visible Spectra Titrations.